A methoxy-substituted nitrodibenzofuran-based protecting group with an improved two-photon action cross-section for thiol protection in solid phase peptide synthesis

Taysir K. Bader,[†] Feng Xu,[†] Michael H. Hodny, David A. Blank and Mark D. Distefano[*]

Department of Chemistry, University of Minnesota, Minneapolis, MN 55455, USA

[†]Both authors contributed equally to this work

*Corresponding Author

E-mail: diste001@umn.edu

Abstract: Photoremovable caging groups are useful for biological applications since the deprotection process can be initiated by illumination with light without the necessity of adding additional reagents such as acids or bases that can perturb biological activity. In solid phase peptide synthesis (SPPS), the most common photoremovable group used for thiol protection is the o-nitrobenzyl group and related analogues. In earlier work, we explored the use of the nitrodibenzofuran (NDBF) group for thiol protection and found it to exhibit a faster rate towards UV photolysis relative to simple nitroveratryl-based protecting groups and a useful two-photon cross-section. Here we describe the synthesis of a new NDBF-based protecting group bearing a methoxy substituent and use it to prepare a protected form of cysteine suitable for SPPS. This reagent was then used to assemble two biologically relevant peptides and characterize their photolysis kinetics in both UV- and two-photon-mediated reactions; a two-photon action cross-section of 0.71 – 1.4 GM for the new protecting group was particularly notable. Finally, uncaging of these protected peptides by either UV or two-photon activation was used to initiate their subsequent enzymatic processing by the enzyme farnesyltransferase. These experiments highlight the utility of this new protecting group for SPPS and biological experiments.

INTRODUCTION

Thiol groups play key roles in a diverse range of biological processes ranging from acting as active site nucleophiles in enzymatic reactions to participating in disulfide bonds to stabilize protein structure as well as serving as sites for post-translational modifications.[1-3] The ability to mask a thiol group with a protecting group allows the resulting "caged" biomolecule to be maintained in an inactive state prior to "uncaging" it by deprotection. Photoremovable caging groups[4] are useful for biological applications since the uncaging process can be initiated by illumination with light without the necessity of adding additional reagents such as acids or bases that can perturb biological activity.[5,6] Light activated processes are particularly well suited for applications in live cells where it is generally not possible to use reagent-based deprotection conditions due to cellular toxicity.[7] Photoremovable protecting groups are also advantageous due to the unique features associated with light activation since uncaging can be triggered with high spatiotemporal control; the specific location and time of deprotection can be controlled by the position and timing of illumination. The spatial precision of uncaging can be improved using two-photon (TP) activation provided the protecting group chromophore manifests a usable TP action cross section; the development of caged neurotransmitters has benefited substantially from this feature.[8] TP activation also reduces potential phototoxicity since irradiation is performed at double the wavelength employed for UV excitation, which is in the visible or near IR region of the electromagnetic spectrum.

In solid phase peptide synthesis (SPPS), a vast number of protecting groups have been developed for cysteine.[9] However, for light-mediated deprotection, the most common protecting group used for thiol protection is the o-nitrobenzyl group (NB)[10] and related analogues including o-nitroveratryl (NV) (Figure 1).[7,11-14] While robust and useful for many applications, such

protecting groups do not exhibit useful TP action cross-sections, thus limiting their utility. To circumvent this limitation,

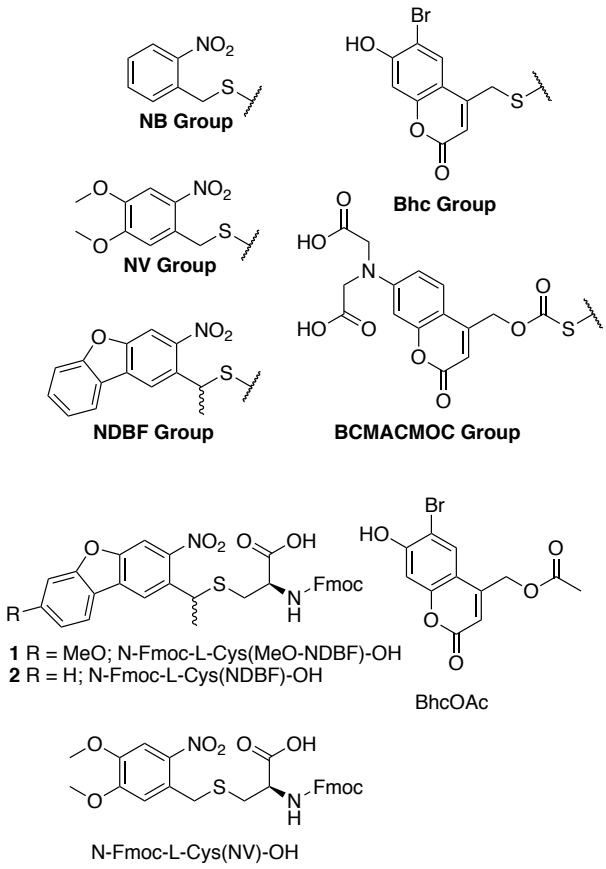

Figure 1. Representative photoremovable protecting groups used for the protection of the thiol group of cysteine and building blocks suitable for SPPS used here.

several groups have investigated the use of other protecting groups based on coumarin, quinoline and dibenzofuran scaffolds.[15-18] Thiol protecting groups based on a coumarin core have been studied and employed for a range of applications.[18-21] Protecting groups employing a thioether bond such as Bhc are more stable than those featuring a thiocarbonate linkage (BCMACMOC). However, irradiation of the former is often accompanied by isomerization without photocleavage[18,20] while the latter can undergo rearrangement when unprotected thiols or primary amine groups are present within the same peptide.[20] In earlier work, we explored the

use of the nitrodibenzofuran (NDBF) group for thiol protection and found it to exhibit a faster rate towards UV photolysis relative to simple NV-based protecting groups.[18] Moreover, it manifested a useful TP cross-section that could be particularly applicable to biological experiments performed in live cells. Previous work with the NV group suggests that its photochemical properties can be modulated via substitution of the aryl ring.[22] Here we describe the synthesis of a new NDBF-based protecting group bearing a methoxy substituent and use it to prepare Fmoc-Cys(MeO-NDBF)-OH (**1**), a building block suitable for SPPS. In the design of this moiety, we elected to preserve the ethyl group used in **2** as the point of thiol linkage (resulting in an additional stereogenic center) since photolysis of such compounds leads to the production of ketone products that have less putative cellular toxicity compared with the aldehyde products that are formed from simpler groups such as NV.[23] This reagent was then used to assemble two biologically relevant peptides and characterize their photolysis kinetics in both UV- and TP-mediated reactions. Finally, uncaging of these protected peptides by either UV or TP activation was used to initiate their subsequent enzymatic processing by the enzyme farnesyltransferase. These experiments highlight the utility of this new protecting group for SPPS and biological experiments.

RESULTS AND DISCUSSION

Synthetic Chemistry. In our earlier work, N-Fmoc-L-Cys(NDBF)-OH (**2**) was prepared starting from dibenzofuran. For the preparation of N-Fmoc-L-Cys(MeO-NDBF-OH) (**1**), a new, and more general route (Scheme 1), was developed to facilitate the synthesis of substituted dibenzofurans. The precursor, 2-bromo-5-methoxyphenol, containing the desired methoxy group was treated with 4-fluoro-2-nitrobenzaldehyde to yield diarylether **3**. Protection of the aldehyde as an acetal followed by palladium-catalyzed aryl coupling and deprotection afforded aldehyde **6** that was then converted to the racemic secondary alcohol, **7**, using trimethylaluminum. That alcohol was

then activated to the corresponding bromide that was then used to alkylate N-Fmoc-L-cysteine methyl ester under acidic conditions[24] to produce the fully protected amino acid **9**. Hydrolysis of that ester using trimethyltin hydroxide[25] gave N-Fmoc-L-Cys(MeO-NDBF)-OH (**1**), a protected form of cysteine suitable for solid phase peptide synthesis; mild conditions are essential for the hydrolysis of **9** to avoid potential racemization of the protected cysteine residue.

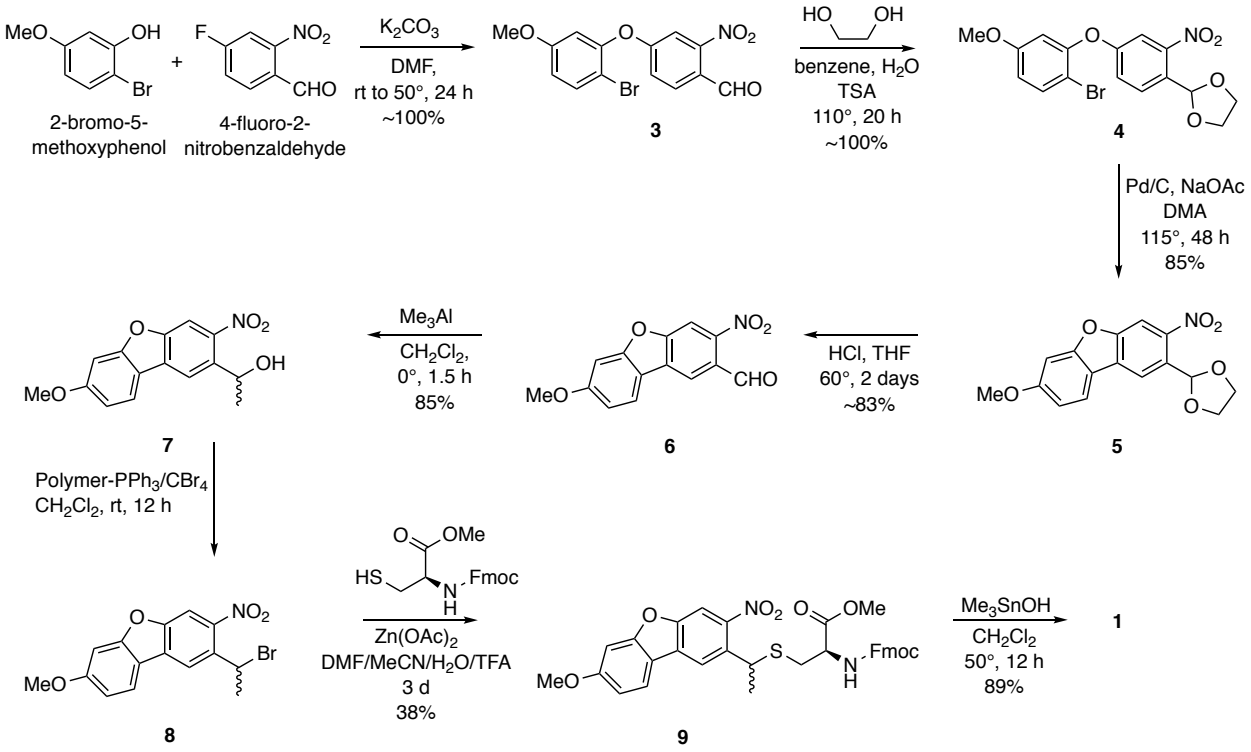

Scheme 1. Synthesis of N-Fmoc-L-Cys(MeO-NDBF)-OH (**1**).

With the desired building block in hand, a series of peptides (**10**-**18**, Figure 2) based on two different sequences incorporating the caged cysteine residue were prepared. First, a 15-residue peptide based on the sequence of a-factor, a yeast pheromone, was prepared starting with Fmoc-Ala on Wang resin. Fmoc-deprotection and two cycles of standard SPPS using an automated synthesizer yielded a VIA tripeptide on resin. Next, N-Fmoc-L-Cys(MeO-NDBF)-OH (**1**) was coupled offline with ninhydrin monitoring to insure complete reaction; to increase the

coupling efficiency, the coupling time was extended to 4 hours for this modified cysteine residue. At that point, automated peptide synthesis was resumed to complete the synthesis. After final Fmoc-deprotection, the peptide was cleaved from the resin under acidic conditions,

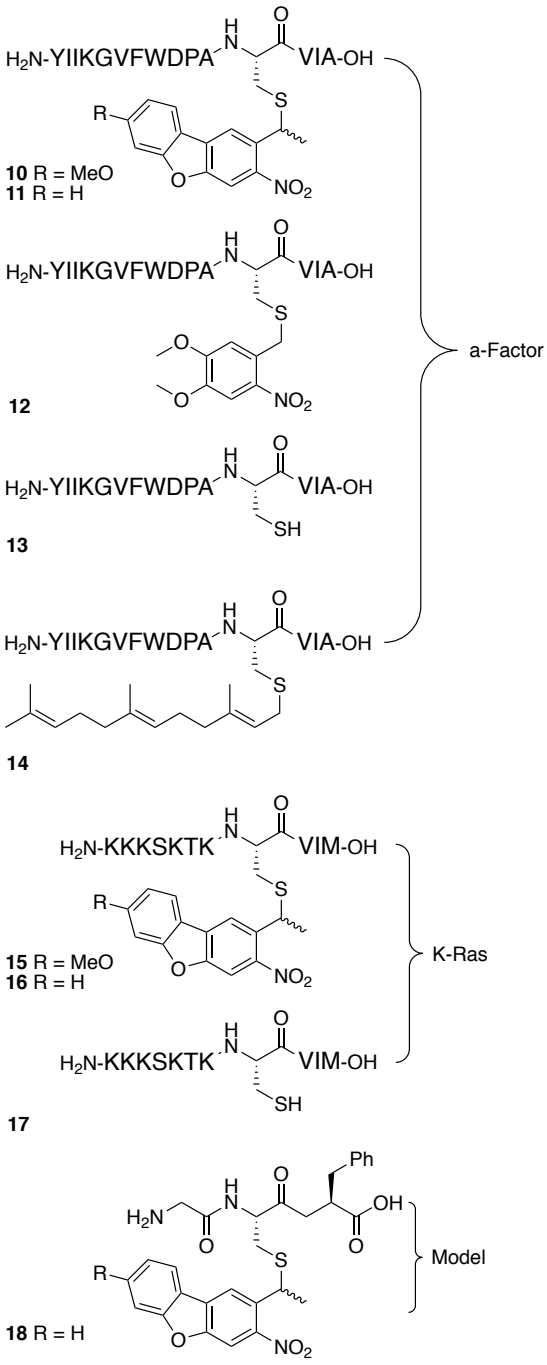

Figure 2. Synthetic peptides containing MeO-NDBF-, NBDF- and NV-protected cysteine residues prepared in this study.

precipitated with ether, and the resulting crude material purified via reversed-phase HPLC to yield the desired peptide. The final peptide, **10**, was analyzed via LC-MS/MS to confirm the sequence (Table S1). a-Factor-based peptides **11** and **12** containing NDBF- and NV-protected cysteine were also prepared and characterized in a similar manner (see Tables S2 and S3). A second peptide sequence based on the C-terminus of the human K-Ras protein was also synthesized. Forms of that peptide containing either Cys(MeO-NDBF) (**15**) or Cys(NDBF) (**16**) were prepared. Following purification of the complete peptides, their sequences were again confirmed via LC-MS/MS analysis (Tables S4 and S5).

In the initial preparation and purification of **10**, the HPLC chromatogram of the crude peptide revealed the presence of two double peaks: a main double peak corresponding to ~70-80% of the total integrated area, and a minor double peak corresponding to ~20-30% of the total integrated area. The double peak pattern was clearer for the NDBF-protected peptides **11** and **16** (Figures S1 and S2). For each peptide, all four peaks exhibited identical m/z values and MS/MS fragmentation patterns. We attribute the two species present in each of the double peaks as resulting from a mixture of two epimers due to the stereogenic center adjacent to the dibenzofuran since bromide **8** was used as a racemic mixture. We attribute the major double peak to be from the desired L-cysteine-containing peptides and the minor double peak to be from D-cysteine-containing peptides that arise due to racemization of the protected cysteine either during the hydrolysis of ester **9** or in the subsequent activation of **1** during SPPS. This structural assignment is supported by the fact that peak doubling was not observed with peptide **12** (Figure S3) which does not have the additional stereogenic center present in **10** and **11** (since the NV group lacks the methyl group present in the NDBF and MeO-NDBF protecting groups); however, **12** did have one major and one minor peak of identical mass, presumably due to racemization of the cysteine as noted above. This hypothesis was further corroborated when photolysis of the combined double peaks (from **11**) led to the generation of two product

peaks (**13**) exhibiting the same m/z ratio, whereas photolysis of the purified major double peak lead to the generation of a single product peak (Figure S4). While it was possible to remove the minor components via HPLC separation and use the resulting material for subsequent experiments, this may not always be possible depending on the specific peptide sequence under study. Hence, the epimerization process was studied in more detail to obtain a more optimized synthetic procedure.

To better understand the origin of the epimerization observed here, we first elected to study the hydrolysis of a Mosher's amide of NDBF-protected cysteine methyl ester (**23a**) to the corresponding acid (**24a**). Accordingly, that compound was prepared from **21a** by removal of the Fmoc group followed by acylation with (*S)*-Mosher's acid chloride [(S)-(+)-α-methoxy- α-(trifluoromethyl)phenylacetyl chloride] to yield the desired cysteine methyl ester derivative (**23a**). Inspection of the ^{19}F NMR revealed the presence of two signals at -69.03 and -68.92 ppm, consistent with the presence of two diastereomers (with equal integration) due to the epimeric mixture, resulting from the stereogenic center present in the NDBF group. Hydrolysis of the ester to the corresponding acid (**24a**) under conditions necessary to obtain complete conversion (Me_3SnOH, DCE, 75°, 12 h) and subsequent ^{19}F NMR analysis showed only two signals (at -69.02 and -68.92 ppm, Figure 3A) suggesting that no epimerization had occurred in the hydrolysis reaction; even when ester **23a** was subjected to more forcing conditions (Me_3SnOH, DCE, 85°, overnight), no additional peaks in the ^{19}F NMR were observed. To confirm the absence of epimerization, the authentic product (the diastereomeric ester containing D-cysteine) was independently prepared by reacting bromide **19** with N-Fmoc-D-cysteine methyl ester followed by Fmoc removal and acylation with (*S)*-Mosher's acid chloride to yield **23b**. Analysis of that material via ^{19}F NMR showed two signals at -68.86 and -68.82 ppm that are different than those present in the material produced from L-cysteine demonstrating that the two cysteine derivatives (prepared from the enantiomers of cysteine) can be clearly distinguished via ^{19}F

NMR. Hydrolysis of the D-cysteine analogue (**23b**) yielded the corresponding acid (**24b**) whose ^{19}F NMR manifested two signals at -68.80 and 68.78 ppm (Figure 3B); an ^{19}F NMR of a mixture of **24a** and **24b** confirms these chemical shift differences are real (Figure 3C). This result validates the use of ^{19}F NMR to monitor this epimerization process and suggests that no significant level of epimerization occurs in the hydrolysis of **9** to **1**.

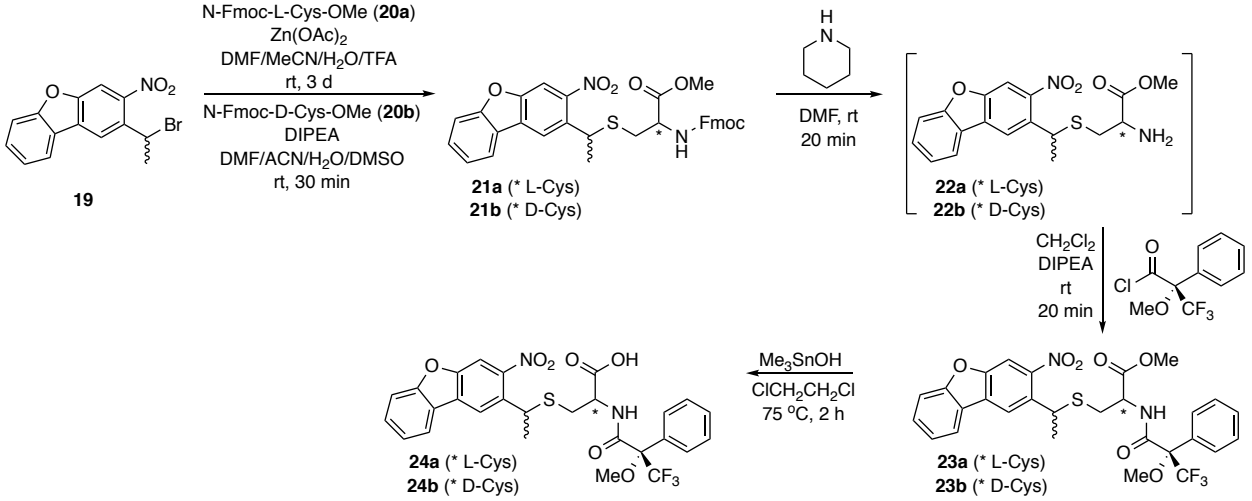

Scheme 2. Synthesis of Mosher's amides of NDBF-protected cysteine for subsequent stereochemical analysis.

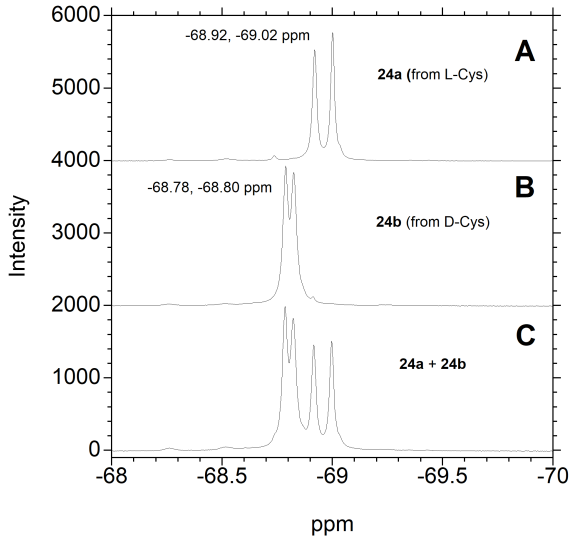

Figure 3. Study of the hydrolysis of a Mosher amide of NDBF-protected L-cysteine via ^{19}F NMR. A: ^{19}F NMR of compound **24a**, obtained after hydrolysis of **23a**. B: ^{19}F NMR of compound **24b**, prepared from D-cysteine. This corresponds to the product that would form from cysteine

racemization during coupling leading to an epimeric peptide product. ^{19}F NMR of a mixture of compounds **24a** and **24b**, showing the difference in chemical shifts between the two epimers.

Next, we examined the potential for epimerization during SPPS. Karas et al. previously reported that variable amounts of racemization occur in the activation of N-Fmoc-L-Cys(NV)-OH depending on the precise coupling conditions used.[14] We initially adjusted our synthetic conditions and employed the optimal conditions described by them, consisting of activation and coupling of **1** with 4 equivalents of N,N'-diisopropylcarbodiimide (DIC) and 6-chloro-1-hydroxybenzotriazole (Cl-HOBt) for 1 hour , for the synthesis of **10**. However, LC-MS/MS analysis of the resulting material after synthesis still showed significant epimerization (Figure S5). To confirm that the epimerization was occurring in the activation/coupling step of the protected cysteine residue, a model tripeptide GC(NDBF)F (**18**) was prepared and subjected to prolonged treatment (2 h) with 20% piperidine/DMF to duplicate the exposure to base that the embedded cysteine residue would experience (12 deprotection steps) necessary to complete the synthesis of a-Factor. Comparison of chromatograms obtained of the tripeptide before and after extensive piperidine treatment showed that no additional epimerization had occurred (Figure S6), suggesting that cysteine racemization must be occurring in the activation step. To minimize potential racemization, several different coupling conditions for the caged cysteine residue were investigated by synthesizing peptide **18** and subsequent LC-MS/MS analysis. Of the conditions surveyed, the use of benzotriazole-1-yl-oxy-tris-pyrrolidino-phosphonium hexafluorophosphate (PyBOP), 1-hydroxy-7-azabenzotriazole (HOAt) and DIEA gave the best results with less than 2% racemization being observed. To confirm the utility of these revised conditions, peptide **15** was resynthesized using 4 equivalents PyBOP/HOAT/DIEA for 30 min at a concentration of 150 mM. After global deprotection and resin cleavage with Reagent K, LC-MS analysis (Figure 4) showed less than 2% of the epimerized product was present. Overall, these results indicate that NDBF-based protection of cysteine can be used to efficiently prepare

caged peptides. However, careful reaction monitoring is important to minimize potential racemization during SPPS.

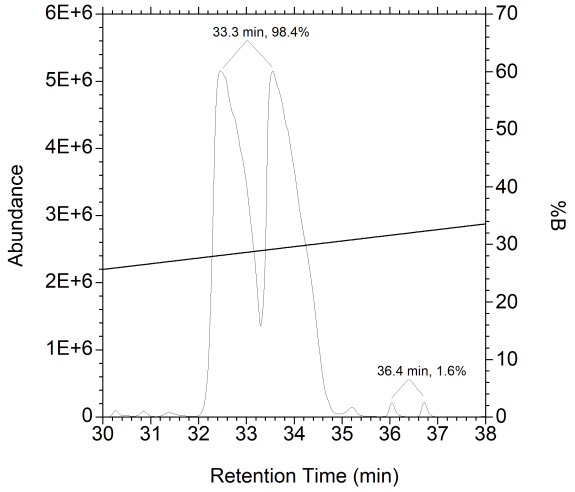

Figure 4. LC-MS of crude peptide **15** synthesized using PyBOP, HOAT and DIEA shows minimal epimerized product. The desired peptide elutes as a double peak centered at 33.3 min. Note the near complete absence of epimerized product at 36.4 min. The coupling conditions for **1** to resin-bound VIM consisted of 4 equivalents of PyBOP, HOAT and DIEA at 150 mM in DMF for 30 min.

Photochemistry. Previous work with o-nitrobenzyl-based protecting groups showed that the addition of methoxy substituents to the nitrobenzyl chromophore shifted the absorbance maximum to lower energy; that was accompanied by a decrease in the quantum yield for photolysis. Comparison of the UV spectra of the parent compound, N-Fmoc-L-Cys(NDBF)-OH (**2**), and N-Fmoc-L-Cys(MeO-NDBF)-OH (**1**), shown in Figure 5, indicates an increase in the absorbance maximum from 320 to 355 nm, consistent with the aforementioned simple o-nitrobenzyl-based system; in fact the absorbance maximum for **1** is quite similar to that of the simpler nitroveratryl group present in N-Fmoc-L-Cys(NV)-OH. Inspection of the UV spectra also shows that the extinction coefficients of the compounds at their λ_{max} vary less than 2-fold with the MeO-NDBF-protected residue exhibiting the highest value. At 350 nm, the wavelength used for the UV irradiation experiments described below, the extinction coefficient for the MeO-

NDBF-protected residue is 1.9-fold higher than that for the NDBF-protected parent compound (Table 1).

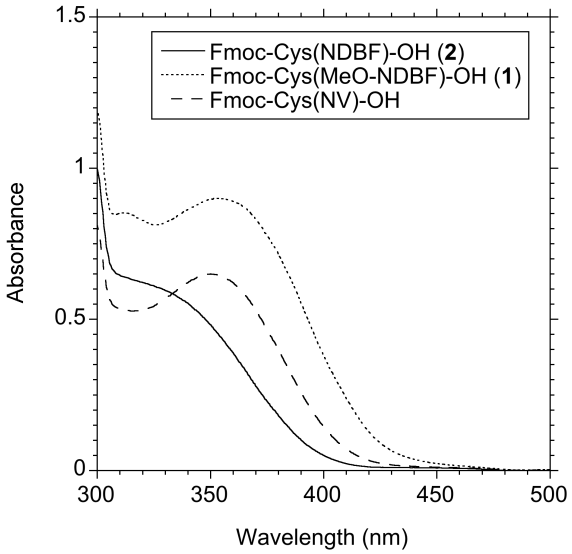

Figure 5. UV spectra of protected forms of cysteine suitable for SPPS used in this study.

Photolysis of peptides **10** and **11** using a Rayonet reactor centered at 350 nm and subsequent LC-MS analysis showed that the two protecting groups uncage at comparable rates (Figure S7). Since the bulbs used in these experiments manifest a fairly broad spectral bandwidth (~ 50 nm at half height), it is not possible to determine the quantum yields of these two protecting groups from these experiments. However, it is clear from an operational perspective (using a Rayonet reactor common to many laboratories performing photolysis experiments) that these two protecting groups have similar UV photolysis properties. Those results are in stark contrast to those obtained with peptide **12** that incorporates an NV-protected cysteine where the rate of photolysis is 25-fold slower compared with peptide **10** (containing a MeO-NDBF-protected cysteine residue); using 14 bulbs in a Rayonet reactor, peptides **10** and **11** are essentially completed deprotected in less than 30 seconds; for comparison, at that point, ~90% of the NV-protected peptide remains unreacted (Figure S7). Those results are similar to

what we previously reported[18] in comparing the monomeric precursors Fmoc-Cys(NDBF)-OMe and Fmoc-Cys(NV)-OMe and highlight a key feature of NDBF-based thiol protection, namely that it is much more sensitive to UV photolysis compared with the simpler NV group.

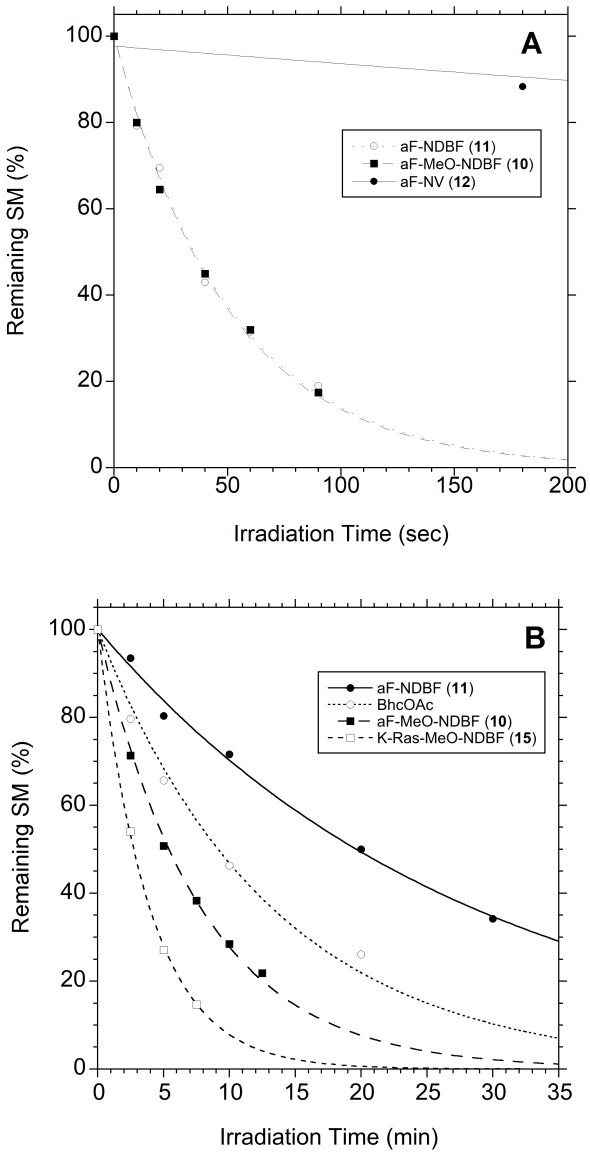

Figure 6. Photolysis of caged peptides via one and TP excitations. Above: Kinetic analysis of photolysis of MeO-NDBF-, NBDF- and NV-containing a-Factor-based peptides (**10**, **11** and **12**, respectively) using a 350 nm LED reactor. Below: Kinetic analysis of photolysis of NBDF- and MeO-NDBF-containing a-Factor-based peptides (**10** and **11**, respectively) and MeO-NDBF-containing K-Ras-based peptide (**15**) using a 800 nm Ti:Saphire laser employing BhcOAc as a reference standard. For both the UV and TP photolysis reactions, each reaction was performed in triplicate and the resulting data averaged and used to create the above plots.

To quantify the photophysical properties of peptides **10** and **11** in more detail, photolysis reactions were performed at low concentration to minimize any inner filter effect using an apparatus (Figure S8) equipped with 350 nm LEDs with a narrower spectral bandwidth (~ 10 nm at half height, Figure S9). After determining the intensity of the light source via ferrioxylate actinometry, the apparatus was used to determine the rate of photolysis for peptides **10**, **11** and **12** (Figure 6A, Figure S10 and Table S6) and calculate their respective quantum yields. Values of 0.53, 0.70 and 0.023 were obtained for **10**, **11** and **12**, respectively (Table 1). It should be noted that the value obtained for peptide **11** that incorporates an NDBF-protected thiol is comparable to the value reported for NDBF-EGTA (0.7), a caged alcohol. These results quantitatively illustrate the greater efficiency of NDBF-based protecting groups as photoremovable moieties compared with NV-based compounds and serve to highlight their utility for uncaging applications.

Table 1. Photophysical properties of caged molecules employed in this study.

Protected Cysteine	(λ_{max})[a] (nm)	ε (λ_{max})[a] ($M^{-1}cm^{-1}$)	ε (350 nm)[a] ($M^{-1}cm^{-1}$)	Φ (350)[c] (mol/ein)	δ_u (800 nm)[d] (GM)
N-Fmoc-L-Cys(MeO-NDBF)-OH (**1**)	355	8,780	8,750	0.53[e]	0.71[e] 1.4[f]
N-Fmoc-L-Cys(NDBF)-OH (**2**)	320[b]	5,990	4,600	0.70[g]	0.20[g]
N-Fmoc-L-Cys(NV)-OH	350	6,290	6,290	0.023[h]	-

[a]Measured in H_2O/CH_3CN (1:1, v/v). [b]Fmoc-Cys(NDBF)-OH (**2**) exhibits a broad maximum. [c]Measured in 50 mM sodium phosphate buffer (PB), pH 7.4 containing 15 mM DTT. [d]Measured in H_2O/CH_3CN (1:1, v/v) containing 0.1% TFA. [e]Measured using peptide **10.** [f]Measured using peptide **15.** [g]Measured using peptide **11**. [h]Measured using peptide **12**.

One of the most important features of the NDBF protecting group is that it manifests a significant TP action cross-section for uncaging, making it useful for biological experiments. Accordingly, we wanted to study the rates of photolysis of peptides **10** and **11** upon TP activation. Thus, solutions of the peptides were irradiated at 800 nm using a Ti:Saphire laser followed by LC-MS analysis. Interestingly, peptide **10** containing the MeO-NDBF-protected cysteine residue uncaged at a rate 3.6-fold greater than peptide **11** containing the parent NDBF-protected cysteine (Figure 6B). Furthermore, irradiation of the K-Ras-derived, MeO-NDBF-containing peptide **15** manifested an additional 2-fold rate increase compared to the MeO-NDBF-containing a-Factor-derived peptide **10**. Using BhcOAc as a standard, we estimate the TP action cross-section for MeO-NDBF deprotection to be 0.7 GM for **10** and 1.4 GM for **15**. Presumably, the observed variation in the TP action cross-section of different peptides incorporating the same chromophore reflects differences in the local structure/environment around the chromophore; such results have been observed in homologues of GFP where the fluorophore is constant throughout.[26] Overall, these results constitute a significant improvement in TP photolysis efficiency and suggests that the MeO-NDBF protecting group could be particularly useful for TP activation of peptides containing caged cysteines in cells or even tissue.

Enzymatic reactions initiated by thiol uncaging. Caged peptide substrates have potentially significant utility in cell-based biological experiments since they are unreactive prior to photolysis. Peptides can be incubated with cells and allowed to accumulate before activation with light. As a prelude to such cell-based experiments, we sought to investigate whether photolysis of peptides containing MeO-NDBF protected cysteine residues could be used to liberate peptides that could serve as substrates for enzymatic reactions. Protein farnesylation involves the transfer of the isoprenyl group from farnesyl diphosphate (FPP) to proteins bearing C-terminal CaaX-box sequences.[27] Protein farnesyltransferase (PFTase) which catalyzes this

reaction has been intensely studied as a possible therapeutic target for a number of diseases including cancer.[28,29] Initially, peptide **10** was incubated in the presence of PFTase and the substrate FPP and irradiated for 30 sec in a Rayonet photoreactor using three 350 nm bulbs. Analysis of the resulting photolysis reaction via LC-MS before and after photolysis indicated that essentially all of the starting peptide **10** (Figure S11A, before photolysis) had been converted to the corresponding farnesylated product **14** (Figure S11C, after photolysis); in the absence of PFTase, the deprotected thiol, **13**, was the major species (Figure S11B, no PFTase).

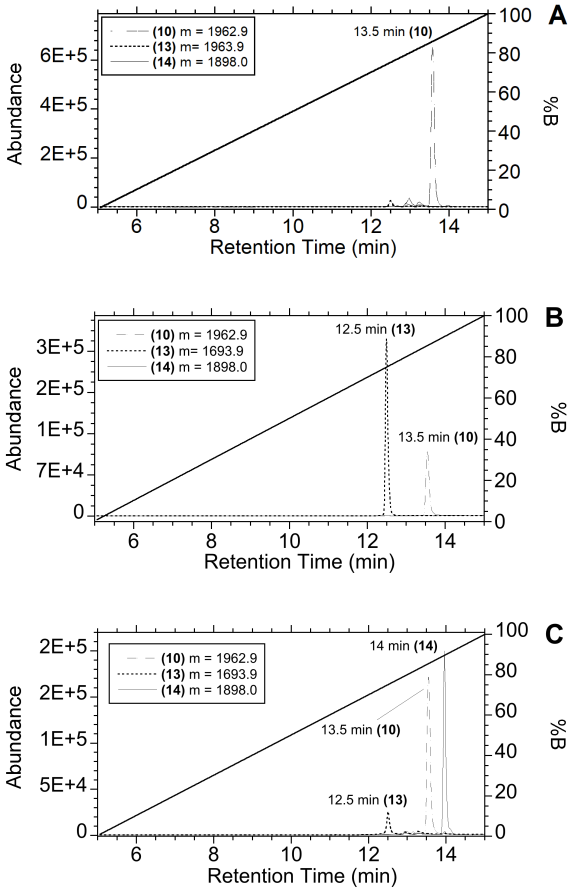

Figure 7. Analysis of PFTase-catalyzed farnesylation after TP-activated photolysis of **10**. In each case, reactions were monitored by LC-MS with single ion monitoring (SIM) of the protected peptide (**10**), the uncaged free thiol (**13**) and the farnesylated product (**14**). Panel A: LC-MS analysis of a reaction containing **10** and PFTase before irradiation at 800 nm. Panel B: LC-MS analysis of a reaction containing **10** without PFTase after irradiation at 800 nm. Panel C: LC-MS analysis of a reaction containing **10** with PFTase after irradiation at 800 nm.

Next, we explored the TP-mediated process. Accordingly, peptide **10** was incubated in the presence of PFTase and FPP and irradiated at 800 nm for 10 minutes using the laser system described above. Analysis of the resulting photolysis reaction via LC-MS before and after photolysis indicated substantial conversion of the starting peptide **10** (Figure 7A, before photolysis) to the corresponding farnesylated product **14** (Figure 7C, after photolysis) with a small amount of the free thiol (**13**) remaining. In contrast, in the absence of PFTase, the major species present after irradiation was the free thiol (**13**) (Figure 7B, after photolysis without PFTase). To explore the dose dependence of this photochemical reaction, samples containing **10**, PFTase and FPP were irradiated at 800 nm for different times and the amounts of starting peptide (**10**) and farnesylated product (**14**) were quantified from LC-MS analysis. A plot of that data (Figure 8) showed a clear relationship between light exposure and product formation. Importantly, under these conditions, significant quantities of the farnesylated product (~20%) were easily detected within the first five minutes of irradiation, highlighting the efficiency of this process.

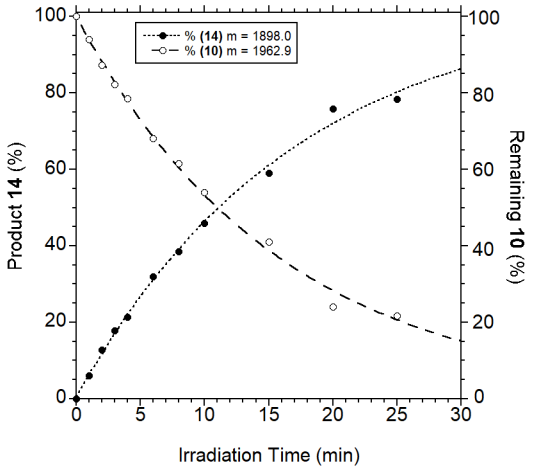

Figure 8. Quantification of starting peptide **10** and enzymatically farnesylated product **14** from TP-activated photolysis of **10** at 800 nm conducted for different durations in the presence of PFTase and FPP.

CONCLUSIONS

In this work, the efficiency of TP-mediated thiol deprotection in cysteine-containing peptides was improved using a new methoxy-substituted analogue of NDBF. An efficient synthesis was developed to prepare Fmoc-Cys(MeO-NDBF)-OH (**1**), a protected form of cysteine suitable for SPPS; installation of the methoxy substituent increased the absorption maximum from 320 nm (NDBF) to 355 nm (MeO-NDBF). The cysteine analogue was incorporated into two known bioactive peptides including a-Factor precursor (**10**, a pentadecapeptide) and a fragment from the C-terminus of K-Ras (**15**, an undecapeptide). UV irradiation of these MeO-NDBF-protected peptides resulted in deprotection at rates comparable to those of peptides masked with the parent NDBF group but 25-fold faster compared to an NV-protected peptide due to the larger quantum yield measured for the NDBF-based caging groups. However, TP activation at 800 nm showed significant differences between the two caging groups with the TP action cross-sections for **10** and **15** determined to be 0.71 and 1.4 GM, respectively using BhcOAc as a standard. These are 3.5- and 7-fold higher for **10** and **15**, respectively, compared to the previously reported value for the parent NDBF group of 0.2 GM, also reproduced here using peptide **11**. Finally, deprotection of peptide **10** using either UV or 800 nm light rapidly liberated the free thiol form (**13**) which was efficiently enzymatically transformed to its farnesylated congener (**14**) via the action of PFTase. These experiments set the stage for future cell-based experiments using this more efficiently removable protecting group. Finally, the results described here, demonstrating an increase in TP action cross-section upon introduction of a methoxy substituent, suggest additional exploration of the NDBF scaffold is warranted.

EXPERIMENTAL

General Details. HPLC and LC-MS Grade H_2O and CH_3CN as well as HOATwere purchased from Fisher Scientific (Pittsburgh PA). Fmoc-Cys-OH was purchased from Chem-Impex International (Wood Dale, IL). All other protected amino acids and resins were purchased from

P3 BioSystems (Louisville, KY). HCTU was purchased from Oakwood Chemical (Estill, SC). PyAOP was purchased from EMD Millipore (Burlington, MA). Other solvents and reagents used were purchased from Sigma-Aldrich (St. Louis, MO) and were used without further purification. ^{1}H NMR data of synthetic compounds were recorded at 500 MHz on a Bruker Avance III HD Instrument at 25 °C. Liquid chromatography – mass spectrometry (LC-MS) analysis was performed using an Agilent 1200 series LCMSD SL single quadrupole system equipped with a C3 column (Agilent ZORBAX 300SB-C3, 5 µM, 4.6 x 250 mm) and a variable wavelength detector. An H_2O/CH_3CN solvent system containing 0.1% HCO_2H was used, consisting of solvent A (H_2O with 0.1% HCO_2H) and solvent B (CH_3CN with 0.1% HCO_2H). High resolution mass spectrometry and MS/MS fragmentation of peptides was performed using a Thermo Scientific Elite Orbitrap instrument. High resolution mass spectra of organic compounds were acquired using either a Bruker BioTOF II ESI/TOF-MS, or an Applied Biosystems-Sciex 5800 MALDI-TOF instrument. High performance liquid chromatography (HPLC) purification was performed using an Agilent 1100 series instrument equipped with a diode-array detector and C18 columns (Agilent ZORBAX 300SB-C18 5 µM 9.4 x 250 mm, or Agilent Pursuit C18 5 µM 250 x 21.2mm, respectively), and using an H_2O/CH_3CN system containing trifluoroacetic acid (TFA) consisting of solvent A (H_2O with 0.1% TFA) and solvent B (CH_3CN with 0.1% TFA).

4-(2-bromo-5-methoxyphenoxy)-2-nitrobenzaldehyde (3). 4-fluoro-2-nitrobenzaldehyde (2.29 g, 13.6 mmol) was dissolved in DMF (100 mL). 2-bromo-5-methoxyphenol (2.62 g, 12.9 mmol) and K_2CO_3 (5.4 g, 39 mmol) were then sequentially added and the reaction was purged with Ar (g) and stirred at rt for 6 h and then 50 °C for 12 h in an oil bath. The reaction progress was followed by TLC. After the reaction was deemed complete, the mixture was cooled to rt and poured into aqueous NH_4Cl (200 mL) and extracted with EtOAc (3 x 100 mL). The organic phase was washed with H_2O (500 mL), brine (500 mL), dried with anhydrous $MgSO_4$ and evaporated to dryness. The crude product was purified by column

chromatography (Hexanes/EtOAc, 4:1, v/v) to yield 4.4 g (98%) of product **3** as a pale yellow solid. mp 62-64 °C. ^{1}H NMR ($CDCl_3$, 500 MHz) δ 10.32 (s, 1H), 7.99 (d, *J* = 8.6 Hz, 1H), 7.57 (d, *J* = 8.9 Hz, 1H), 7.50 (d, *J* = 2.3 Hz, 1H), 7.22 (dd, *J* = 2.1, 8.6 Hz, 1H), 6.80 (dd, *J* = 2.8, 8.9 Hz, 1H), 6.72 (d, *J* = 2.8, 1H), 3.81 (s, 3H). ^{13}C{^{1}H} NMR ($CDCl_3$, 125 MHz) δ 186.8, 161.4, 160.6, 151.4, 151.1, 134.5, 131.7, 125.0, 120.8, 113.7, 111.9, 108.9, 106.1, 55.8. HRMS (ESI): Calcd for $C_{14}H_{10}BrNNaO_5$ $[M+Na]^+$: 373.9635; found: 373.9610.

2-(4-(2-bromo-5-methoxyphenoxy)-2-nitrophenyl)-1,3-dioxolane (4). Compound 3 (5 g, 14.2 mmol) was dissolved in benzene (300 mL). Ethylene glycol (5 mL) and p-toluene sulfonic acid monohydrate (500 mg, 2.91 mmol) were added. The reaction was purged with Ar (g) and stirred at 110 °C in an oil bath using a Dean-Stark trap. Reaction progress was monitored by TLC. After completion of this reaction, the mixture was cooled to rt and poured into aqueous $NaHCO_3$ (200 mL), and extracted with EtOAc (3 x 150 mL). The organic phase was washed with H_2O (100 mL), brine (100 mL), dried with anhydrous $MgSO_4$, evaporated to dryness, and purified by column chromatography (Hexanes/EtOAc, 3:1, v/v) to yield 5.1 g (95%) of product **4** as a sticky oil. ^{1}H NMR ($CDCl_3$, 500 MHz) δ 7.74 (d, *J* = 8.7 Hz, 1H), 7.53 (d, *J* = 8.9 Hz, 1H), 7.41 (d, *J* = 2.5 Hz, 1H), 7.15 (dd, *J* = 2.5, 8.7 Hz, 1H), 6.72 (dd, *J* = 2.9, 8.9 Hz, 1H), 6.63 (dd, *J* = 2.9, 1H), 6.40 (s, 1H), 4.04 (s, 4H), 3.78 (s, 3H). ^{13}C{^{1}H} NMR ($CDCl_3$, 125 MHz) δ 160.5, 158.0, 152.3, 149.7, 134.4, 129.5, 127.4, 121.0, 113.0, 112.9, 108.4, 106.2, 99.5, 65.5, 55.9. HRMS (ESI): Calcd for $C_{16}H_{14}BrNNaO_6$ $[M+Na]^+$, 417.9897; found: 417.9886.

2-(1,3-dioxolan-2-yl)-7-methoxy-3-nitrodibenzo[b,d]furan (5). Compound **4** (3 g, 8.1 mmol) was dissolved in dimethylacetamide (60 mL). NaOAc (1.0 g, 12.2 mmol) and Pd/C (0.228 mmol, 239 mg) were added into this mixture. The reaction was stirred at 115 °C in an oil bath and the progress followed by NMR at selected intervals. The reaction was deemed complete after 2 days. After filtration through a pad of Celite®, the filtrate was diluted with EtOAc (80 mL),

and poured into NH_4Cl aqueous solution (200 mL), and extracted with EtOAc (3 x 150 mL). The organic phase was washed with H_2O (100 mL), brine (100 mL), and was then dried over anhydrous $MgSO_4$, evaporated to dryness, and purified by column chromatography (Hexanes/EtOAc, 3:1, v/v) to yield 2.2 g (85%) of product **5**, isolated as a yellow solid. mp 220-222 °C. ^{1}H NMR ($CDCl_3$, 500 MHz) δ 8.26 (s, 1H), 8.15 (s, 1H), 7.88 (d, *J* = 8.6 Hz, 1H), 7.12 (d, *J* = 1.9 Hz, 1H), 7.02 (dd, *J* = 2.0, 8.6 Hz, 1H), 6.63 (s, 1H), 4.12 (s, 4H), 3.93 (s, 3H). $^{13}C\{^1H\}$ NMR ($CDCl_3$, 125 MHz) δ 161.8, 160.2, 155.0, 146.2, 128.91, 128.89, 122.3, 118.6, 115.8, 112.9, 108.9, 100.09, 96.7, 65.5, 56.0. HRMS (ESI): Calcd for $C_{16}H_{13}NNaO_6$ $[M+Na]^+$, 338.0635; found: 338.0619.

7-methoxy-3-nitrodibenzo[b,d]furan-2-carbaldehyde (6). Compound **5** (3 g, 9.5 mmol) was dissolved in a THF/H_2O solvent mixture (100 mL, 3:1, v/v), and then p-toluene sulfonic acid monohydrate (300 mg, 1.74 mmol) as added. The reaction was stirred at 60 ^oC in an oil bath and reaction progress was monitored by TLC. After 24 h THF in the resulting solutions was removed by vacumn and the desired product was precipitated, product **6** was isolated through filtration to yield 2.1 g (83%), as a red solid. mp 205-208 °C. ^{1}H NMR ($CDCl_3$, 500 MHz) δ 10.51 (s, 1H), 8.42 (s, 1H), 8.29 (s, 1H), 7.93 (d, *J* = 8.6 Hz, 1H), 7.16 (d, *J* = 1.9 Hz, 1H), 7.08 (dd, *J* = 2.0, 8.7 Hz, 1H), 3.95 (s, 3H). $^{13}C\{^1H\}$ NMR ($CDCl_3$, 125 MHz) δ 188.2, 162.5, 160.6, 157.2, 147.5, 129.9, 127.8, 122.7, 120.9, 115.3, 113.7, 108.7, 96.8, 56.1. HRMS (ESI): Calcd for $C_{14}H_9NNaO_5$ $[M+Na]^+$, 294.0373; found: 294.0401.

1-(7-methoxy-3-nitrodibenzo[b,d]furan-2-yl)ethan-1-ol (7). Trimethylaluminum (0.55 mL, 1.1 mmol; 2 M solution in hexanes) was added dropwise over 10 min to a solution of **6** (150 mg, 0.55 mmol) in dry CH_2Cl_2 (3 mL) under Ar at 0 ºC. The reaction was stirred at 0 ºC for 1 h, after which it was quenched with ice-cold water (50 mL), followed by addition of 1 M NaOH (5 mL). The mixture was stirred for 30 min, after which time additional CH_2Cl_2 (10 mL) was added

and the resulting organic layer was washed with 1 M NaOH (50 mL), brine (50 mL), dried over $MgSO_4$ and the volatiles were evaporated, affording crude **7**. The crude product was passed through a thin pad of SiO_2 eluted with EtOAc/Hexanes (150 mL, 1:3, v/v) to yield 123 mg (85%) of pure product **7**, as a yellow solid. mp 140-142 °C. ^{1}H NMR (THF-D_8, 500 MHz) δ 8.42 (s, 1H), 8.29 (s, 1H), 7.93 (d, *J* = 8.6 Hz, 1H), 7.28 (d, *J* = 2.2 Hz, 1H), 7.08 (dd, *J* = 1.5, 8.6 Hz, 1H), 5.50-5.45 (m, 1H), 4.71 (d, *J* = 3.74 Hz, 1H), 3.95 (s, 3H), 1.54 (d, *J* = 6.25 Hz, 3H). ^{13}C{^{1}H} NMR (THF-D_8, 125 MHz) δ 161.9, 160.0, 153.7, 145.1, 138.8, 129.0, 122.1, 118.2, 115.6, 112.4, 107.1, 96.5, 64.8, 55.2, 25.2. HRMS (ESI): Calcd for $C_{15}H_{13}NNaO_5$ $[M+Na]^+$, 310.0686; found: 310.0671.

2-(1-bromoethyl)-7-methoxy-3-nitrodibenzo[b,d]furan (8). To compound **7** (126 mg, 0.44 mmol) in CH_2Cl_2 (5 mL) in an ice bath, PPh_3-polymer supported (1.1 mmol, ~ 3 mmol/g, 367 mg), and CBr_4 (273 mg, 0.825 mmol) were introduced. The reaction mixture was stirred at rt overnight. After filtration through a pad of Celite®, the filtrate was collected, and the solvent evaporated. The crude product was purified by column chromatography on SiO_2 (Hex/EtOAc, 5:1, v/v) to give 120 mg (78%) of the desired product, **8**, as a yellow solid. mp 168 °C (decomposed). ^{1}H NMR ($CDCl_3$, 500 MHz) δ 8.29 (s, 1H), 8.05 (s, 1H), 7.91 (d, *J* = 8.6 Hz, 1H), 7.11 (d, *J* = 2.2 Hz, 1H), 7.03 (dd, *J* = 2.2, 8.6 Hz, 1H), 6.04 (q, *J* = 6.8 Hz, 1H), 3.94 (s, 3H), 2.20 (d, *J* = 6.8 Hz, 3H). ^{13}C{^{1}H} NMR ($CDCl_3$, 125 MHz) δ162.0, 160.3, 154.3, 144.9, 133.6, 129.6, 122.4, 120.5, 115.4, 112.9, 108.3, 96.7, 56.0, 43.1, 28.0. HRMS (ESI): Calcd for $C_{15}H_{12}BrNO_4Na$ $[M+Na]^+$, 371.9842; found: 371.9872.

Methyl *N*-(((9*H*-fluoren-9-yl)methoxy)carbonyl)-*S*-(1-(7-methoxy-3-nitrodibenzo[*b*,*d*]furan-2-yl)ethyl)-*L*-cysteinate (9). Product **8**, Fmoc-L-Cysteine methyl ester (327 mg, 0.93 mmol) and $Zn(OAc)_2$ (438 mg, 2.0 mmol) were dissolved in 30 mL of a mixture of DMF/ACN/0.1% TFA in H_2O (4:1:1, v/v/v). The reaction was monitored by TLC (Hexanes/Et_2O,

1:1, v/v) and stopped after 24 h of stirring at rt by pouring the reaction mixture into H_2O (100 mL), and extraction with EtOAc (3 x 30 mL) three times. The organic phase was washed with 100 mL of brine, and was then dried over anhydrous $MgSO_4$, evaporated to dryness, and purified by column chromatography on SiO_2 (Hexanes/EtOAc, 3:1, v/v) to give 221 mg (38%) of the desired product **9**, isolated as a yellow sticky oil, as a diastereomeric mixture. ^{1}H NMR ($CDCl_3$, 500 MHz) δ 8.26 (s, 1H), 8.24 (s, 1H), 8.01 (s, 2H), 7.87 (d, *J* = 8.6 Hz, 1H), 7.80 (d, *J* = 8.6 Hz, 1H), 7.77-7.73 (m, 4H), 7.62-7.56 (m, 4H), 7.41-7.38 (m, 4H), 7.32-7.28 (m, 4H), 7.09-6.91 (m, 4H), 5.59-5.55 (m, 2H), 4.92-4.85 (m, 2H), 4.59-4.56 (m, 1H), 4.52-4.49 (m, 1H), 4.39-4.32 (m, 2H), 4.28-4.20 (m, 3H), 4.15-4.11 (m, 1H), 3.92 (s, 3H), 3.88 (s, 3H), 3.77 (s, 3H), 3.71 (s, 3H), 2.98-2.85 (m, 4H), 1.71-1.69 (m, 6H). ^{13}C{^{1}H} NMR($CDCl_3$, 125 MHz) δ171.1, 161.9, 161.8, 160.1, 155.8, 153.9, 146.6, 146.5, 144.0, 143.9, 141.41, 141.38, 141.37, 134.1, 134.0, 129.6, 129.5, 127.9, 127.3, 125.3, 122.4, 122.3, 120.09, 120.07, 119.98, 119.90, 115.5, 112.79, 112.71, 108.14, 108.09, 100.11, 96.66, 96.63, 67.49, 67.45, 55.99, 55.96, 53.77, 53.71, 52.96, 52.93, 47.19, 47.11, 40.0, 39.7, 34.22, 34.10, 23.86, 23.74. HRMS (ESI): Calcd for $C_{34}H_{30}N_2O_8SNa$ $[M+Na]^+$, 649.1615; found: 649.1629.

***N*-(((9*H*-fluoren-9-yl)methoxy)carbonyl)-*S*-(1-(7-methoxy-3-nitrodibenzo[*b*,*d*]furan-2-yl)ethyl)-*L*-cysteine (1).** Ester **9** (300 mg, 0.48 mmol) was dissolved in CH_2Cl_2 (6 mL) and Me_3SnOH (226 mg, 1.25 mmol) was added. The reaction was refluxed for 12 h in an oil bath and monitored by TLC (Hexanes/EtOAc, 1:1, v/v), at which point the solvent was removed in vacuo and the resulting oil dissolved in EtOAc (30 mL). The organic layer was washed with 5% HCl (3 × 10 mL) and brine (3 × 10 mL), dried over $MgSO_4$, and evaporated to give 267 mg of the desired product (89%) as a yellow foam, present as a diastereomeric mixture. mp 64-66 °C. ^{1}H NMR ($CDCl_3$, 500 MHz) δ 8.25 (s, 1H), 8.21 (s, 1H), 7.97 (d, *J* = 7.6 Hz, 2H), 7.85 (d, *J* = 8.5 Hz, 1H), 7.79 (d, *J* = 8.6 Hz, 1H), 7.75-7.73 (m, 4H), 7.60-7.55 (m, 4H), 7.45-7.38 (m, 4H), 7.32-7.26 (m, 4H), 7.06-6.91 (m, 4H), 5.63-5.60 (m, 2H), 4.93-4.89 (m, 2H), 4.60-4.59 (m, 1H), 4.52-

4.50 (m, 1H), 4.36-4.34 (m, 2H), 4.30-4.21 (m, 3H), 4.15-4.11 (m, 1H), 3.89 (s, 3H), 3.87 (s, 3H), 3.01-2.89 (m, 4H), 1.71-1.68 (m, 6H). $^{13}C\{^{1}H\}$ NMR($CDCl_3$, 125 MHz) δ 161.8, 160.1, 156.0, 153.9, 146.5, 146.4, 143.0, 141.41, 141.38, 141.36, 133.98, 134.0, 129.6, 129.5, 127.8, 127.2, 125.3, 122.4, 122.3, 120.09, 120.07, 119.93, 119.90, 115.47, 115.44, 112.75, 112.71, 108.19, 96.6, 67.59, 67.57, 55.98, 55.96, 53.42, 53.41, 47.16, 47.05, 39.77, 39.70,33.76, 33.73, 31.09, 23.77, 23.73. HRMS (ESI): Calcd for $C_{33}H_{28}N_2O_8NaS$ $[M+Na]^+$, 635.1459; found: 635.1479.

Methyl N-(((9H-fluoren-9-yl)methoxy)carbonyl)-S-(1-(3-nitrodibenzo[b,d]furan-2-yl)ethyl)-D-cysteinate (**21b**). N-Fmoc-D-Cysteine methyl ester **20b** (179 mg, 0.5 mmol) and **19** (160 mg, 0.5 mmol) were dissolved in 5 mL of a mixture of DMSO/DMF/ACN/ H_2O (3:3:1:1, v/v/v/v), and then, DIPEA (0.1 mL) was added into this solution. The reaction was monitored by TLC (Hexanes/EtOAc, 5:1, v/v) and stopped after 30 min of stirring at rt by pouring the reaction mixture into H_2O (100 mL), and extraction with EtOAc (3 x 30 mL). The organic phase was washed with 100 mL of brine, and was then dried over anhydrous $MgSO_4$, evaporated to dryness, and purified by column chromatography on SiO_2 (Hexanes/EtOAc, 5:1 to 3:1, v/v) to give 160 mg (53%) of the desired product **21b**, isolated as a yellow sticky oil, as a diastereomeric mixture. ^{1}H NMR ($CDCl_3$, 500 MHz) δ 8.42 (s, 1H), 8.39 (s, 1H), 8.07-8.00 (m, 4H), 7.65-7.55 (m, 10H), 7.79-7.77 (m, 4H), 7.65-7.56 (m, 8H), 7.47-7.33 (m, 10H), 5.59 (d, *J* = 7.7 Hz, 2H), 4.90-4.84 (m, 2H), 4.62-4.58 (m, 1H), 4.56-4.52 (m, 1H), 4.43-4.36 (m, 2H), 4.32-4.24 (m, 3H), 4.19-4.12 (m, 2H), 3.80 (s, 3H), 3.74 (s, 3H), 3.01-2.87 (m, 4H), 1.76-1.73 (m, 6H). $^{13}C\{^{1}H\}$ NMR($CDCl_3$, 125 MHz) δ 170.9, 158.3, 155.65, 155.56, 153.7, 147.74, 147.69, 143.9, 143.8, 141.29, 141.27, 141.23, 136.6, 133.6, 133.5, 129.47, 129.45, 129.42, 129.25, 129.01, 128.90, 127.78, 127.70, 127.1, 125.2, 123.80, 123.78, 123.76, 122.6, 122.4, 121.83, 121.81, 121.76, 121.0, 120.9, 120.04, 120.02, 119.95, 119.21, 112.25, 112.22, 112.19, 108.4, 108.2,

67.34, 67.29, 65.9, 53.6, 53.5, 52.82, 52.80, 47.1, 47.0, 29.8, 29.5, 34.1, 34.0, 27.1, 24.8, 23.7, 23.6. HRMS (ESI): Calcd for $C_{33}H_{28}N_2NaO_7S$ $[M+Na]^+$, 619.1515; found: 619.1507.

Methyl S-(1-(3-nitrodibenzo[b,d]furan-2-yl)ethyl)-N-((S)-3,3,3-trifluoro-2-methoxy-2-phenylpropanoyl)-L-cysteinate (23a). Methyl ester **21a** (100 mg, 0.168 mmol) was dissolved in 1 mL of a mixture of DMF/piperidine (4:1, v/v). The reaction was monitored by TLC (Hexanes/EtOAc, 5:1, v/v) and stopped after 30 min of stirring at rt, the solvents were removed using a stream of air, and the crude product was purified by column chromatography on SiO_2 (Hexanes/EtOAc, 5:1, v/v, to EtOAc) to remove the byproduct and remaining starting materials. The purified product **22a** and Mosher's acid chloride [(S)-(+)-α-methoxy- α-(trifluoromethyl)phenylacetyl chloride] (51 mg, 0.2 mmol) were dissolved in 1 mL dry CH_2Cl_2, then DIEPA (0.1 mL) was added into this mixture. The reaction was monitored by TLC (Hexanes/EtOAc, 5:1, v/v) and stopped after 20 min of stirring at rt, the solvents were removed under vacuum, and the crude product was purified by column chromatography on SiO_2 (Hexanes/EtOAc, 5:1, v/v) to give 85 mg (86%) of the desired product **23a**, isolated as a yellow sticky oil. ^{1}H NMR ($CDCl_3$, 500 MHz) δ 8.43 (s, 1H), 8.36 (s, 1H), 8.09-8.06 (m, 4H), 7.66-7.52 (m, 11H), 7.48-7.41 (m, 9H), 4.88-4.76 (m, 4H), 3.77 (s, 3H), 3.69 (s, 3H), 3.44 (s, 3H), 3.42 (s, 3H), 3.09-2.99 (m, 2H), 2.94-2.88 (m, 2H), 1.77 (d, *J* = 6.9 Hz, 2H), 1.73 (d, *J* = 6.9Hz, 2H). $^{13}C\{^1H\}$ NMR($CDCl_3$, 125 MHz) δ 170.4, 170.3, 166.3, 166.2, 158.32, 158.28, 153.7, 147.8, 147.7, 133.4, 133.2, 129.6, 129.5, 129.1, 128.9, 128.6, 127.9, 123.7 (q, J = 289.9 Hz, *C*F_3), 123.81, 123.79, 122.39, 122.37, 121.9, 121.8, 121.0, 120.8, 112.25, 112.19, 108.24, 108.19, 84.13 (q, *J* = 28.0 Hz, *C*-CF_3), 83.92 (q, *J* = 28.0 Hz, *C*-CF_3), 55.1, 52.84, 52.80, 51.89, 51.83, 43.5, 39.7, 39.3, 33.7, 33.3, 23.6, 23.4. ^{19}F NMR ($CDCl_3$, 470 MHz) δ -68.9, -69.0. HRMS (ESI): Calcd for $C_{28}H_{25}F_3N_2NaO_7S$ $[M+Na]^+$, 613.1227; found: 613.1234.

S-(1-(3-nitrodibenzo[b,d]furan-2-yl)ethyl)-N-((S)-3,3,3-trifluoro-2-methoxy-2-phenylpropanoyl)-L-cysteine (24a). Ester **23a** (80 mg, 0.136 mmol) was dissolved in 1 mL of $ClCH_2CH_2Cl$, and Me_3SnOH (49 mg, 0.271 mmol) was added. The reaction was heated at 75 °C in an oil bath for 2 h and then cooled down to rt. The solvent was removed in vacuo and the resulting oil was purified by column chromatography on SiO_2 (CH_2Cl_2/CH_3OH, 100:5, v/v) to give 71 mg (91%) of the desired product **24a**, isolated as a yellow sticky oil. ^{1}H NMR ($CDCl_3$, 500 MHz) δ 8.42 (s, 1H), 8.34 (s, 1H), 8.08-8.03 (m, 4H), 7.72 (d, *J* = 7.6 Hz, 1H), 7.65-7.55 (m, 10H), 7.47-7.36 (m, 9H), 4.89-4.74 (m, 4H), 3.42 (s, 3H), 3.40 (s, 3H), 3.12-2.88 (m, 4H), 1.75 (d, *J* = 6.1 Hz, 2H), 1.71 (d, *J* = 6.4Hz, 2H). ^{13}C{^{1}H} NMR($CDCl_3$, 125 MHz) δ166.6, 166.5, 158.29, 158.25, 153.6, 147.7, 147.5, 133.4, 133.2, 131.9, 131.8, 129.60, 129.53, 129.1,129.45, 129.43, 129.1, 128.9, 128.6, 127.9, 123.7 (q, J = 289.9 Hz, *C*F_3), 123.8, 122.4, 121.9, 121.8, 121.0, 120.9, 112.16, 108.25, 108.18, 84.02 (q, *J* = 26.9 Hz, *C*-CF_3), 83.92 (q, *J* = 27.0 Hz, *C*-CF_3), 55.1, 52.0, 51.8, 39.5, 39.2, 33.4, 33.0, 29.7, 29.2, 23.5, 23.4. ^{19}F NMR ($CDCl_3$, 470 MHz) δ -68.9, -69.0. HRMS (ESI): Calcd for $C_{27}H_{22}F_3N_2O_7S$ $[M-H]^+$, 575.1105; found: 613.1085.

Methyl S-(1-(3-nitrodibenzo[b,d]furan-2-yl)ethyl)-N-((S)-3,3,3-trifluoro-2-methoxy-2-phenylpropanoyl)-D-cysteinate (23b). Methyl ester **21b** (100 mg, 0.168 mmol) was dissolved in 1 mL of a mixture of DMF/piperidine (4:1, v/v). The reaction was monitored by TLC (Hexanes/EtOAc, 5:1, v/v) and stopped after 30 min of stirring at rt, the solvents were removed using a stream of air, and the crude product was purified by column chromatography on SiO_2 (Hexanes/EtOAc, 5:1, v/v, to EtOAc) to remove the byproduct and remaining starting materials. The purified product **22b** and Mosher's acid chloride (51 mg, 0.2 mmol) were dissolved in 1 mL dry CH_2Cl_2, then DIEPA (0.1 mL) was added into this mixture. The reaction was monitored by TLC (Hexanes/EtOAc, 5:1, v/v) and stopped after 30 min of stirring at rt, the solvents were under vacuum, and the crude product was purified by column chromatography on SiO_2 (Hexanes/EtOAc, 5:1, v/v) to give 80 mg (81%) of the desired product **23b**, isolated as a yellow

sticky oil. ^{1}H NMR ($CDCl_3$, 500 MHz) δ 8.35 (s, 1H), 8.31 (s, 1H), 8.04-8.00 (m, 4H), 7.65-7.57 (m, 9H), 7.51 (d, *J* = 7.9 Hz, 1H), 7.46-7.38 (m, 10H), 4.88-4.70 (m, 4H), 3.79 (s, 3H), 3.72 (s, 3H), 3.51 (s, 6H), 3.01-2.96 (m, 2H), 2.88-2.82 (m, 2H), 1.68 (d, *J* = 6.9 Hz, 2H), 1.65 (d, *J* = 6.9Hz, 2H). ^{13}C{^{1}H} NMR($CDCl_3$, 125 MHz) δ 170.4, 170.3, 166.4, 166.3, 158.29, 158.26, 153.6, 147.67, 147.65, 133.24, 133.15, 132.42, 132.39, 129.6, 129.5, 129.0, 128.8, 128.49, 128.47, 127.8, 127.6, 123.62 (q, *J* = 290.0 Hz, *C*F_3), 123.60 (q, *J* = 290.2 Hz, *C*F_3),123.81, 123.79, 122.35, 122.34, 121.9, 121.7, 120.9, 120.8, 112.26, 112.20, 108.24, 108.19, 84.0 (q, *J* = 26.4 Hz, *C*-CF_3), 83.9 (q, *J* = 26.4 Hz, *C*-CF_3), 55.19, 55.18, 52.88, 52.86, 51.92, 51.39, 39.6, 39.2, 33.7, 33.3, 23.5, 23.4. ^{19}F NMR ($CDCl_3$, 470 MHz) δ -68.8, -68.9. HRMS (ESI): Calcd for $C_{28}H_{25}F_3N_2NaO_7S$ $[M+Na]^+$, 613.1227; found: 613.1250.

S-(1-(3-nitrodibenzo[b,d]furan-2-yl)ethyl)-N-((S)-3,3,3-trifluoro-2-methoxy-2-phenylpropanoyl)-D-cysteine (24b). Ester **23b** (80 mg, 0.136 mmol) was dissolved in 1 mL of $ClCH_2CH_2Cl$, and Me_3SnOH (49 mg, 0.271 mmol) was added. The reaction was heated at 75 °C in an oil bath for 2 h and then cooled down to rt. The solvent was removed in vacuo and the resulting oil was purified by column chromatography on SiO_2 (CH_2Cl_2/CH_3OH, 100:5, v/v) to give 69 mg (90%) of the desired product **24b**, isolated as a yellow sticky oil. ^{1}H NMR ($CDCl_3$, 500 MHz) δ 8.31 (s, 1H), 8.28 (s, 1H), 8.03-7.90 (m, 4H), 7.60-7.52 (m, 11H), 7.41-7.36 (m, 9H), 4.78-4.74 (m, 4H), 3.46 (s, 6H), 3.02-2.99 (m, 2H), 2.89-2.85 (m, 2H), 1.64 (d, *J* = 4.9 Hz, 2H), 1.60 (d, *J* = 5.6Hz, 2H). ^{13}C{^{1}H} NMR($CDCl_3$, 125 MHz) δ 166.6, 158.23, 158.19, 153.6, 147.56, 147.49, 133.3, 133.2, 132.41, 130.9, 129.52, 129.46, 129.41, 129.39, 128.89, 128.81, 128.79, 128.45, 128.44, 127.81,127.69, 123.2 (q, *J* = 292.0 Hz, *C*F_3), 123.7, 122.4, 121.9, 121.8, 120.9, 120.8, 112.1, 108.2, 84.0 (q, *J* = 25.9 Hz, *C*-CF_3), 83.8 (q, *J* = 26.3 Hz, *C*-CF_3), 55.18, 52.27, 51.66, 39.5, 39.2, 33.6, 33.1, 30.9, 23.4, 23.3. ^{19}F NMR ($CDCl_3$, 470 MHz) δ -68.79, -68.81. HRMS (ESI): Calcd for $C_{27}H_{22}F_3N_2O_7S$ $[M-H]^+$, 575.1105; found: 575.1118.

General Procedure for Solid-Phase Peptide Synthesis (SPPS). Peptides were synthesized using an automated solid-phase peptide synthesizer (PS3, Protein Technologies Inc., Memphis, TN) employing Fmoc/HCTU-based chemistry. Fmoc-Met-Wang or Fmoc-Ala-Wang resin (0.03 mmol) was placed in the reaction vessel and deprotected twice using 20% piperidine in dimethylformamide (DMF) for 5 min each time. Four equivalents of amino acids and HCTU were activated in 0.4 M N-methylmorpholine (NMM) for 1 min before adding to the resin. Standard incubation time for each coupling was 20 min. Manual coupling of caged Fmoc-Cys derivatives was performed in a polypropylene filter syringe equipped with a polypropylene stopcock. Four equivalents of the protected cysteine were activated with 4 equivalents of HCTU in 1 mL 0.4 M NMM for 10 min before adding to the resin. The reaction completion was tested every hour using a ninhydrin assay.[30] All caged Fmoc-Cys derivatives required 4 h for completion. Once the ninhydrin assay confirmed the absence of any free amines, the resin was washed thoroughly with DMF before placing back on the synthesizer and resuming the synthesis as previously described. Once complete, approximately half of the resin was transferred to a syringe filter and washed three times with CH_2Cl_2. Global deprotection and resin cleavage was accomplished via treatment with 5 mL reagent K (82.5% TFA, 5% phenol, 5% water, 5% thioanisole, and 2.5 % ethanedithiol) for 2 h. Cleaved peptides were precipitated with Et_2O and centrifuged before decanting the Et_2O layer (repeated 3 times total). The resulting crude peptide was dried via a stream of dry N_2, then dissolved in 8 mL of a mixture of H_2O/CH_3CN (1:1, v/v) containing 0.1% TFA, aided by sonication. The solution was filtered using a 0.2 μm PTFE filter and then purified using preparative reverse-phase (RP)-HPLC. Once pure peptides were obtained, their concentrations were quantified in solution using the ε_{350} value measured for the caged Fmoc-Cys derivatives (**1**, **2** or Fmoc-Cys(NV)-OH). Stock solutions were generated by dilution in H_2O/CH_3CN (1:1, v/v) containing 0.1% TFA to a final concentration of 300 μM and stored at -20 °C.

NH_2-YIIKGVFWDPAC(MeO-NDBF)VIA-OH (10). ESI-MS calcd for $C_{98}H_{136}N_{18}O_{23}S$ $[M+2H]^{2+}$ 982.9883, found 982.9879. 33.6 mg were obtained after cleavage of approximately half of the resin.

NH_2-YIIKGVFWDPAC(NDBF)VIA-OH (11). ESI-MS. calcd for $C_{97}H_{134}N_{18}O_{22}S$ $[M+2H]^{2+}$ 967.9854, found 967.9826. 19.0 mg were obtained after cleavage of approximately half of the resin.

NH_2-YIIKGVFWDPAC(NV)VIA-OH (12). ESI-MS. calcd for $C_{92}H_{134}N_{18}O_{23}S$ $[M+2H]^{2+}$ 945.9829, found 945.9790. 10.5 mg were obtained after cleavage of approximately half of the resin.

NH_2-KKKSKTKC(MeO-NDBF)VIM-OH (15). ESI-MS. calcd for $C_{71}H_{121}N_{17}O_{18}S_2$ $[M+2H]^{2+}$ 781.9253, found 781.9243. 17.7 mg were obtained after cleavage of approximately half of the resin.

NH_2-KKKSKTKC(NDBF)VIM-OH (16). ESI-MS. calcd for $C_{70}H_{119}N_{167}O_{17}S_2$ $[M+2H^{2+}$ 766.9200, found 766.9193. 9.0 mg obtained after cleavage of approximately half of the resin.

Model Tripeptide NH_2-GC(NDBF)F-OH (18). Peptide **18** was synthesized manually on a 0.01 mmol scale using the conditions described in the General Procedure for Solid-Phase Peptide Synthesis (SPPS) section. Compound **2** (6 equiv) along with PyBOP, HOAT, and DIEA (6 equiv each) were dissolved in DMF at 50 mM concentration and coupled to Phe-Wang resin for 1 h. After synthesis, a small amount of the peptide was cleaved from resin using 95% TFA with 2.5% CH_2Cl_2 and 2.5% H_2O for 20 min. The solvent was then removed using a gentle stream of dry N_2, which took approximately 40 min. The resulting residue was brought to dryness using a rotary evaporator. DMF (200 µL) was used to dissolve the peptide and the

solution was filtered using a GHP filter before acquiring a LC-MS chromatogram with single ion monitoring to observe the epimerized product. The gradient consisted of an isocratic hold at 1% buffer A for 10 min to fully remove the DMF, followed by a 1-100% gradient over 100 min (1% increase per min). The remaining resin was incubated in 6 mL of 20% piperidine in DMF for 2 h to simulate 12 coupling steps in the synthesis of a full dodecapeptide and another LC-MS chromatogram was obtained as before to probe for epimerization. ESI-MS. calcd for $C_{12}H_{29}N_4O_7S$ $[M+H]^+$ 565.2, found 565.2.

Coupling Optimization on Complete Peptides to Reduce Epimerization. Peptide **10** was synthesized on a 0.01 mmol scale using procedure described in the General Procedure for Solid-Phase Peptide Synthesis (SPPS) section. However, compound **1** (4 equiv) was coupled using 4 equiv of N,N'-Diisopropylcarbodiimide (DIC) and 6-Chloro-1-hydroxybenzotriazole (Cl-HOBT) in DMF at 150 mM concentration for 1 h. Peptide **15** was synthesized on the same scale, but using 4 equiv of Benzotriazole-1-yl-oxy-tris-pyrrolidino-phosphonium hexafluorophosphate (PyBOP), 1-Hydroxy-7-azabenzotriazole (HOAT), and N,N-diisopropylethylamine (DIEA) for 30 min. LC-MS chromatograms with single ion monitoring were acquired using an isocratic hold at 1% buffer A for 5 min, followed by a 1-100% gradient over 100 min (1% increase per min).

General Procedure for UV Photolysis of Caged Peptides in Rayonet Reactor. Peptides were diluted in 50 mM sodium phosphate buffer (PB), pH 7.4 containing 1 mM DTT to a final concentration of 100 μM. The solutions were transferred into the quartz tubes and irradiated in using 14 x 350 nm bulbs (14 W, RPR-3500 Å). Aliquots (50 μL) were withdrawn at various intervals ranging from 0 to 30 sec (up to 240 sec for peptide **12**), and 40 μL were subjected to LC-MS analysis. It is important to note that photolysis in H_2O/CH_3CN (1:1, v/v) containing 0.1% TFA or in PB buffer containing 1 mM DTT led to production of compounds with an m/z corresponding to the desired free thiols + 32 mass units, believed to be the

corresponding sulfinic acid (Figure S4A-B). Photolysis in PB buffer containing 15 mM DTT showed only the desired free thiols (Figure S4C-D).

General Procedure for UV Photolysis of Caged Peptides in LED Reactor. Photolysis was conducted in a home-built LED reactor equipped with 8 X 350 nm LEDs (FoxUV, 5.5mm) evenly spaced in a radial arrangement. A round quartz tube (10 x 50 mm) with 1 mm wall thickness was positioned in the middle of the reactor. 200 µL of solution was used for photolysis, resulting in an irradiated surface area of 1 cm^2. Kinetic analyses were performed using caged peptides diluted in 50 mM sodium phosphate buffer (PB), pH 7.4 containing 15 mM DTT to a final concentration of 10 µM. At this concentration, > 90% transmittance occurs, thereby minimizing any inter-filter effect. The samples were irradiated for varying amounts of time ranging from 0 to 90 sec (180 to 1080 for peptide **12**), and then 100 µL aliquots were subjected to LC-MS analysis with UV monitoring at 350 nm and MS scanning over a 500-2000 m/z window. The gradient was isocratic at 1% buffer A for 5 min, followed by a 1-100% gradient over 10 min (10% increase per min). Peaks exhibiting the m/z of the caged peptide were integrated in the UV chromatogram, and the amount of remaining caged peptide was calculated using the formula: *Remaining SM (%) = (Peak area after irradiation)/(Peak area of unirradiated sample)*100*. The quantum yield of uncaging (Φ) in mols/ein was calculated using the relationship $\Phi = (I\sigma t_{90})^{-1}$, where I is the irradiation intensity in ein·cm^{-2}.sec^{-1}, σ is the decadic extinction coefficient in cm^2·mol (1000·ε), and t_{90} is the irradiation time in seconds required to achieve 90% uncaging.[31] The intensity (I) at 350 nm was measured to be 1.93E-09 ein·cm^{-2}.sec^{-1} via actinometry using 6 mM potassium ferrioxalate as a standard.[32]

Laser apparatus for Two-Photon (TP) irradiation: For the two-photon kinetic experiments, a home-built regeneratively amplified Ti:Sapphire laser operating at 1 kHz with the

pulse power maintained between 68 – 76 mW centered around 800 nm was used. Each pulse had a Gaussian profile with a full width at half maximum of 80 fs. This system is described in detail elsewhere.[33] The beam was sent through a 35 cm focusing lens and then through the sample. Samples (30 μL) were irradiated in a quartz microcuvette (Starna 16.10-Q-10/Z15, 1 mm x 1 mm sample window, 10 mm path length) 15 cm after the focal plane of the lens.

General Procedure for Two-Photon Photolysis of Caged Peptides at 800 nm. Samples were irradiated in a 30 μL quartz cuvette (Starna Cells Corp.). The TP action cross-sections for **10**, **11**, and **15** were measured by comparing the photolysis rates of the peptides with that of BhcOAc as a reference (δ_u = 0.45 at 800 nm). Aliquots (30 μL) containing peptides (100 μM in H_2O/CH_3CN (1:1, v/v) containing 0.1% TFA) were irradiated with the 800 nm laser system for varying amounts of time, ranging from 2.5 to 30 min. Each sample was analyzed by LC-MS using the previously described method. BhcOAc photolysis experiments were conducted in the same manner using a 100 μM solution in 50 mM PB, pH 7.4. Reaction progress data were analyzed as described above, and the first-order decay constants for the two compounds were calculated from by fitting to a first order exponential decay process.[18]

UV and TP-Triggered Enzymatic Reactions. A 7.5 μM solution of peptide **10** was prepared in prenylation buffer (50 mM PB, pH 7.4, 15 mM DTT, 10 mM $MgCl_2$, 50 μM $ZnCl_2$, 20 mM KCl, and 22 μM FPP) and divided into three 50 μL aliquots. Yeast PFTase was added to the first aliquot to give a final concentration of 50 nM, but the resulting sample was not subjected to photolysis. The second aliquot was irradiated in the absence of yeast PFTase, while the third sample was supplemented with yeast PFTase (50 nM) and then photolyzed with UV light using the Rayonet reactor. UV photolysis was conducted for 30 sec at 350 nm as described above using three light bulbs. Each sample was incubated for 90 min at rt to allow the enzymatic reaction to proceed and then the entire sample was analyzed by LC-MS using the

gradient described above, and detected with single ion monitoring (SIM) for the $[M+H]^{+1}$, $[M+2H]^{+2}$, and $[M+3H]^{+3}$ charged states for the caged peptide (1967.9, 982.9, 655.6), the free thiol peptide (1694.9, 847.4, 565.3), and the farnesylated peptide (1900.1, 950.5, 634.0), respectively. The TP experiments were performed in an analogous manner using peptide **10** at identical concentrations as the UV experiment, but using 30 µL aliquots (due to the 30 uL cuvette size). Samples used initially to generate either the free thiol (**13**) or farnesylated product (**14**) were irradiated for 10 min. Samples used to generate the farnesylated product as a function of time were irradiated for varying amounts ranging between 0 and 25 min. The percent remaining starting material was determined by integrating the SIM peaks for the starting peptide (**10**) and farnesylated product (**14**) and inputting into the following formula: *Remaining SM (%) = (SIM of **10**)/[(SIM of **10**) + (SIM of **14**)]*100.*

ASSOCIATED CONTENT

Supporting Information

Additional Figures; Tables of ions observed via LC-MS/MS for protected peptides; ^{1}H NMR, ^{13}C NMR and ^{19}F NMR, for all new compounds; ESI-MS and analytical HPLC chromatograms for reported peptides. This material is available free of charge via the

Internet at http://pubs.acs.org.

AUTHOR INFORMATION

Corresponding Author

*E-mail: Diste001@umn.edu (M.D.D.).

Notes

The authors declare no competing financial interest.

ACKNOWLEDGEMENTS

The authors thank Drs. Matt Hammers and Andrew Healy for valuable consultations. We acknowledge the Mass Spectrometry Core Facility of the Masonic Cancer Center, a comprehensive cancer center designated by the National Cancer Institute, supported by P30 CA77598, where the LC-MS/MS analysis was performed. This work was supported by the National Institute of General Medical Sciences, including R01 GM084152, R21 CA185783 and NSF/CHE 1905204 to M.D.D.

REFERENCES

(1) Haugaard, N. Reflections on the Role of the Thiol Group in Biology. *Annals of the New York Academy of Sciences* **2000**, *899*, 148-158.
(2) Couvertier, S. M.; Zhou, Y.; Weerapana, E. Chemical-proteomic strategies to investigate cysteine posttranslational modifications. *Biochim. Biophys. Acta-Prot. Proteom.* **2014**, *1844*, 2315-2330.
(3) Poole, L. B. The basics of thiols and cysteines in redox biology and chemistry. *Free Radic. Biol. Med.* **2015**, *80*, 148-157.
(4) Klán, P.; Šolomek, T.; Bochet, C. G.; Blanc, A.; Givens, R.; Rubina, M.; Popik, V.; Kostikov, A.; Wirz, J. Photoremovable Protecting Groups in Chemistry and Biology: Reaction Mechanisms and Efficacy. *Chem. Rev.* **2013**, *113*, 119-191.
(5) Shao, Q.; Xing, B. Photoactive molecules for applications in molecular imaging and cell biology. *Chem. Soc. Rev.* **2010**, *39*, 2835-2846.
(6) Silva, J. M.; Silva, E.; Reis, R. L. Light-triggered release of photocaged therapeutics - Where are we now? *Journal of Controlled Release* **2019**, *298*, 154-176.
(7) Uprety, R.; Luo, J.; Liu, J.; Naro, Y.; Samanta, S.; Deiters, A. Genetic encoding of caged cysteine and caged homocysteine in bacterial and mammalian cells. *ChemBioChem* **2014**, *15*, 1793-1799.
(8) Ellis-Davies, G. C. R. Two-Photon Uncaging of Glutamate. *Frontiers in Synaptic Neuroscience* **2019**, *10*, 48.
(9) Isidro-Llobet, A.; Álvarez, M.; Albericio, F. Amino Acid-Protecting Groups. *Chem. Rev.* **2009**, *109*, 2455-2504.
(10) Kaplan, J. H.; Forbush, B.; Hoffman, J. F. Rapid photolytic release of adenosine 5'-triphosphate from a protected analog: utilization by the sodium:potassium pump of human red blood cell ghosts. *Biochemistry* **1978**, *17*, 1929-1935.
(11) Chang, C.-y.; Niblack, B.; Walker, B.; Bayley, H. A photogenerated pore-forming protein. *Chem. Biol.* **1995**, *2*, 391-400.
(12) DeGraw, A. J.; Hast, M. A.; Xu, J.; Mullen, D.; Beese, L. S.; Barany, G.; Distefano, M. D. Caged Protein Prenyltransferase Substrates: Tools for Understanding Protein Prenylation. *Chem. Biol. Drug Des.* **2008**, *72*, 171-181.
(13) Nguyen, D. P.; Mahesh, M.; Elsässer, S. J.; Hancock, S. M.; Uttamapinant, C.; Chin, J. W. Genetic Encoding of Photocaged Cysteine Allows Photoactivation of TEV Protease in Live Mammalian Cells. *J. Am. Chem. Soc.* **2014**, *136*, 2240-2243.

(14) Karas, J. A.; Scanlon, D. B.; Forbes, B. E.; Vetter, I.; Lewis, R. J.; Gardiner, J.; Separovic, F.; Wade, J. D.; Hossain, M. A. 2-nitroveratryl as a photocleavable thiol-protecting group for directed disulfide bond formation in the chemical synthesis of insulin. *Chemistry* **2014**, *20*, 9549-9552.
(15) Furuta, T.; Wang, S. S. H.; Dantzker, J. L.; Dore, T. M.; Bybee, W. J.; Callaway, E. M.; Denk, W.; Tsien, R. Y. Brominated 7-hydroxycoumarin-4-ylmethyls: photolabile protecting groups with biologically useful cross-sections for two photon photolysis. *Proc. Nat. Acad. Sci. USA* **1999**, *96*, 1193-1200.
(16) Momotake, A.; Lindegger, N.; Niggli, E.; Barsotti, R. J.; Ellis-Davies, G. C. The nitrodibenzofuran chromophore: a new caging group for ultra-efficient photolysis in living cells. *Nat. Methods* **2006**, *3*, 35-40.
(17) Zhu, Y.; Pavlos, C. M.; Toscano, J. P.; Dore, T. M. 8-Bromo-7-hydroxyquinoline as a Photoremovable Protecting Group for Physiological Use: Mechanism and Scope. *J. Am. Chem. Soc.* **2006**, *128*, 4267-4276.
(18) Mahmoodi, M. M.; Abate-Pella, D.; Pundsack, T. J.; Palsuledesai, C. C.; Goff, P. C.; Blank, D. A.; Distefano, M. D. Nitrodibenzofuran: a One- and Two-Photon Sensitive Protecting Group that is Superior to Brominated Hydroxycoumarin for Thiol Caging in Peptides. *J. Am. Chem. Soc.* **2016**, *138*, 5848-5859.
(19) Wosnick, J. H.; Shoichet, M. S. Three-dimensional Chemical Patterning of Transparent Hydrogels. *Chem. Mater.* **2007**, *20*, 55-60.
(20) Kotzur, N.; Briand, B.; Beyermann, M.; Hagen, V. Wavelength-Selective Photoactivatable Protecting Groups for Thiols. *J. Am. Chem. Soc.* **2009**, *131*, 16927-16931.
(21) Abate-Pella, D.; Zeliadt, N. A.; Ochocki, J. D.; Warmka, J. K.; Dore, T. M.; Blank, D. A.; Wattenberg, E. V.; Distefano, M. D. Photochemical Modulation of Ras-Mediated Signal Transduction using Caged Farnesyltransferase Inhibitors: Activation via One- and Two-Photon Excitation. *ChemBioChem* **2012**, *13*, 1009-1016.
(22) Aujard, I.; Benbrahim, C.; Gouget, M.; Ruel, O.; Baudin, J.-B.; Neveu, P.; Jullien, L. o-Nitrobenzyl Photolabile Protecting Groups with Red-Shifted Absorption: Syntheses and Uncaging Cross-Sections for One- and Two-Photon Excitation. *Chemistry – A European Journal* **2006**, *12*, 6865-6879.
(23) LoPachin, R. M.; Gavin, T. Molecular mechanisms of aldehyde toxicity: a chemical perspective. *Chem. Res. Tox.* **2014**, *27*, 1081-1091.
(24) Xue, C.-B.; Becker, J. M.; Naider, F. Efficient Regioselective Isoprenylation of Peptides in Acidic Aqueous Solution using Zinc Acetate as Catalyst. *Tetrahedron. Lett.* **1992**, *33*, 1435-1438.
(25) Nicolaou, K. C.; Estrada, A. A.; Zak, M.; Lee, S. H.; Safina, B. S. A Mild and Selective Method for the Hydrolysis of Esters with Trimethyltin Hydroxide. *Angew. Chem. Int. Ed.* **2005**, *44*, 1378-1382.
(26) Molina, R. S.; Tran, T. M.; Campbell, R. E.; Lambert, G. G.; Salih, A.; Shaner, N. C.; Hughes, T. E.; Drobizhev, M. Blue-Shifted Green Fluorescent Protein Homologues Are Brighter than Enhanced Green Fluorescent Protein under Two-Photon Excitation. *J. Phys. Chem. Lett.* **2017**, *8*, 2548-2554.
(27) Palsuledesai, C. C.; Distefano, M. D. Protein prenylation: enzymes, therapeutics and biotechnology applications. *ACS Chem. Biol.* **2015**, *10*, 51-62.
(28) Kohl, N. E.; Omer, C. A.; Conner, M. W.; Anthony, N. J.; Davide, J. P.; deSolms, S. J.; Giuliani, E. A.; Gomez, R. P.; Graham, S. L.; Hamilton, K. Inhibition of farnesyltransferase induces regression of mammary and salivary carcinomas in ras transgenic mice. *Nat. Med.* **1995**, *1*, 792-797.
(29) Berndt, N.; Hamilton, A. D.; Sebti, S. Ø. M. Targeting protein prenylation for cancer therapy. *Nat Rev Cancer* **2011**, *11*, 775-791.

(30) Kaiser, E.; Colescott, R. L.; Bossinger, C. D.; Cook, P. I. Color test for detection of free terminal amino groups in the solid-phase synthesis of peptides. *Anal. Biochem.* **1970**, *34*, 595-598.
(31) Tsien, R. Y.; Zucker, R. S. Control of cytoplasmic calcium with photolabile tetracarboxylate 2-nitrobenzhydrol chelators. *Biophys, J.* **1986**, *50*, 843-853.
(32) Hatchard, C. G.; Parker, C. A.; Bowen, E. J. A new sensitive chemical actinometer - II. Potassium ferrioxalate as a standard chemical actinometer. *Proc. R. Soc. Lond. A.* **1956**, *235*, 518-536.
(33) Underwood, D. F.; Blank, D. A. Ultrafast Solvation Dynamics: A View from the Solvent's Perspective Using a Novel Resonant-Pump, Nonresonant-Probe Technique. *J. Phys. Chem. A* **2003**, *107*, 956-961.

TOC Graphic

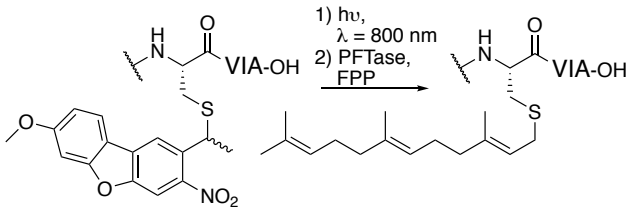

Supporting Information

A methoxy-substituted nitrodibenzofuran-based protecting group with an improved two-photon action cross-section for thiol protection in solid phase peptide synthesis

Taysir K. Bader,[†] Feng Xu,[†] Michael H. Hodny, David A. Blank and Mark D. Distefano[*]

Department of Chemistry, University of Minnesota, Minneapolis, MN 55455, USA

[†]Both authors contributed equally to this work.

*Corresponding Author

E-mail: diste001@umn.edu

Table of Contents

Additional Figures and Tables (cited in text)

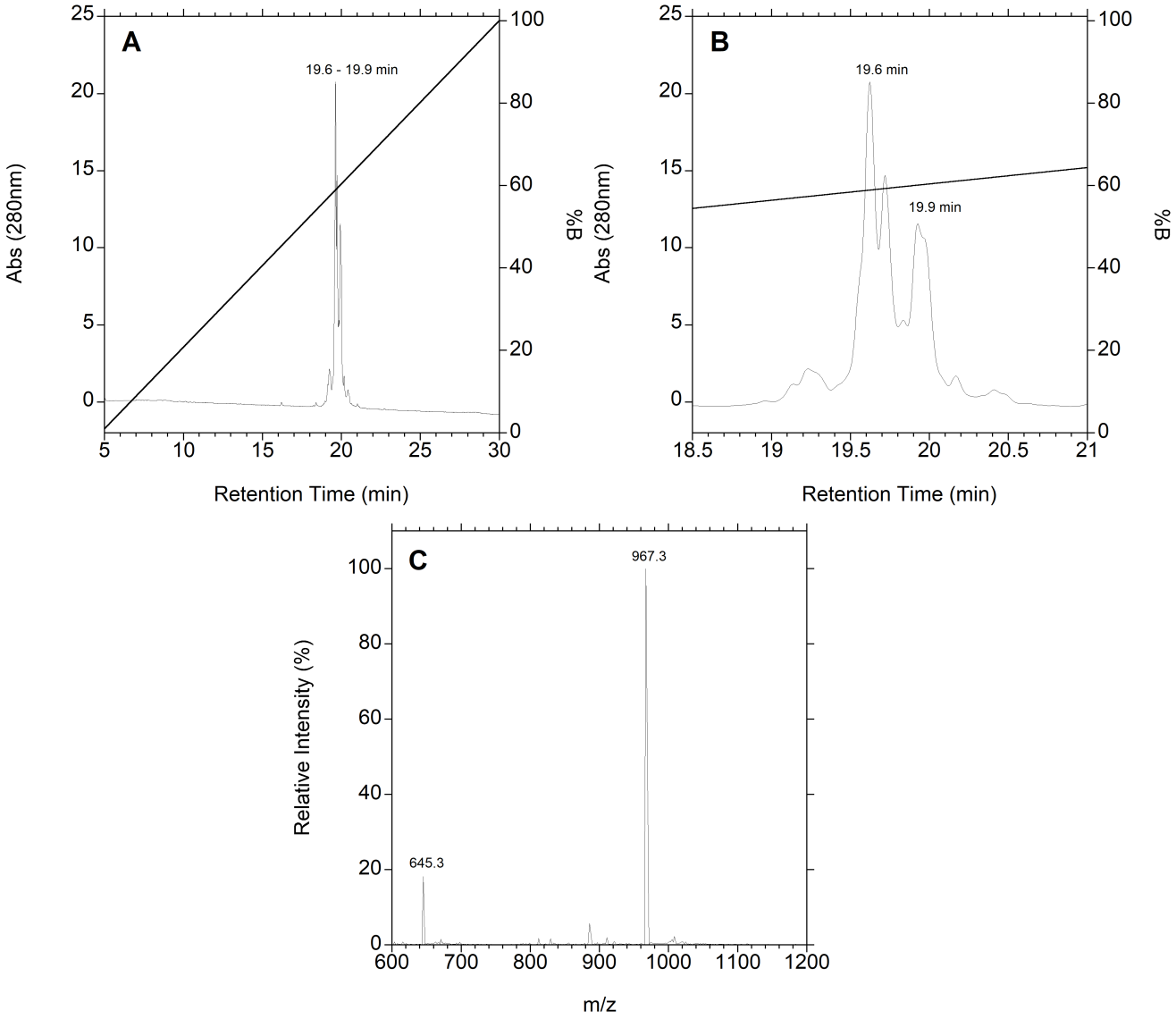

Figure S1. LC-MS analysis of a-Factor-C(NDBF)-VIA (**11**) before purification. **A**. UV monitoring at 280 nm. **B.** Expanded region highlighting split peak pattern. The double peak centered at 19.6 minutes is attributed to the product containing L-Cys, while the double peak centered at 19.9 min is believed to from the epimerized product containing D-Cys. Each of those peaks is doubled due to the presence of an epimeric mixture at the 3 position of the NBDF group resulting from the stereogenic center due to the presence of the methyl group at that position. **C.** Extracted Mass Spectrum of TIC chromatogram of all peaks. $[M+2H]^{+2}$, and $[M+3H]^{+3}$ are indicated.

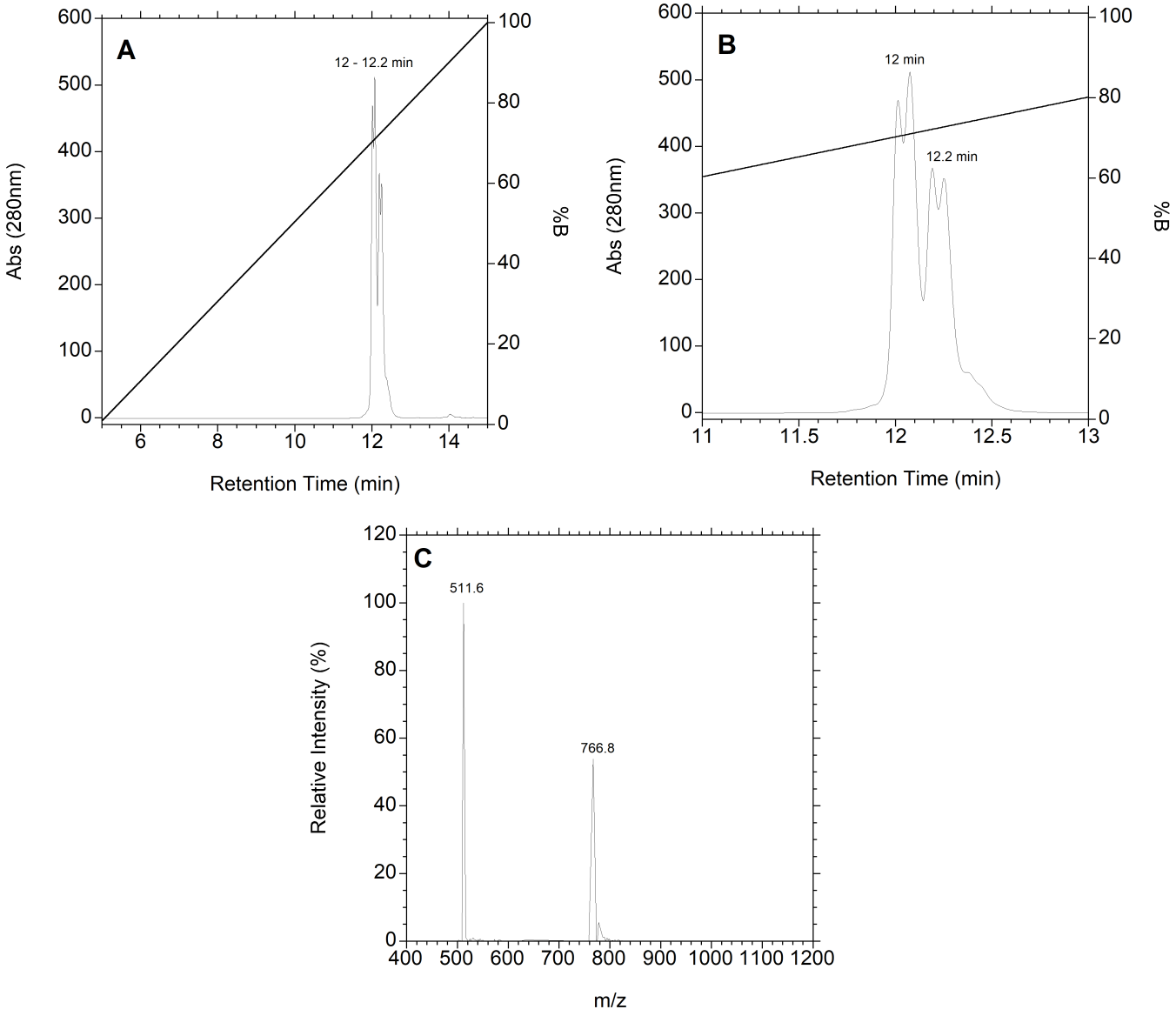

Figure S2. LC-MS analysis of K-Ras-C(NDBF)-VIA (**16**) before purification. **A**. UV monitoring at 280 nm. **B.** Expanded region highlighting the split peak pattern. The double peak centered at 12.0 minutes is attributed to the product containing L-Cys, while the double peak centered at 12.2 min is believed to from the epimerized product containing D-Cys. Each of those peaks is doubled due to the presence of an epimeric mixture at the 3 position of the NBDF group resulting from the stereogenic center due to the presence of the methyl group at that position. **C.** Extracted Mass Spectrum of TIC chromatogram of all peaks. $[M+2H]^{+2}$, and $[M+3H]^{+3}$ are indicated.

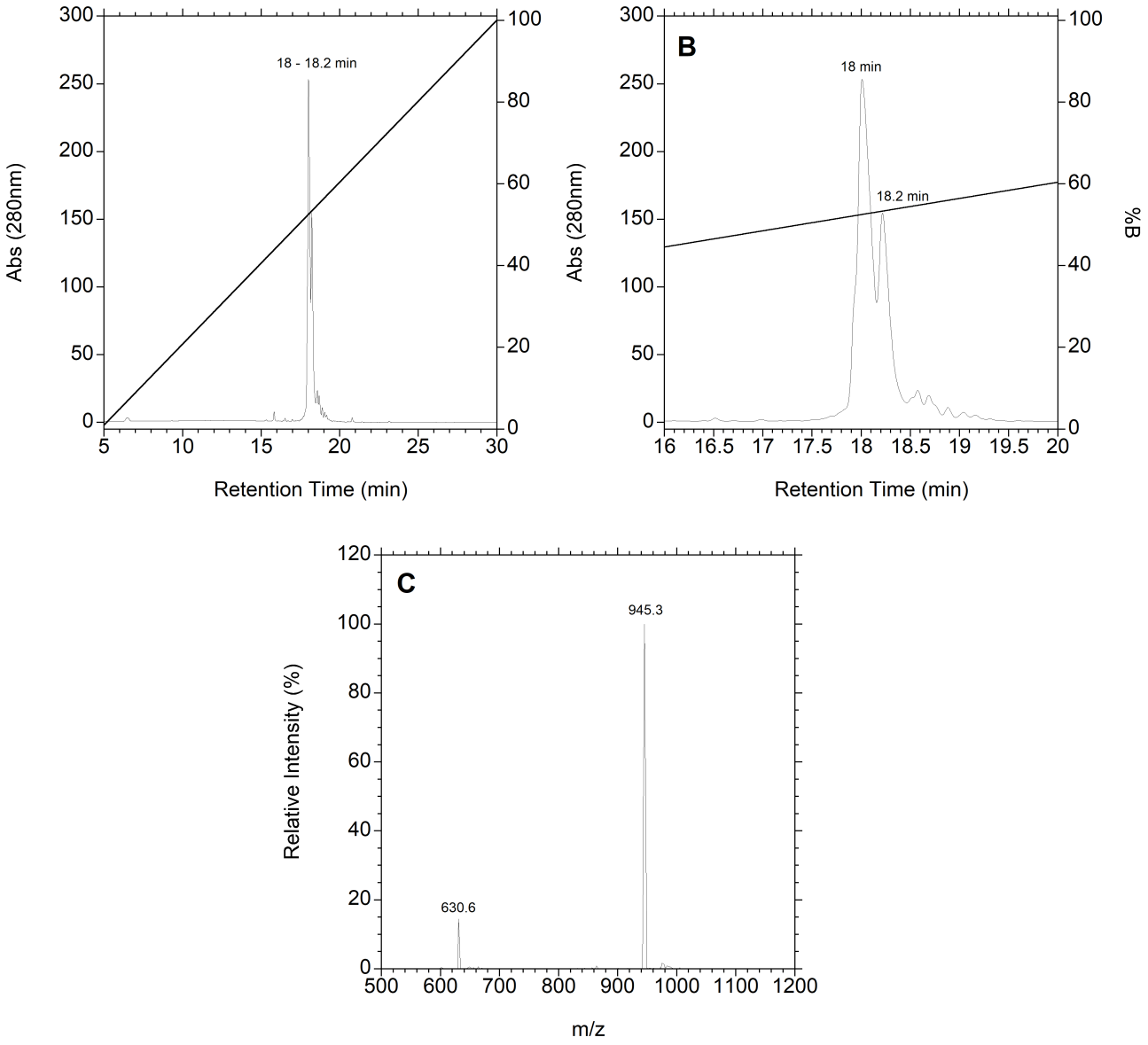

Figure S3. LC-MS analysis of a-Factor-C(NV)-VIA (**12**) before purification. **A**. UV monitoring at 280 nm. **B.** Expanded region highlighting two peaks observed instead of four as was observed in the NDBF derivative. The single peak centered at 18.0 minutes is attributed to the product containing L-Cys, while the single peak centered at 18.2 min is believed to from the epimerized product containing D-Cys. Each of those peaks is not doubled since the NV group lacks the stereogenic center present in NDBF. **C.** Extracted Mass Spectrum of TIC chromatogram of all peaks. $[M+2H]^{+2}$, and $[M+3H]^{+3}$ are indicated.

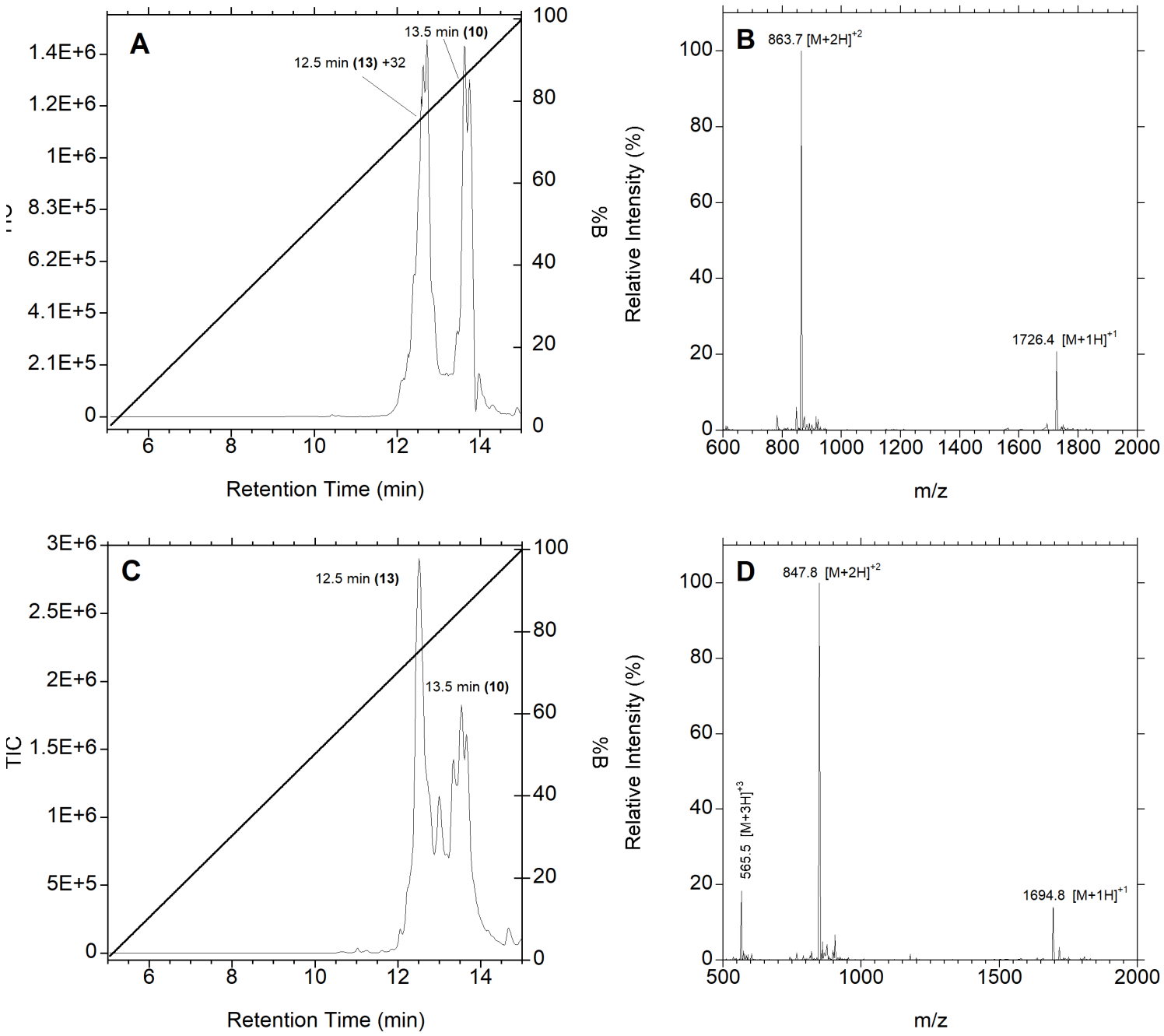

Figure S4. Effect of DTT on oxidation state of uncaged free thiol after photolysis. Top panels correspond to peptide (**10**) at 100 μM after UV irradiation for 20 seconds in 50 mM sodium PB with 1 mM DTT. A peak at 12.5 min appeared in the TIC (**A**) after irradiation, and the corresponding mass spectrum (**B**) showed the mass of peptide (**13**) + 32 mass units, believed to be the resulting oxidized sulfinic acid. Bottom two panels show the same peptide irradiated in the presence of 15 mM DTT for 30 seconds. The retention time of the resulting product is still similar in the TIC (**C**), but the corresponding mass spectrum shows only the non-oxidized thiol (**D**).

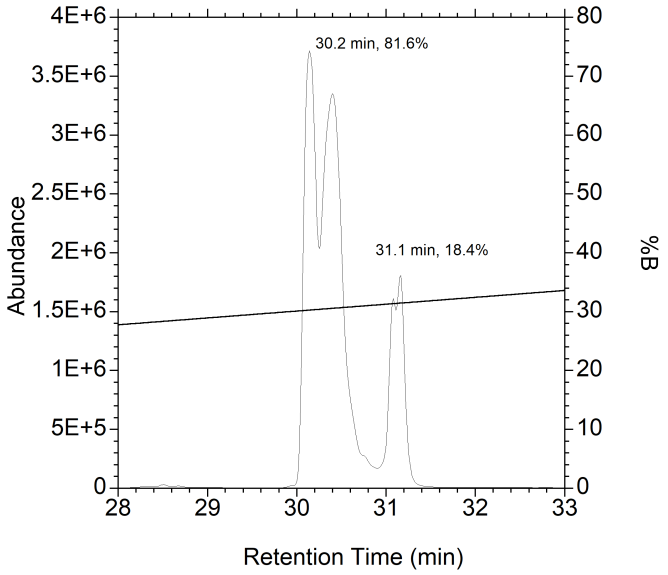

Figure S5. Analysis of a-Factor prepared using coupling conditions described by Karas et al. for N-Fmoc-L-Cys(NV)-OH. LC-MS analysis of peptide **10** synthesized using 4 equiv of N-Fmoc-L-C(MeO-NDBF)-OH (**1**) with 4 equiv DIC and Cl-HOBT at 150 mM for 1 h. A significant amount of the epimeric product containing D-Cys is clearly visible at 31.1 min.

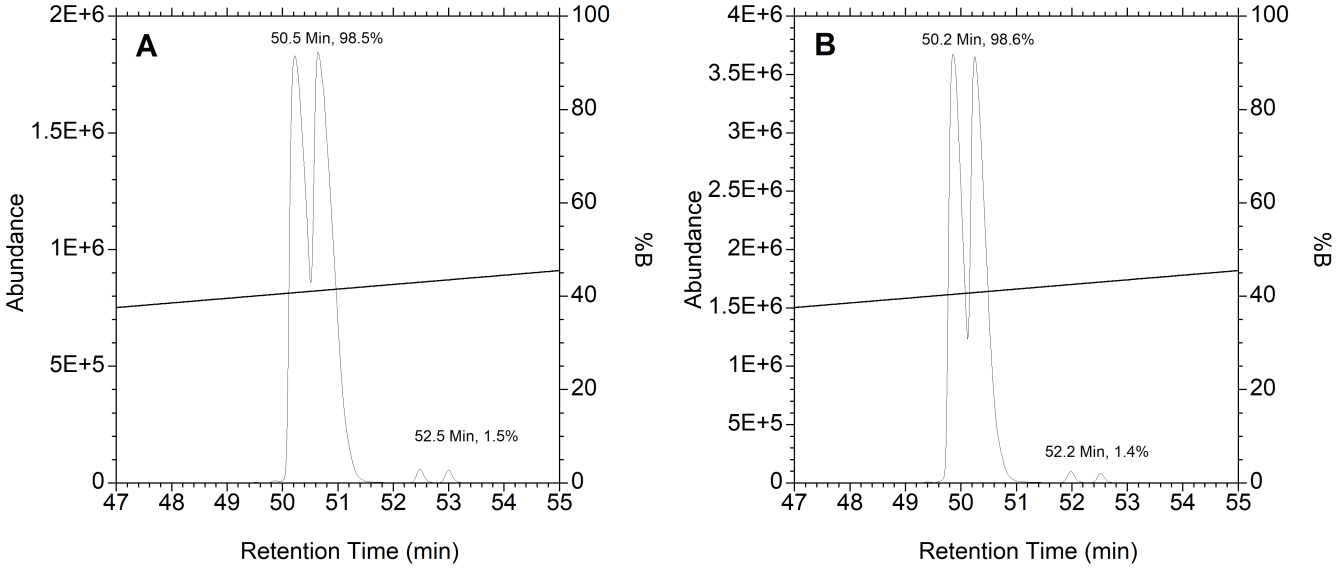

Figure S6. Analysis of extended piperidine treatment on tripeptide GC(NDBF)F (**18**). LC-MS analysis of resin-bound GC(NDBF)F (**18**) before (A) and after (B) incubation with 20% piperidine in DMF for 2 h to duplicate the 12 deprotection steps involved in full length peptide synthesis of a-Factor. No significant change in the ratio of the epimers was observed.

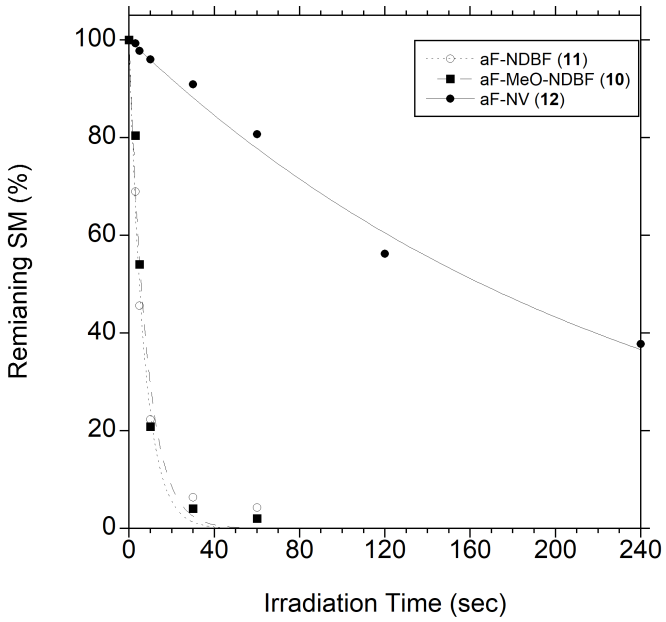

Figure S7. Kinetic analysis of photolysis of a-Factor-based peptides (**10**, **11** and **12**,) using a Rayonet reactor equipped with fourteen 350 nm bulbs.

Figure S8. Photolysis apparatus equipped with eight 350 nm LEDs arranged in a radial manner. Left: Apparatus without top. Right: Apparatus with top showing reaction tube inserted into the center.

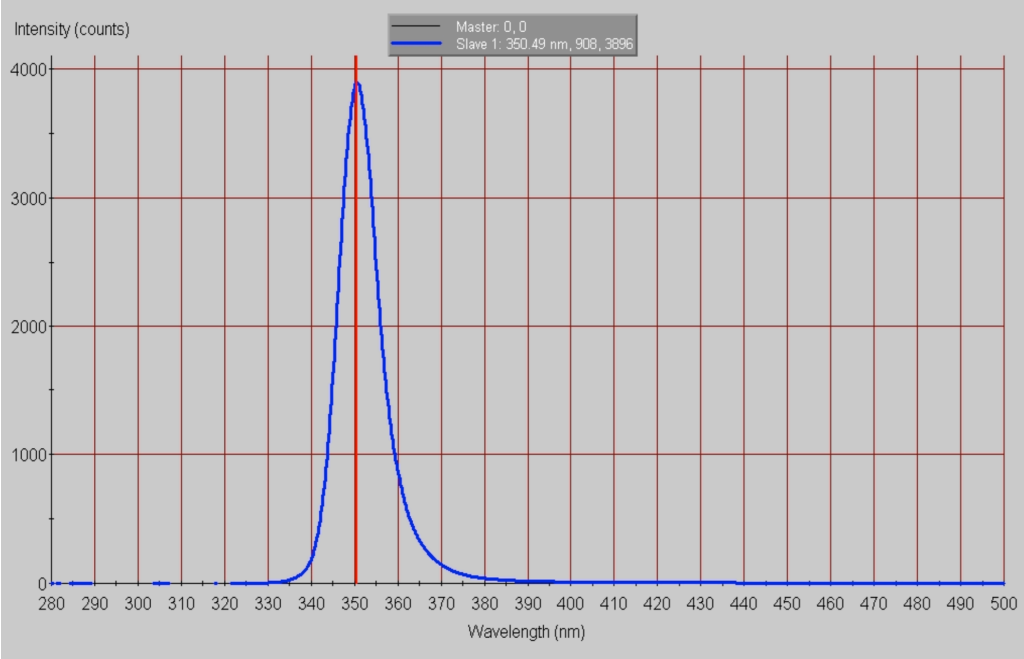

Figure S9. Spectral output of LEDs used in photoreactor. Specifications provided from Fox Group Optoelectronics (FoxUVTM 350nm LED 5.5mm 15 degree v.a. FG350-R5.5WC015). Each LED provides a typical power of 200 µW with a 15° viewing angle.

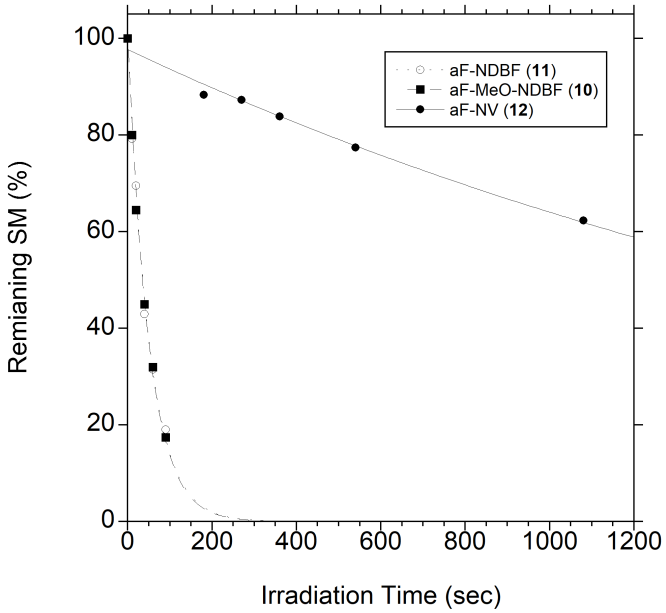

Figure S10. Kinetic analysis of photolysis of a-Factor-based peptides (**10**, **11** and **12**, respectively) using a 350 nm LED reactor. This plot shows the data obtained for NV at longer photolysis times obtained due to its slower reaction rate.

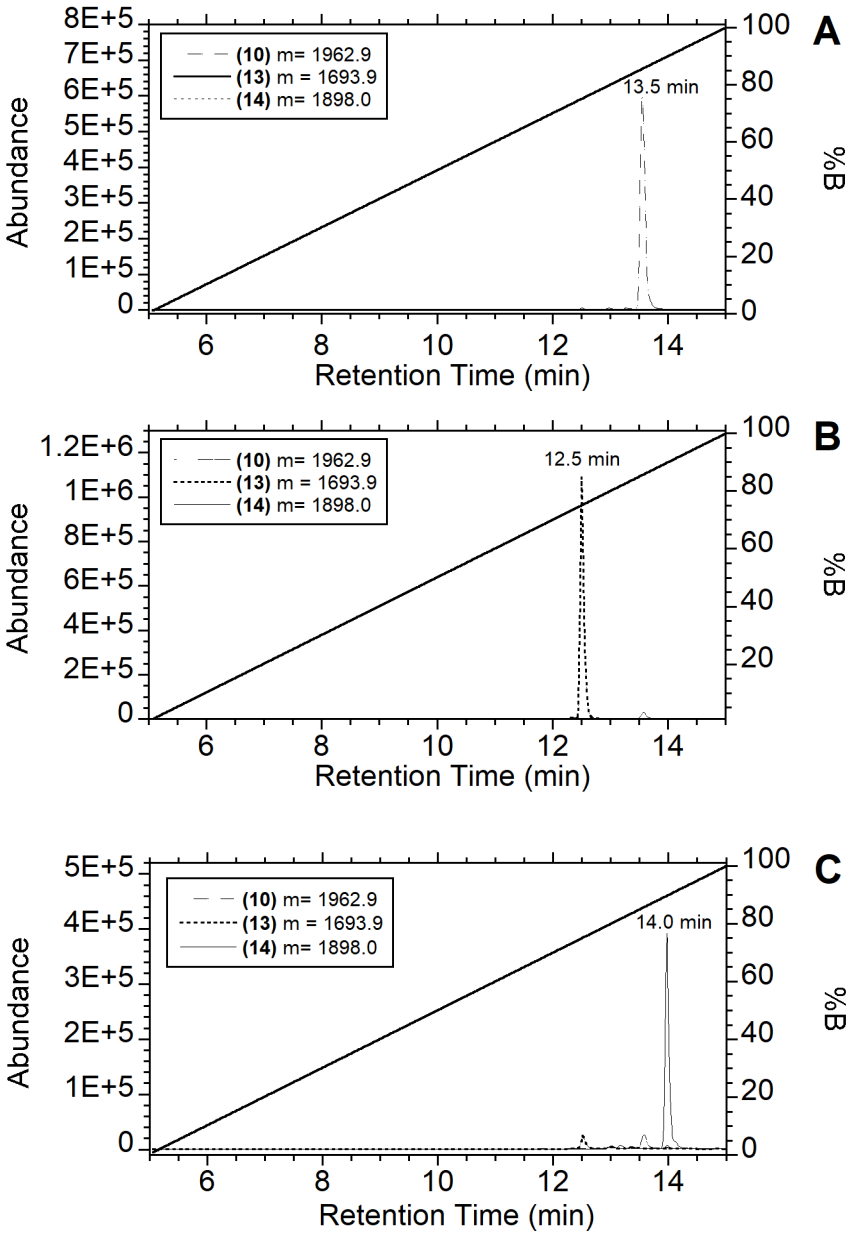

Figure S11. Enzymatic reactions initiated by UV photolysis of caged thiol. All chromatograms are SIM for the $[M+1H]^{+1}$, $[M+2H]^{+2}$, and $[M+3H]^{+3}$ charged states of peptides (**10**), (**13**), and (**14**). **A**. sample with PFTase but no irradiation, showing only the caged peptide (**10**). **B**. Sample irradiated for 30 sec in the absence of PFTase, showing the production of free thiol (**13**). **C**. Sample irradiated for 30 sec with PFTase, showing the production of the farnesylated peptide (**14**).

Table S1. MS/MS fragmentation pattern of a-Factor-C(MeNDBF)-VIA (**10**)

Ion	Observed Ion	Calculated Mass
[M+2H]+2	982.9879	982.98834
[M+2H-MeNDBF]+2	846.4143	847.4485
b9+	1122.53284	1122.5982
b8+	1007.51545	1007.5719
y14+	901.42015	901.459
b7+	821.45745	821.492
b6+	674.42341	674.4236
y6++	646.28254	646.4287
c10++	605.26246	605.8346
b5+	575.35473	575.3552
b4+	518.32568	518.3337
a4+	490.23963	490.3388
b3+	390.23712	390.2387
b6++	337.18609	337.7159
y3+	302.11261	302.2074
z3+	285.19154	285.1809
b2+	277.15432	277.1547
MeNDBF+	270.07579	270.0766
a2+	249.15936	249.1598
y2+	203.13856	203.139
a1+	136.07565	136.0757

Table S2. MS/MS fragmentation pattern of a-Factor-C(NDBF)-VIA (**11**)

Ion	Observed Ion	Calculated Mass
[M+2H]+2	967.9826	967.9854
[M+2H-NDBF]+2	846.4143	847.4485
y10+	1360.5892	1360.6156
b11+	1290.5943	1290.6881
b9+	1122.5313	1290.6881
b8+	1007.5163	1007.5719
b7+	821.4623	821.4920
b6+	674.4239	674.4236
a6+	646.4157	646.4287
b5+	575.3541	575.3552
y8++	557.3352	557.7430
b4+	518.3273	518.3337
a4+	490.2389	490.3388
x6++	398.2733	398.1770
b3+	390.2378	390.2387
b6++	337.1866	337.7159
y3+	302.1128	302.2074
z3+	285.1916	285.1809
b2+	277.1544	277.1547
b4++	259.9593	259.6705
a2+	249.1594	249.1598
NDBF	240.0652	240.0661
y2	203.1387	203.1390
z2+	186.1245	186.1125
a1+	136.0756	136.0757

Table S3. MS/MS fragmentation pattern of a-Factor-C(NV)-VIA (**12**)

Ion	Observed Ion	Calculated Mass
[M+2H]+2	945.9790	945.9829
[M+2H-NV]+2	846.4172	847.4485
b11+	1290.5909	1290.6881
b9+	1122.5276	1122.5982
b14++	901.4246	901.4590
y14++	864.4454	864.4512
b8+	1007.5164	1007.5719
b7+	821.4889	821.4920
a7+	793.4742	793.4971
b6+	674.4235	674.4236
a6+	646.4153	646.4287
c10++	605.2626	605.8346
b5+	575.3559	575.3552
b4+	518.3272	518.3337
a4+	490.2408	490.3388
x6++	398.1360	398.1770
b3+	390.2364	390.2387
b6++	337.1864	337.7159
x4++	314.0072	314.1321
y3+	302.1124	302.2074
y4++	301.0202	301.1424
z3+	285.1915	285.1809
b2+	277.1542	277.1547
c4++	268.3898	268.1838
a2+	249.1593	249.1598
y2+	203.1386	203.1390
NV+	196.0601	196.0610
a1+	136.0757	136.0757

Table S4. MS/MS fragmentation pattern of KRas-C(MeNDBF)-VIM (**15**)

Ion	Observed Ion	Calculated Mass
[M+2H]+2	781.9243	781.9253
[M+2H-MeNDBF]+2	647.3358	647.3909
y9+	1307.5508	1307.6612
b8+	1202.5511	1202.6476
y8+	1179.4726	1179.5663
x7+	1118.5135	1118.6605
y5+	863.5070	863.3916
b7+	829.5275	829.5618
y10++	718.4741	718.3817
b10++	707.3835	707.8685
b6+	701.4668	701.4668
a10++	693.3860	693.9062
b9++	651.8447	651.3617
a9++	637.5642	637.3448
y8++	603.2279	603.2764
b5+	600.4187	600.4192
b4+	472.1529	472.3242
x5++	445.2756	445.1891
a4+	444.1576	444.3293
y5+	432.4872	432.1994
b7++	415.2823	415.2845
a7+	401.2530	401.2871
b3+	385.2913	385.2922
z3+	345.0875	345.1843
c555	309.1916	309.2265
MeNDBF+	270.0755	270.0766
y2+	263.1419	263.1424
b2+	257.1967	257.1972
a4++	222.1597	222.6683

Table S5. MS/MS fragmentation pattern of KRas-C(NDBF)-VIM (**16**)

Ion	Observed Ion	Calculated Mass
[M+2H]+2	766.9193	766.9200
[M+2H-NDBF]+2	647.3351	647.3909
b9+	1271.6037	1271.7055
b8+	1172.5466	1172.6371
y8+	1149.4663	1149.5557
a8+	1144.6447	1144.6421
y6+	934.5338	934.4287
x5+	859.3880	859.3603
y5+	833.3465	833.3810
b7+	829.5283	829.5618
y10++	718.4770	718.3817
b6+	701.4660	701.4668
b10++	692.3758	692.8984
a10++	678.3765	678.9009
a9++	622.3676	600.4192
b5+	600.4180	600.4192
b8++	586.3095	586.8222
a5+	572.2046	572.4242
c4+	4893477.0000	489.3507
b4+	472.3248	472.3242
a4+	444.3774	444.3293
b7++	415.1479	415.2845
b3+	385.2913	385.2922
z4++	344.2287	344.3.11
y2+	263.1480	263.1424
b2+	257.1966	257.1972
NDBF+	240.0649	240.0661

Table S6. Photochemical and photophysical data used for calculating Φ.

Protected Cysteine	(λ_{max}) (nm)	ε (λ_{max}) ($M^{-1}cm^{-1}$)	ε (350 nm) ($M^{-1}cm^{-1}$)	I ($ein \cdot cm^{-2} \cdot sec^{-1}$)	k (1P) (1/sec)	k (2P) (1/sec)	t_{90} (sec)	Φ·ε ($1000 \cdot cm^2 \cdot mol^{-1}$)	Φ (350 nm) (mols/ein)	δ_u (800 nm) (GM)
Fmoc-Cys(MeO-NDBF)-OH (**1**)	355	8,780	8,750	1.93E-9	0.0200±0.0005	0.128±0.002	115	4500	0.53	0.71[b]
						0.254±0.004				1.4[c]
Fmoc-Cys(NDBF)-OH (**2**)	320[a]	5,990	4,600	1.93E-9	0.0197±0.0006	0.035±0.001	117	4400	0.70	0.20[d]
Fmoc-Cys(NV)-OH	350	6,290	6,290	1.93E-9	$4.6E^{-4} \pm 2E^{-5}$	-	5456	95	0.023	-

Quantum yield and actinometry calculations

Calculation of quantum yield (Φ): Φ was determined using the expression $\Phi = (I\sigma t_{90})^{-1}$, where I is the irradiation intensity in ein·cm^{-2}·mol^{-1} (determined by ferrioxalate actinometry (Hatchard, C. G.; Parker, C. A. *Proc. R. Soc. Lond.*, A **1956**, *235*, 518-536), σ is the decadic extinction coefficient (1000· ε) in cm^2·mol^{-1}, and t_{90} is the irradiation time in seconds required to reach 90% uncaging. This expression first appeared in (Tsien, R. Y.; Zucker, R. S. *Biophys. J.* **1986**, *50*, 843-853), and is derived from (Livingston, R. In *Photochromism*; Brown, G. H., Ed.; Wiley: New York, 1971; pp 13-44.). However, the derivation is never fully explained, so it is shown here.

Φ is defined as the following:

$$\Phi = \frac{number\ of\ molecules\ decomposed\ or\ formed}{number\ of\ photons\ absorbed}$$

From this definition, the following formula can be established for a photochemical uncaging system, where n_C is number of caged molecules:

$$\Phi = \frac{dn_C/dt}{d(h\nu)/dt}$$

Which can then be expressed as the following, where k is the reaction constant for a first order reaction in units of 1/sec, and I_{Abs}^{S} is the number of photons absorbed by the starting material in ein/sec:

$$\Phi = \frac{k}{I_{Abs}^{S}}$$

I_{Abs}^{S} is equal to I*σ, where I is intensity in units of ein·cm^{-2}·sec^{-1}, and σ is the decadic extinction coefficient in cm^2·mol^{-1} (ε *1000 dm^3·cm^{-1}·mol^{-1}). The expression becomes:

$$\Phi = \frac{k}{I\sigma}$$

Since absorbance (and ε by extension) is recorded in base 10 log values, k value should also be in base 10 log. Thus k' value is used, where k' = k/2.303. The expression then becomes

$\Phi = \frac{k\prime}{I\sigma}$ Eq. (1)

The rate constant k is derived from the following expression, where y is the percent of caged compound left, and t is the time of irradiation in sec:

$$y = 100e^{-kt}$$

By substituting y = 10, or time required to achieved 90% uncaging, the expression becomes:

$$10 = 100e^{-kt_{90}}$$

$$\Rightarrow log10 = log100e^{-kt_{90}}$$

$$\Rightarrow \frac{k}{2.303} = \frac{1}{t_{90}}$$

$$\Rightarrow k' = \frac{1}{t_{90}}$$

By substitution into Eq. (1) the expression becomes:

$$\Phi = \frac{1}{I\sigma t_{90}}$$

This is the expression used to calculate the quantum yield, where I is irradiation intensity in terms on units of ein·cm^{-2}·sec^{-1}, σ is the decadic extinction coefficient in cm^2·mol^{-1} (ε *1000 dm^3·cm^{-1}·mol^{-1}), and t_{90} is irradiation time in seconds required to achieve 90% uncaging.

Actinometry: Actinometry was conducted using a solution of potassium ferrioxalate at 6.00 mM in 0.5 M H_2SO_4. 200 µL aliquots of this solution were irradiated for 30, 60, 90, 150, and 180 sec. Irradiation of this solution converts Fe(III) to Fe(II), which can then be chelated by phenanthroline, resulting in a red colored solution. The irradiated aliquots were subsequently diluted to 5 mL using 2.3 mL 0.5 M H_2SO_4, 2 mL 0.6 M NaOAc in 0.18 M H_2SO_4, and 0.5 mL of 1 mg/mL phenanthroline in H_2O and allowed to incubate for 30 min, after which the absorbance

of solution at 512 nm was measured in a 96-well plate. A standard curve was also constructed using ferrous sulfate heptahydrate as a source of Fe(II), and diluted in the same buffer system to yield stock solutions with Fe(II) concentrations of 0.100, 0.0800, 0.0600, 0.0400, 0.0300, 0.0200, and 0.0100 mM. The absorbance of these solutions was measured in the same 96-well plate and used to determine the mols of Fe(II) produced after irradiation. The mols of Fe(II) produced were plotted against the time of irradiation in sec, and the slope of that plot was used as a the rate of mols produced per second irradiation (mols/sec). The rate was divided by the quantum yield of potassium ferrioxalate at 350 nm (1.21) (Hatchard, C. G.; Parker, C. A. *Proc. R. Soc. Lond. A* **1956**, *235*, 518-536), to yield I in units of ein·cm^{-2}·mol^{-1}. This was repeated three times using three freshly made solutions, yielding an average intensity of 1.93E-09 ein·cm^{-2}·mol^{-1}.

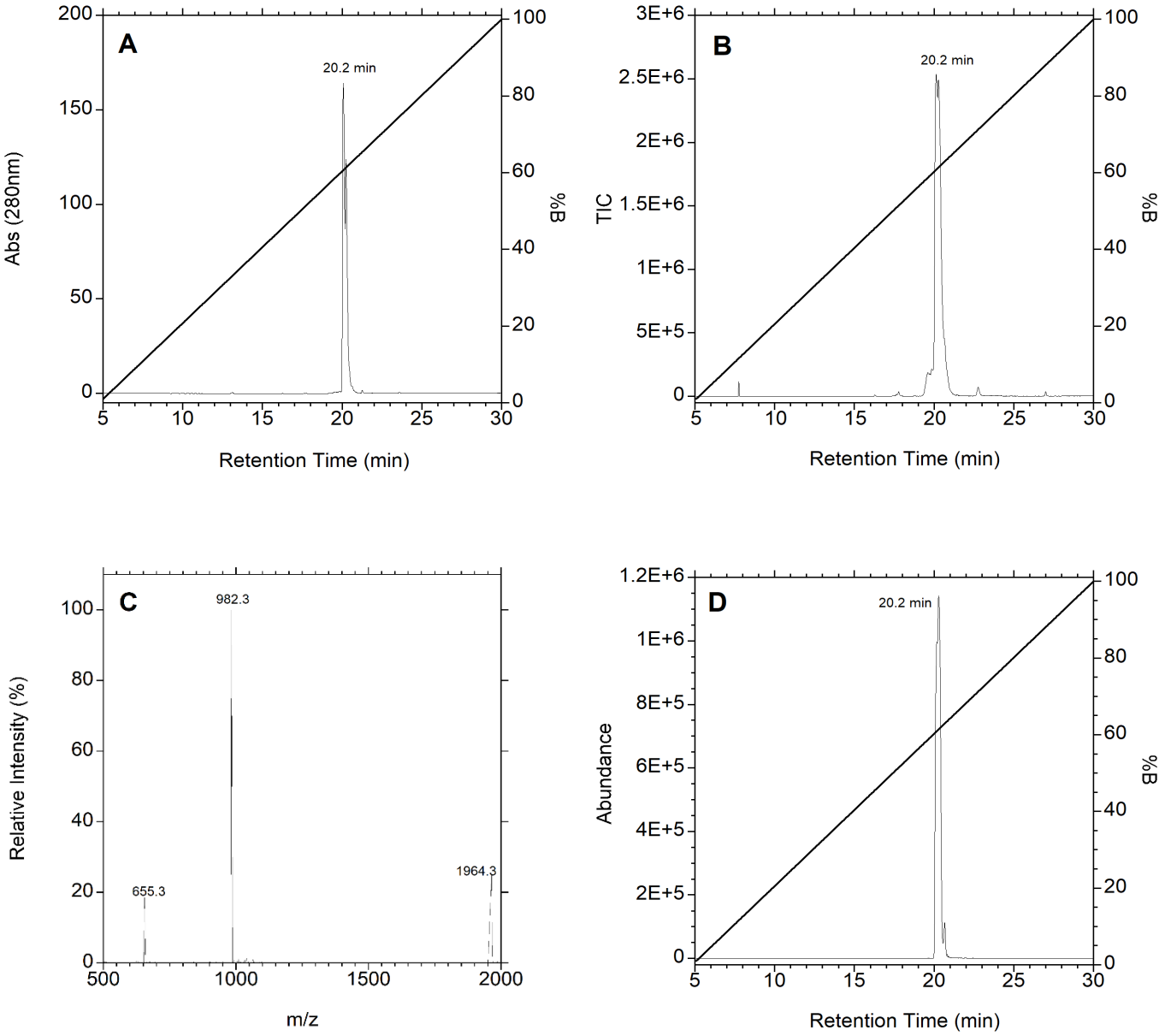

Figure S12. LC-MS analysis of a-Factor-C(MeO-NDBF)-VIA (**10**). **A**. UV monitoring at 280 nm. **B.** Total Ion Chromatogram with scan range 500-2000 m/z. **C.** Extracted Mass Spectrum of TIC peak showing $[M+1H]^{+1}$, $[M+2H]^{+2}$, and $[M+3H]^{+3}$ charged states. **D.** Extracted ion chromatogram of 982.3 ion

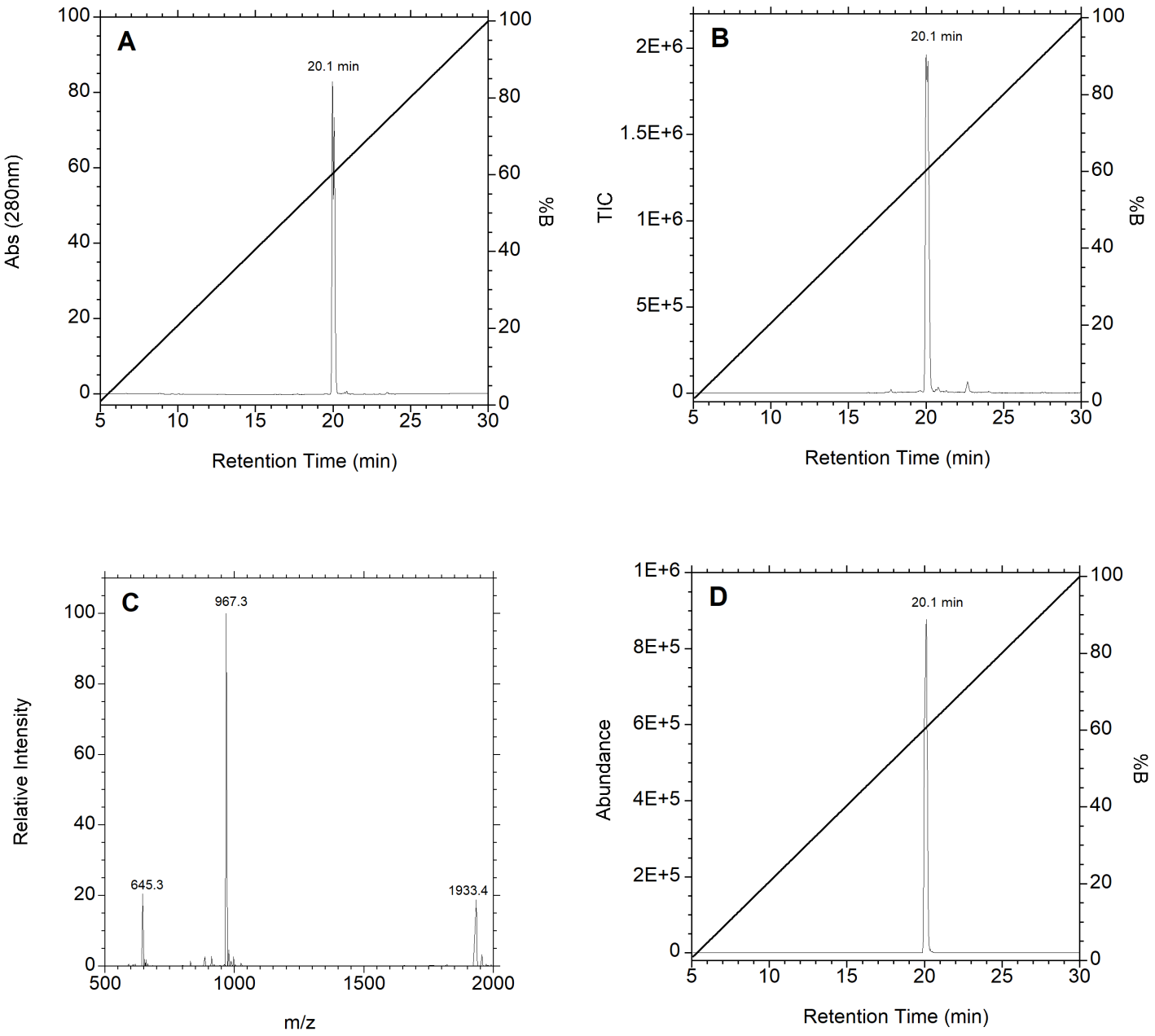

Figure S13. LC-MS analysis of a-Factor-C(NDBF)-VIA (**11**). **A**. UV monitoring at 280 nm. **B.** Total Ion Chromatogram with scan range 500-2000 m/z. **C.** Extracted Mass Spectrum of TIC peak showing $[M+1H]^{+1}$, $[M+2H]^{+2}$, and $[M+3H]^{+3}$ charged states. **D.** Extracted ion chromatogram of 967.3 ion

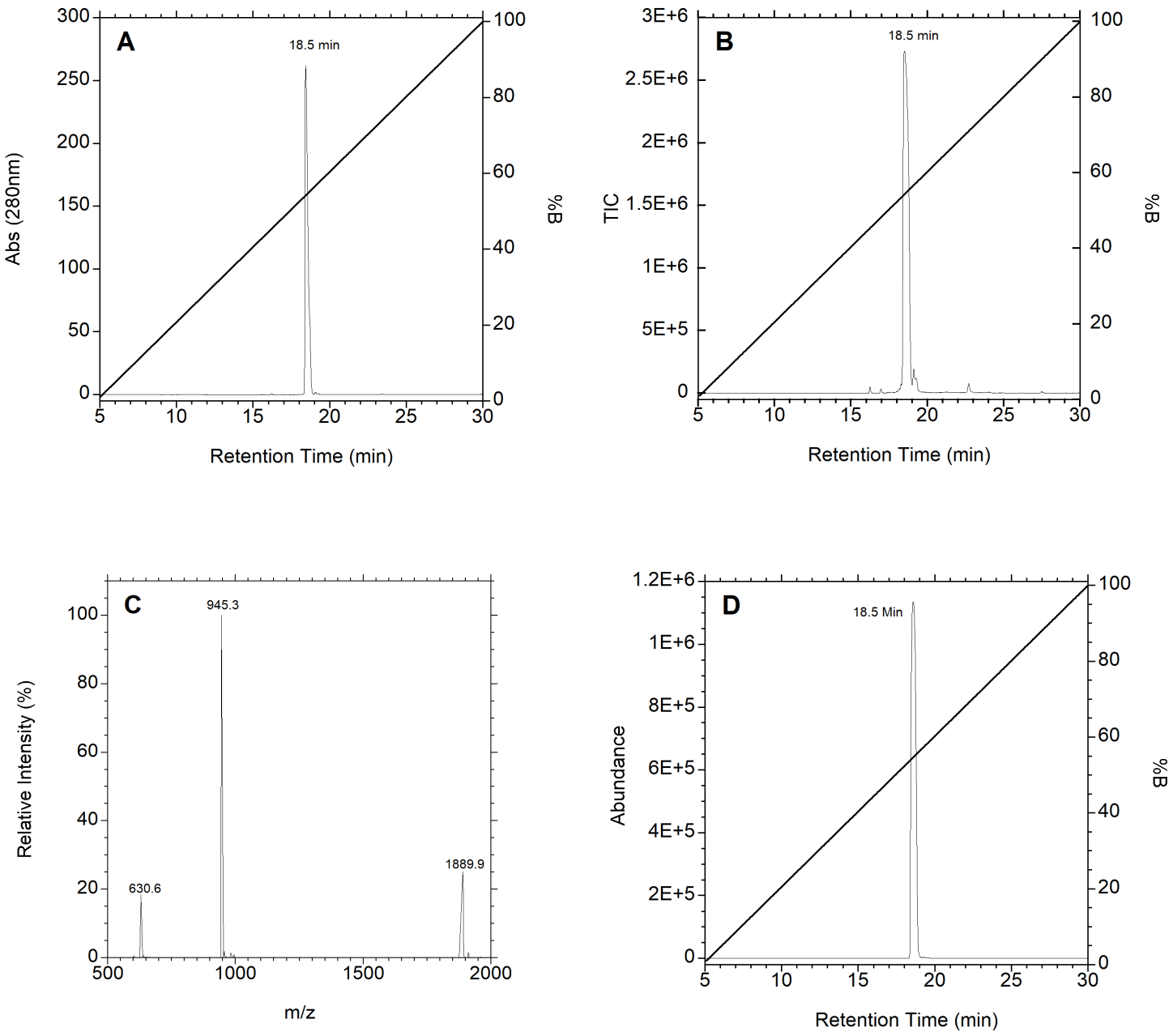

Figure S14. LC-MS analysis of a-Factor-C(NV)-VIA (**12**). **A.** UV monitoring at 280 nm. **B.** Total Ion Chromatogram with scan range 500-2000 m/z. **C.** Extracted Mass Spectrum of TIC peak showing $[M+1H]^{+1}$, $[M+2H]^{+2}$, and $[M+3H]^{+3}$ charged states. **D.** Extracted ion chromatogram of 967.3 ion

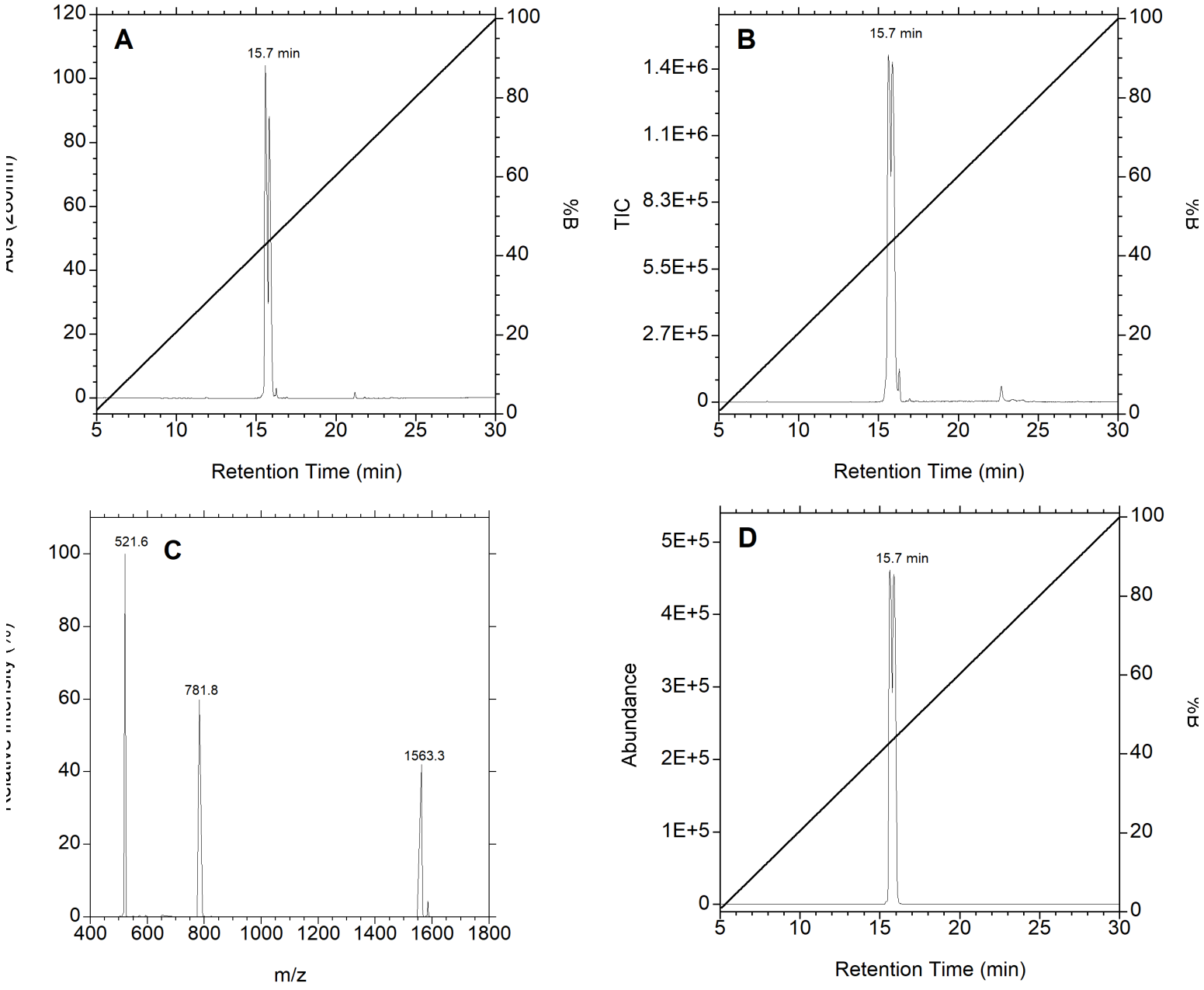

Figure S15. LC-MS analysis of KRas-C(MeO-NDBF)-VIM (**15**). **A.** UV monitoring at 280 nm. **B.** Total Ion Chromatogram with scan range 400-1800 m/z. **C**. Extracted Mass Spectrum of TIC peak showing $[M+1H]^{+1}$, $[M+2H]^{+2}$, and $[M+3H]^{+3}$ charged states. **D.** Extracted ion chromatogram of 521.6 ion

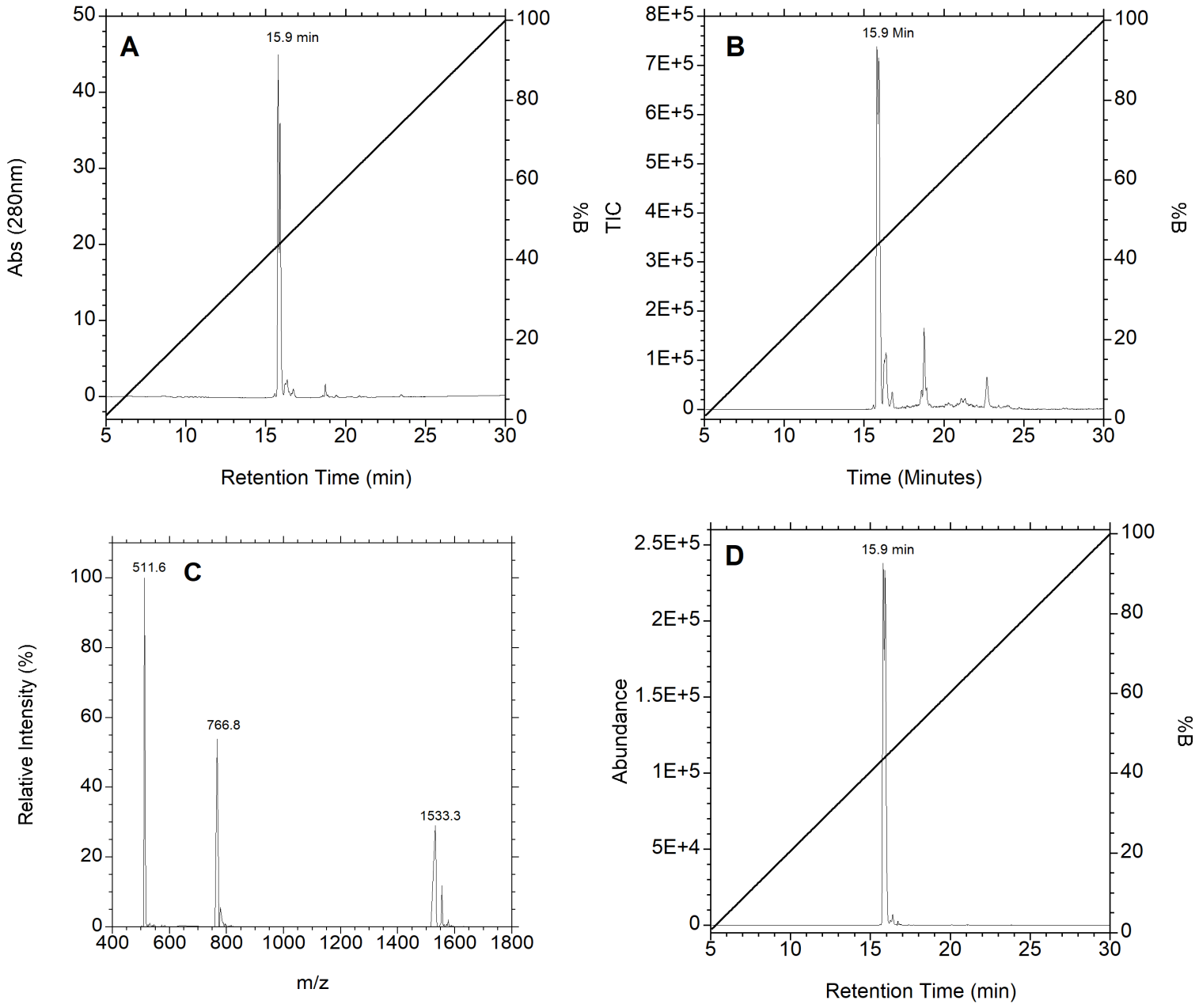

Figure S16. LC-MS analysis of KRas-C(NDBF)-VIM (**16**). **A.** UV monitoring at 280nm. **B.** Total Ion Chromatogram with scan range 400-1800 m/z. **C.** Extracted Mass Spectrum of TIC peak showing $[M+1H]^{+1}$, $[M+2H]^{+2}$, and $[M+3H]^{+3}$ charged states. **D.** extracted ion chromatogram of 511.6 ion

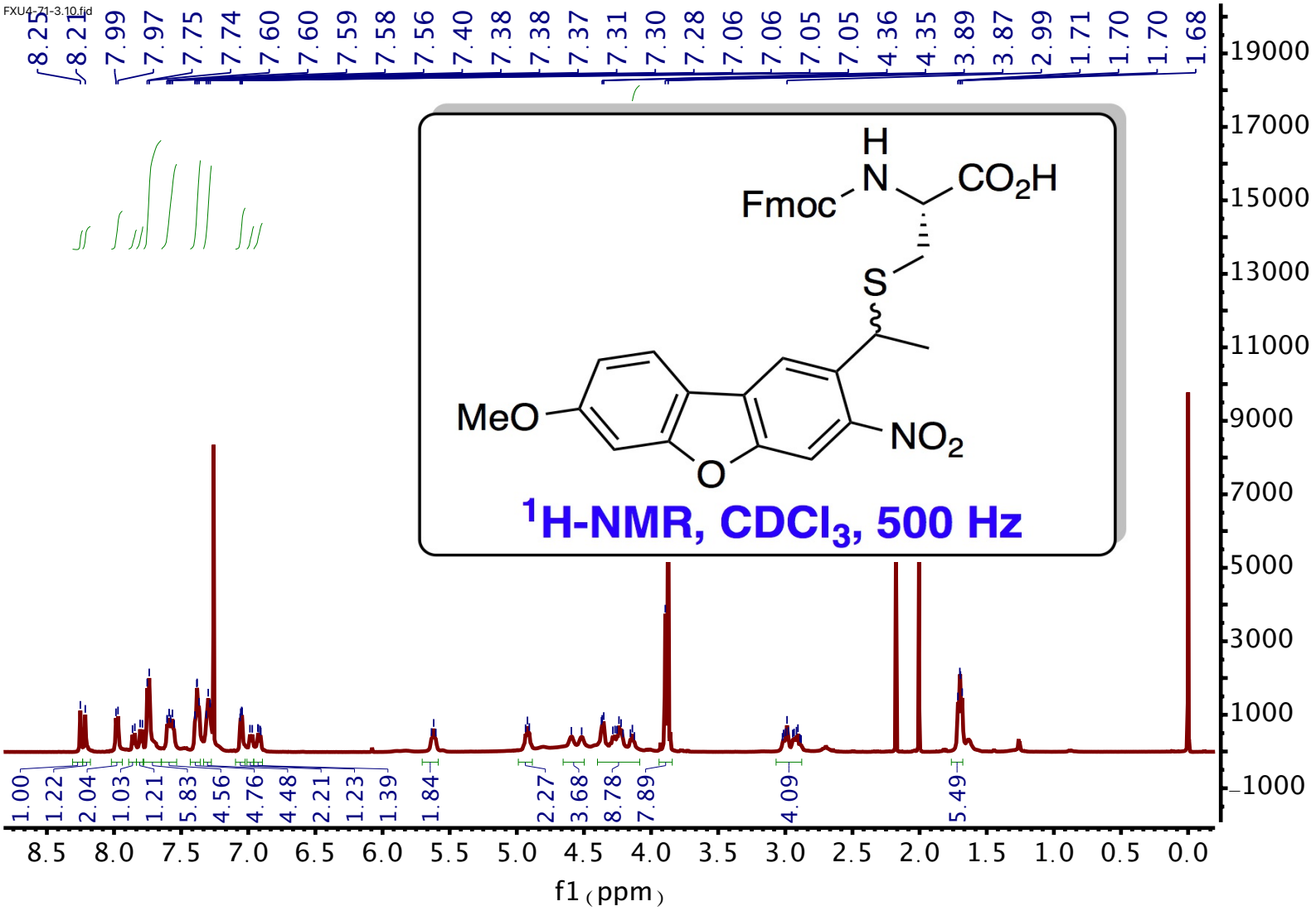

Compound **1**: ^{1}H NMR

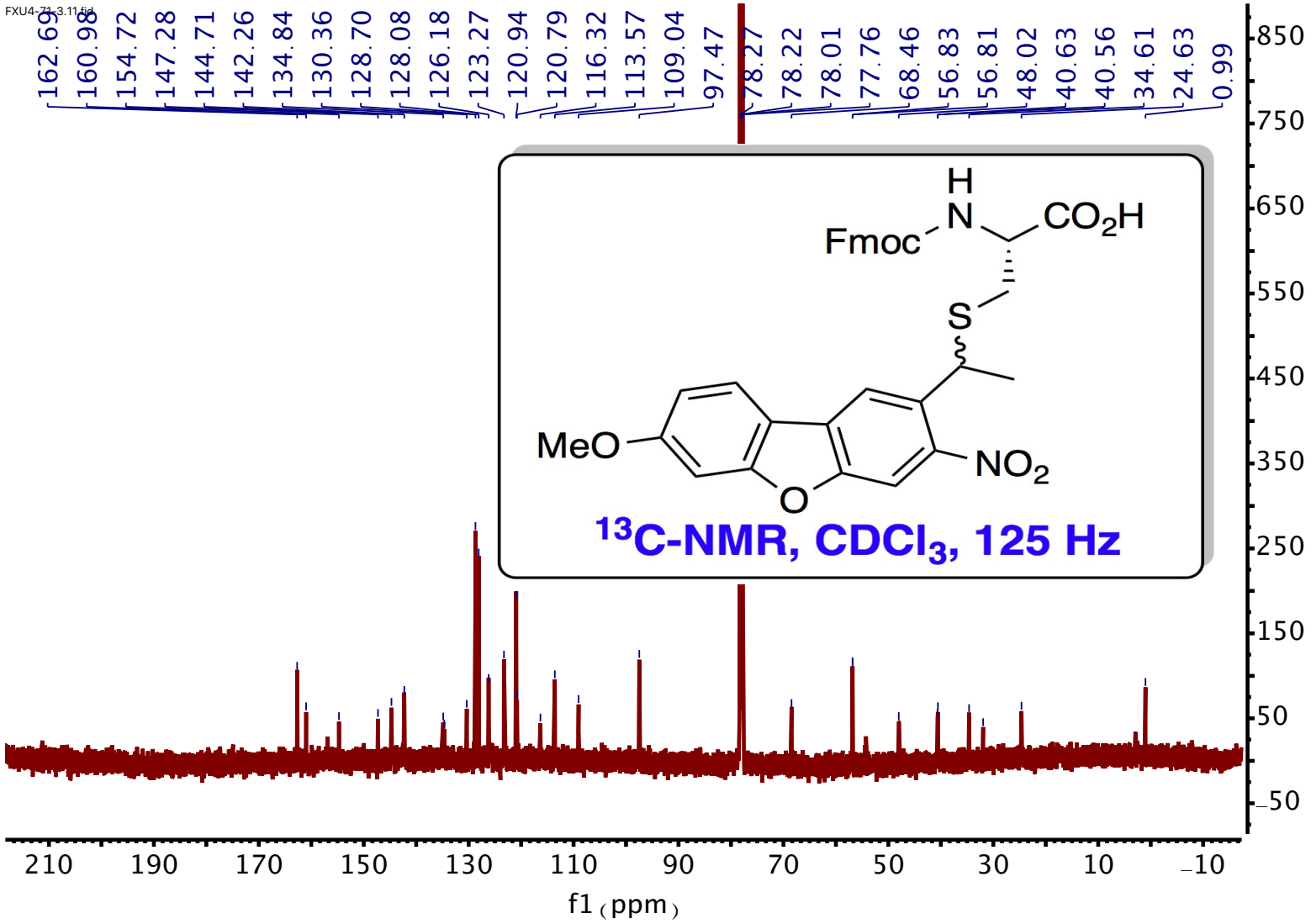

Compound **1**: ^{13}C NMR

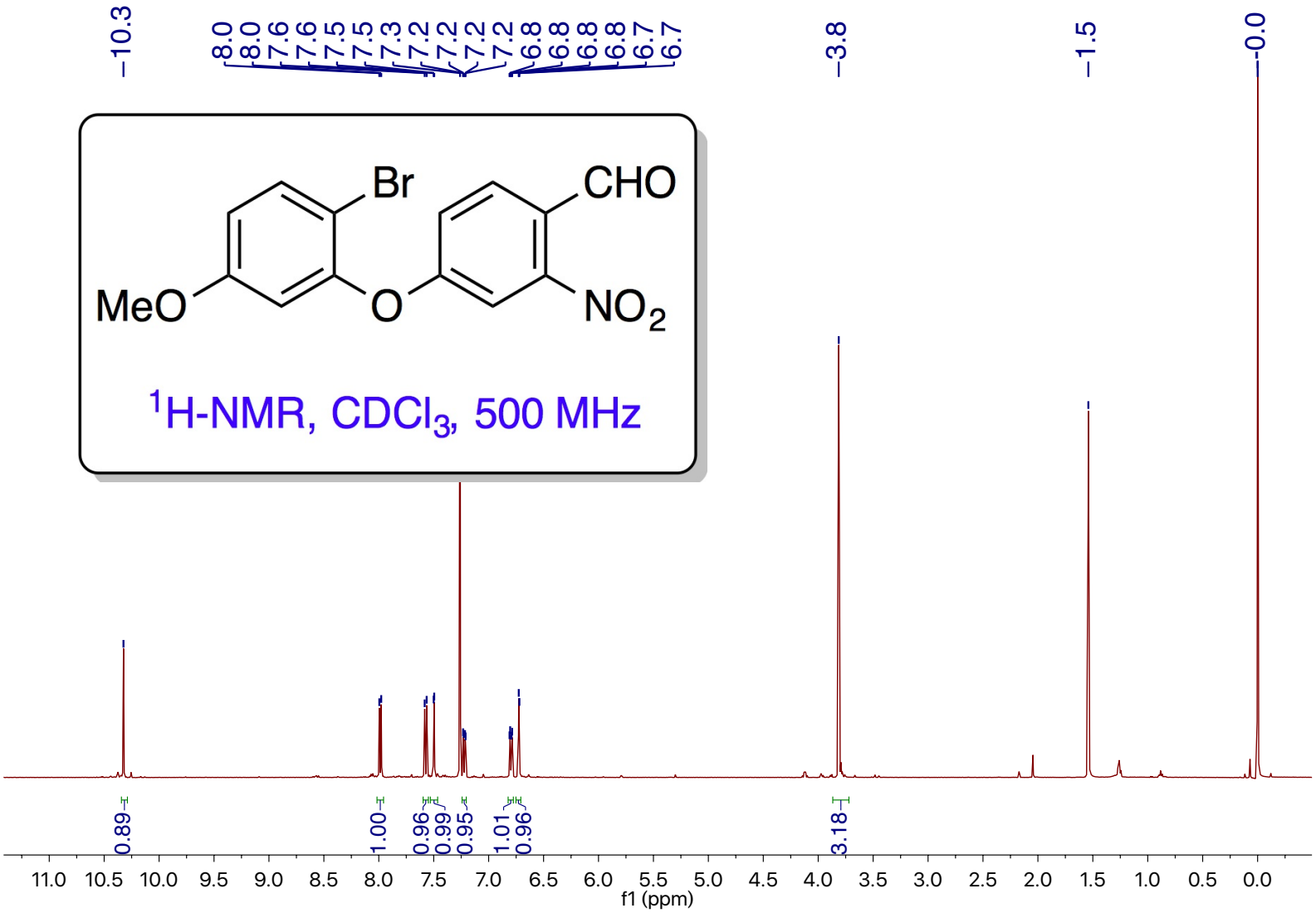

Compound **3**: ^{1}H NMR

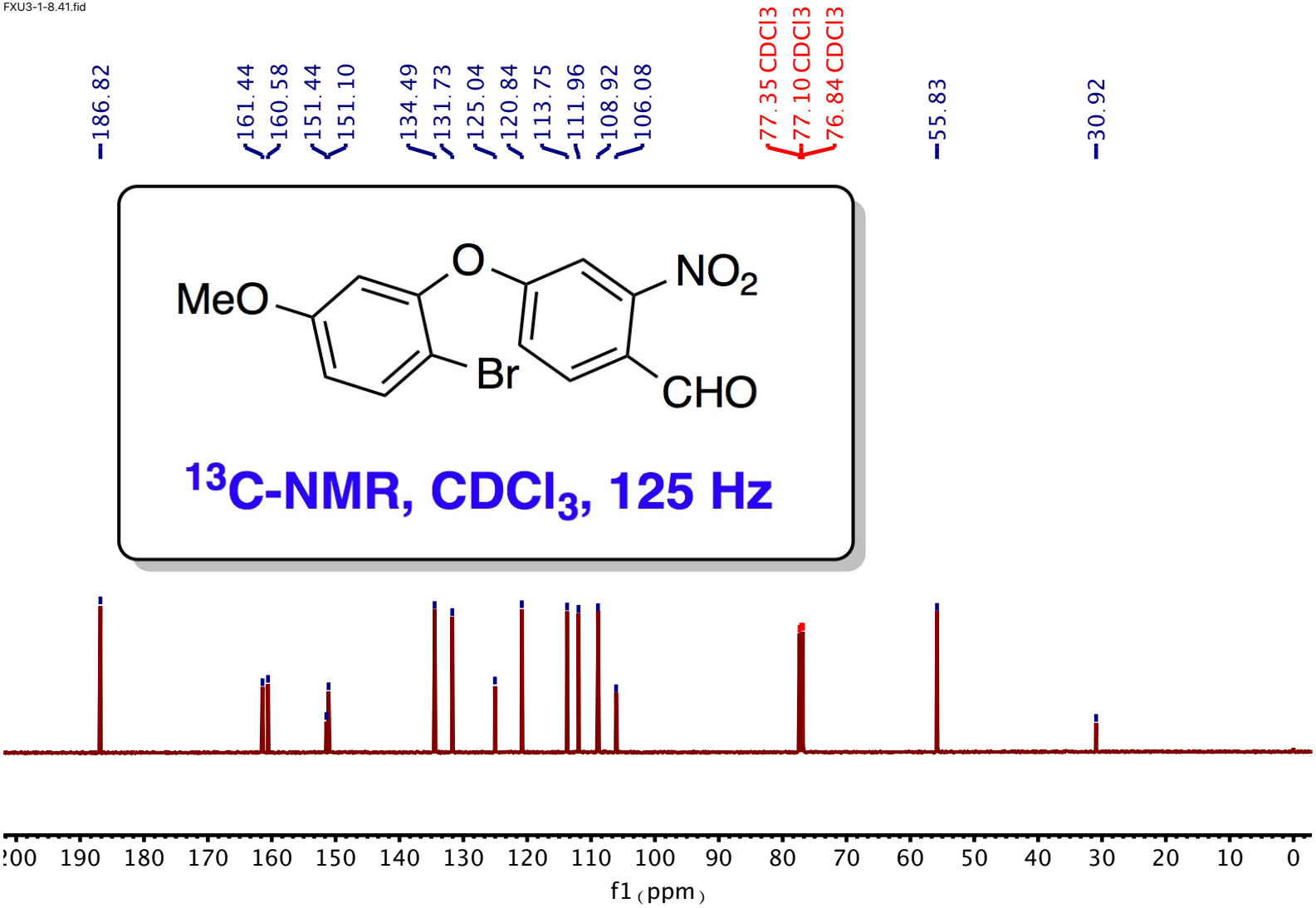

Compound **3**: ^{13}C NMR

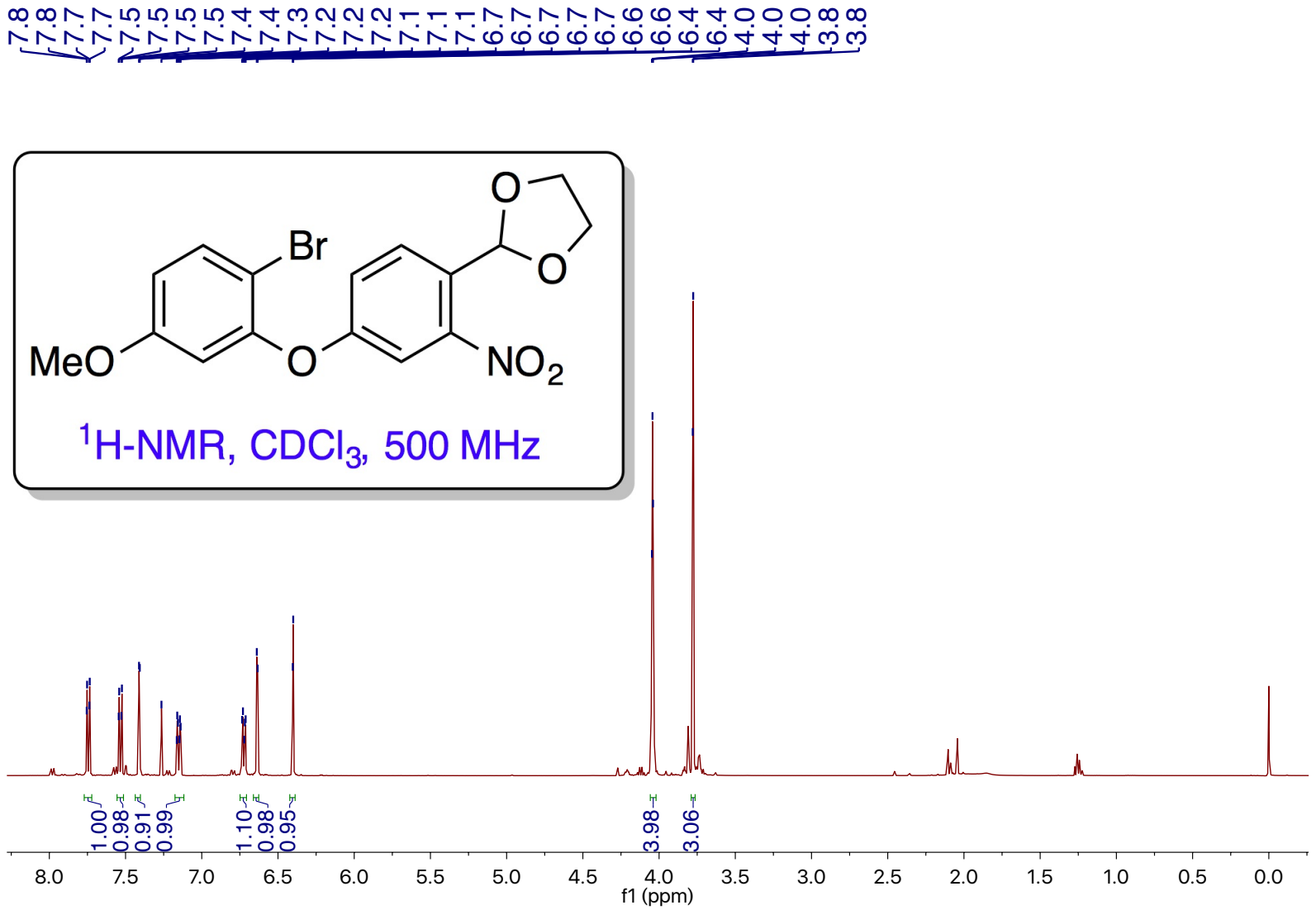

Compound **4**: ^{1}H NMR

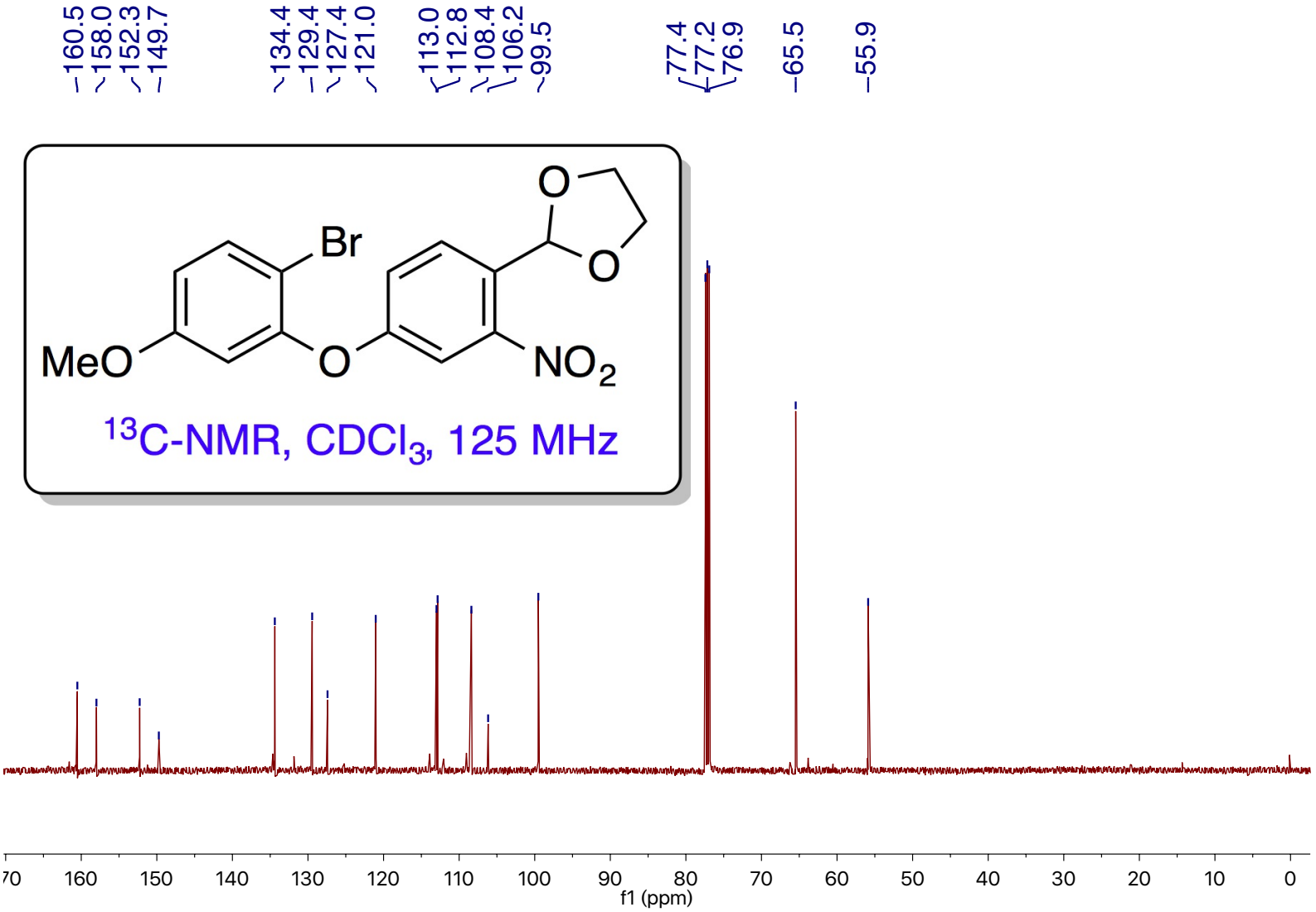

Compound **4**: ^{13}C NMR

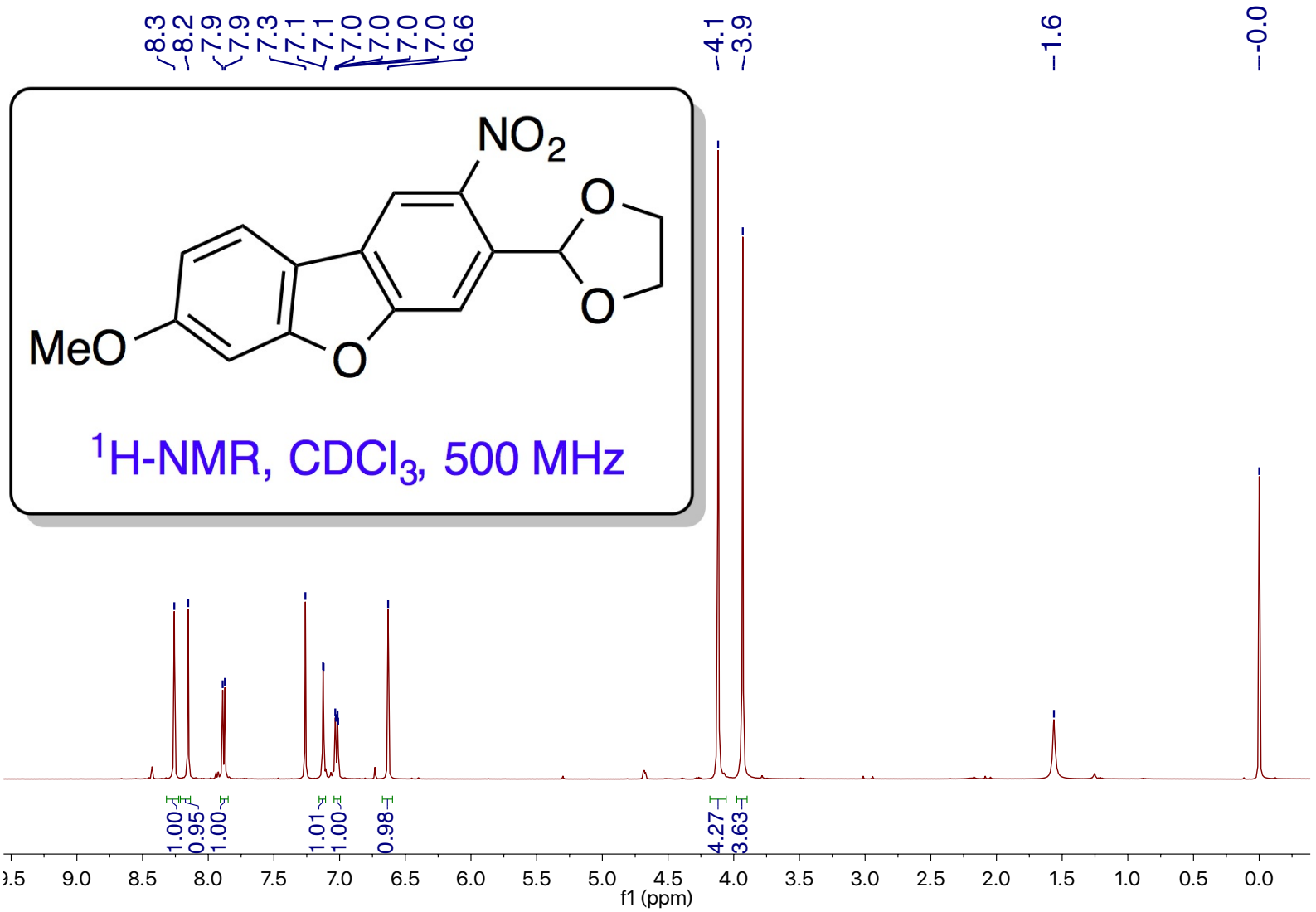

Compound **5**: ^{1}H NMR

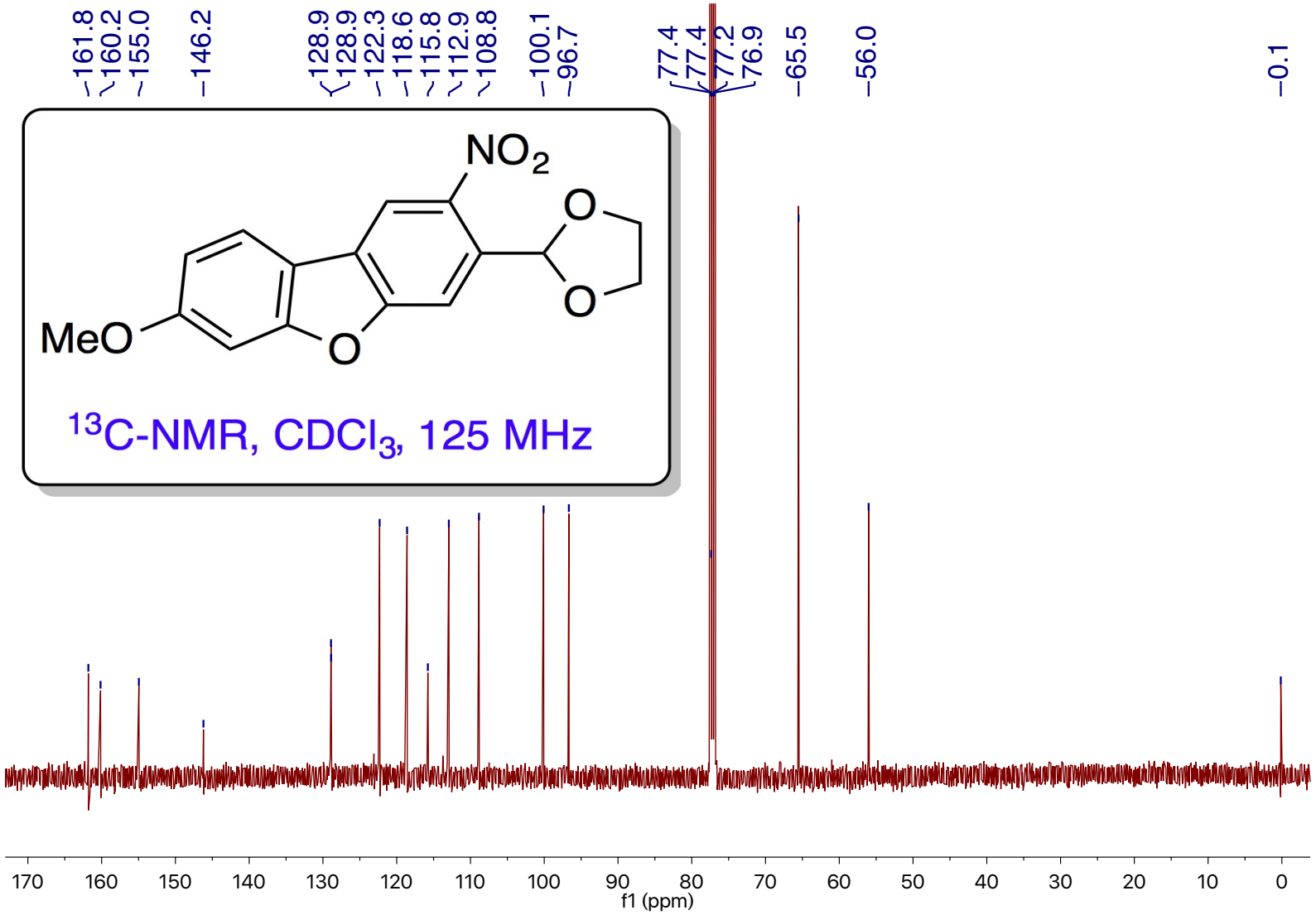

Compound **5**: ^{13}C NMR

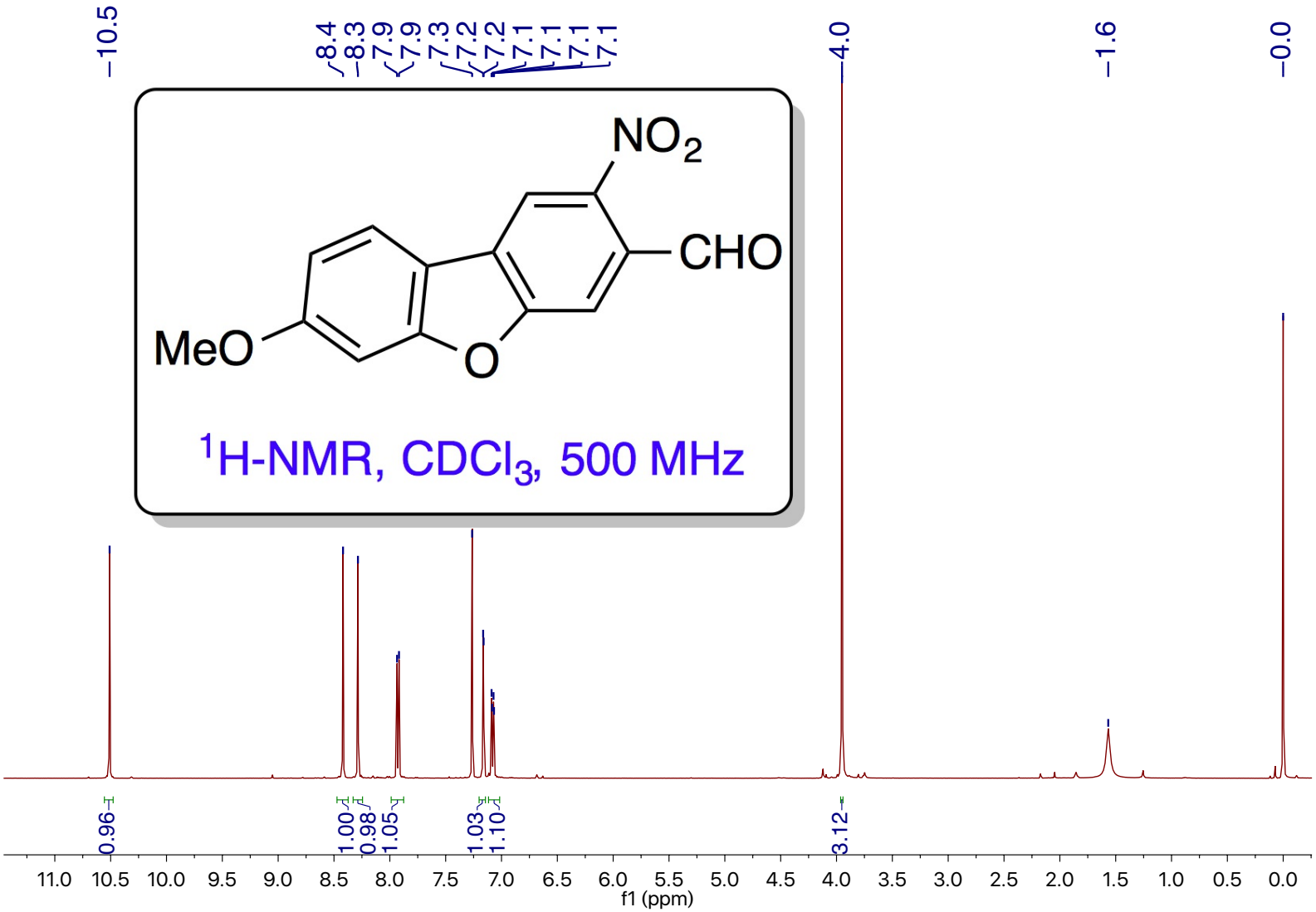

Compound **6**: ^{1}H NMR

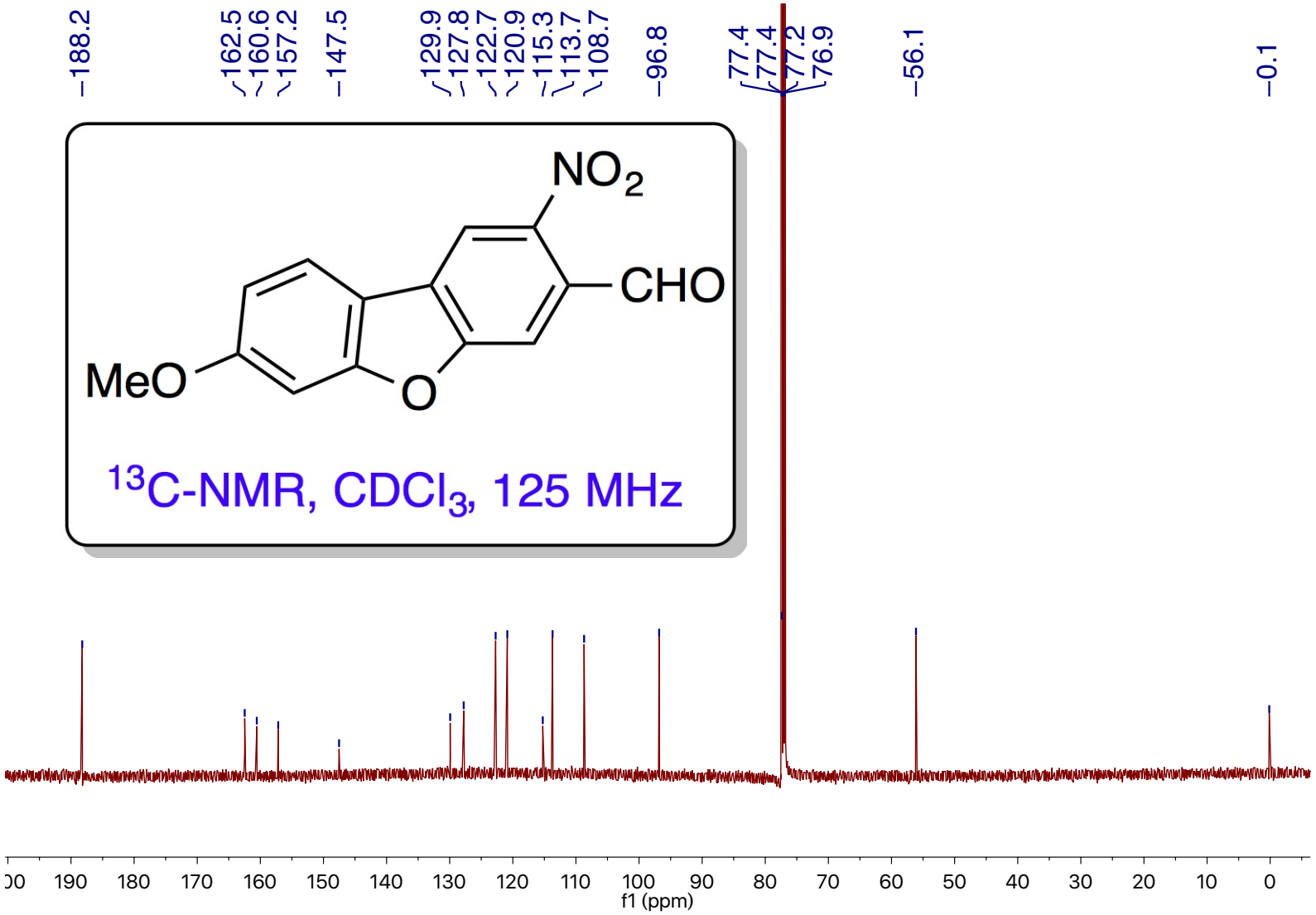

Compound **6**: ^{13}C NMR

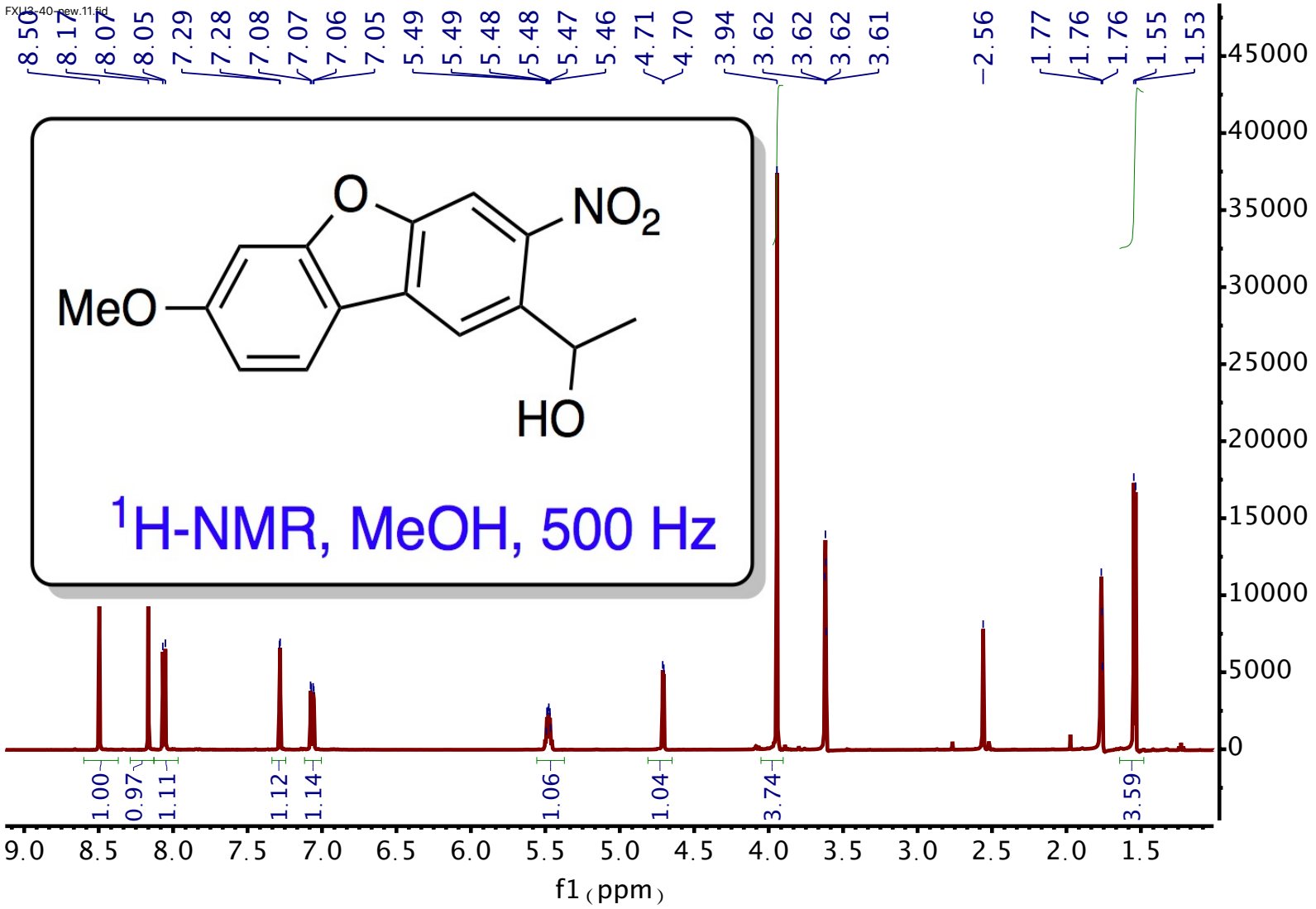

Compound **7**: ^{1}H NMR

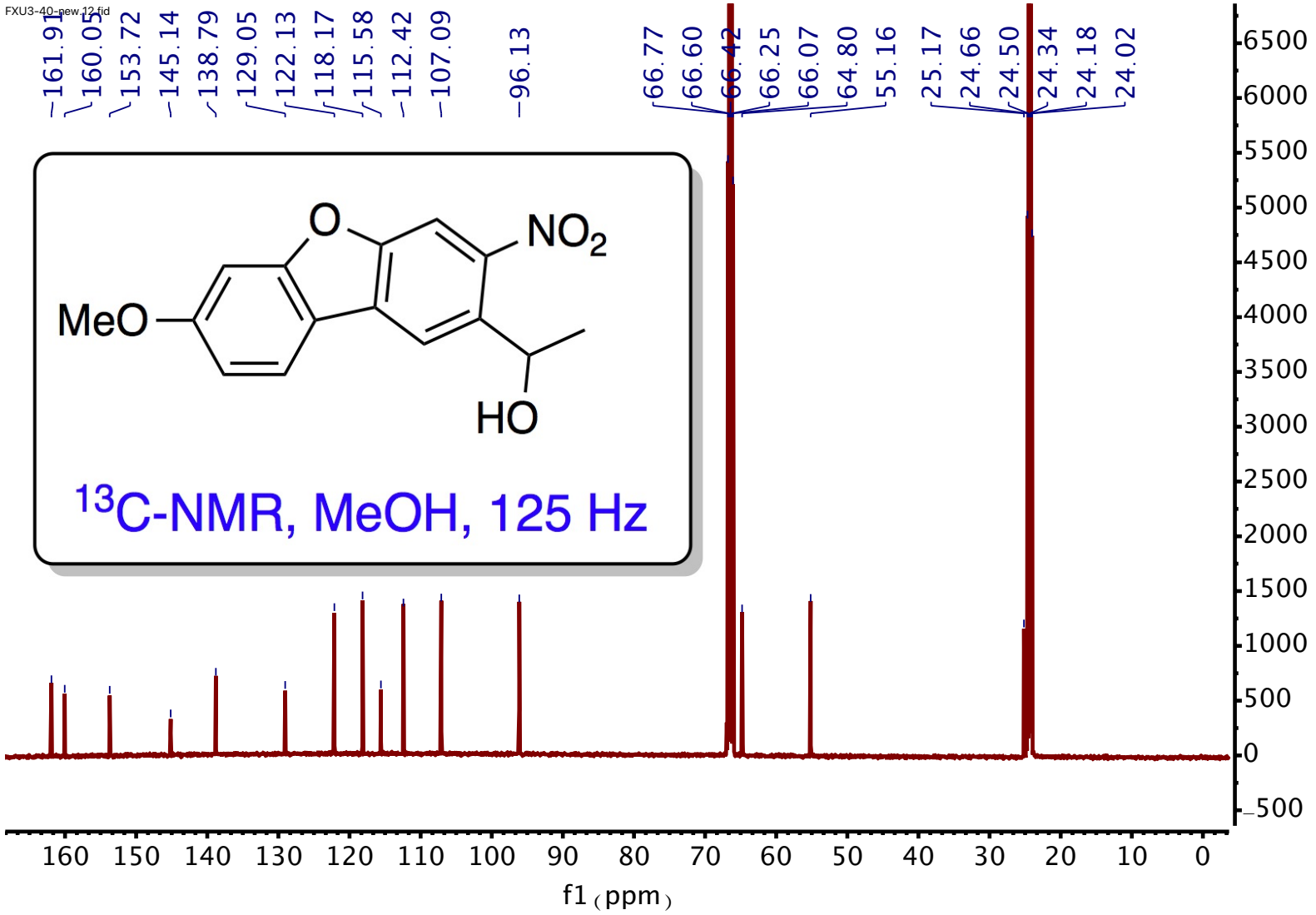

Compound **7**: ^{13}C NMR

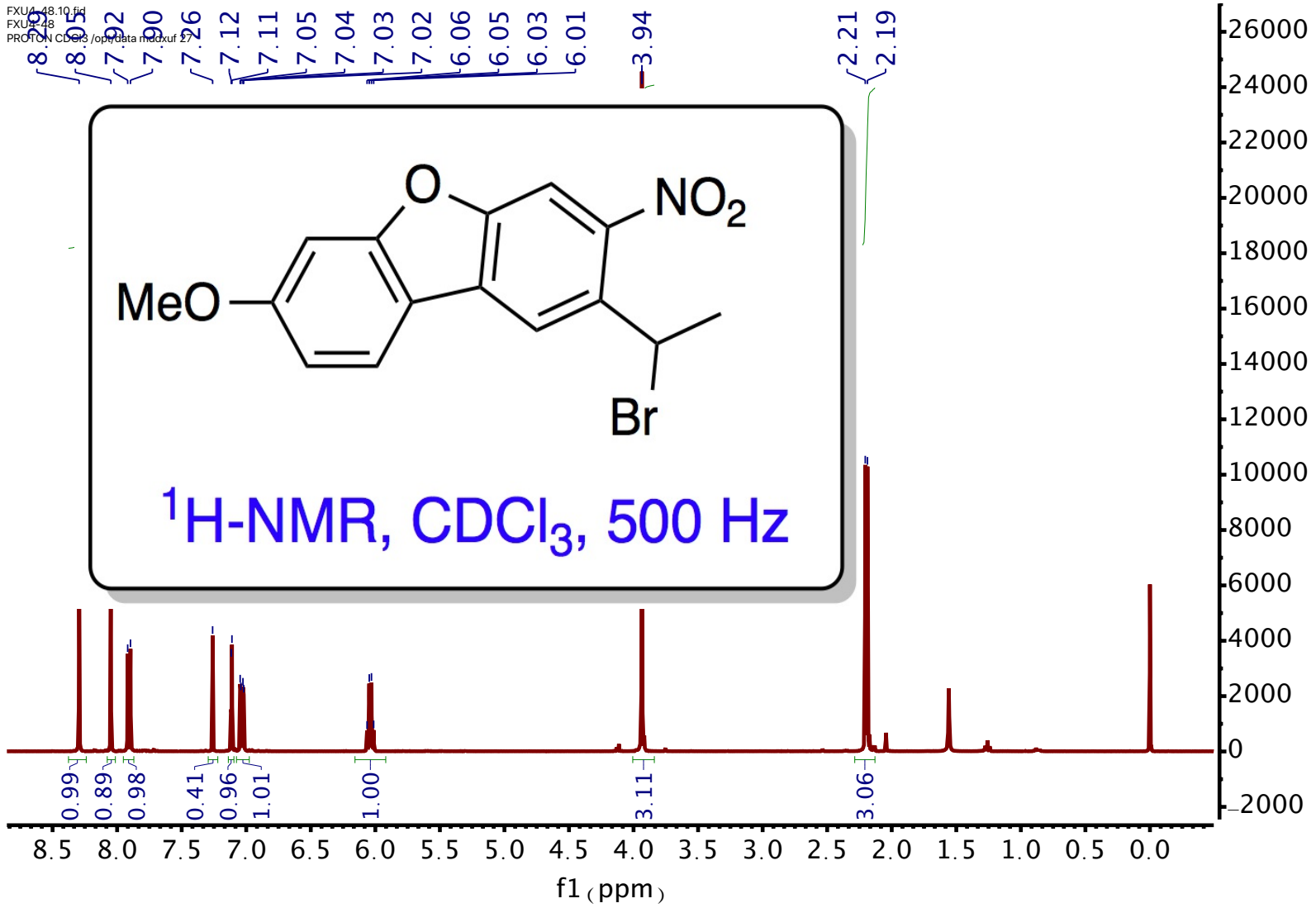

Compound **8**: ^{1}H NMR

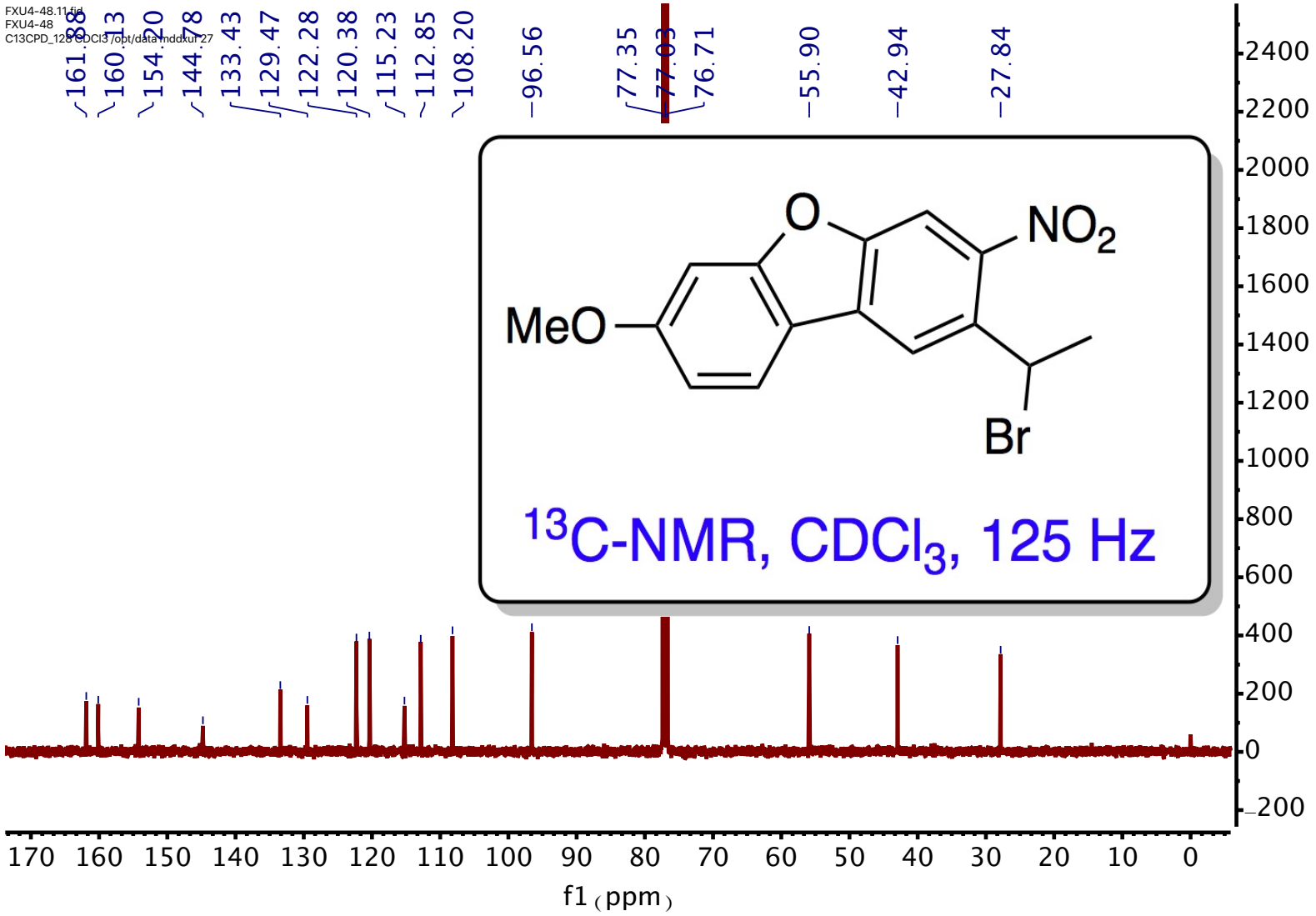

Compound **8**: ^{13}C NMR

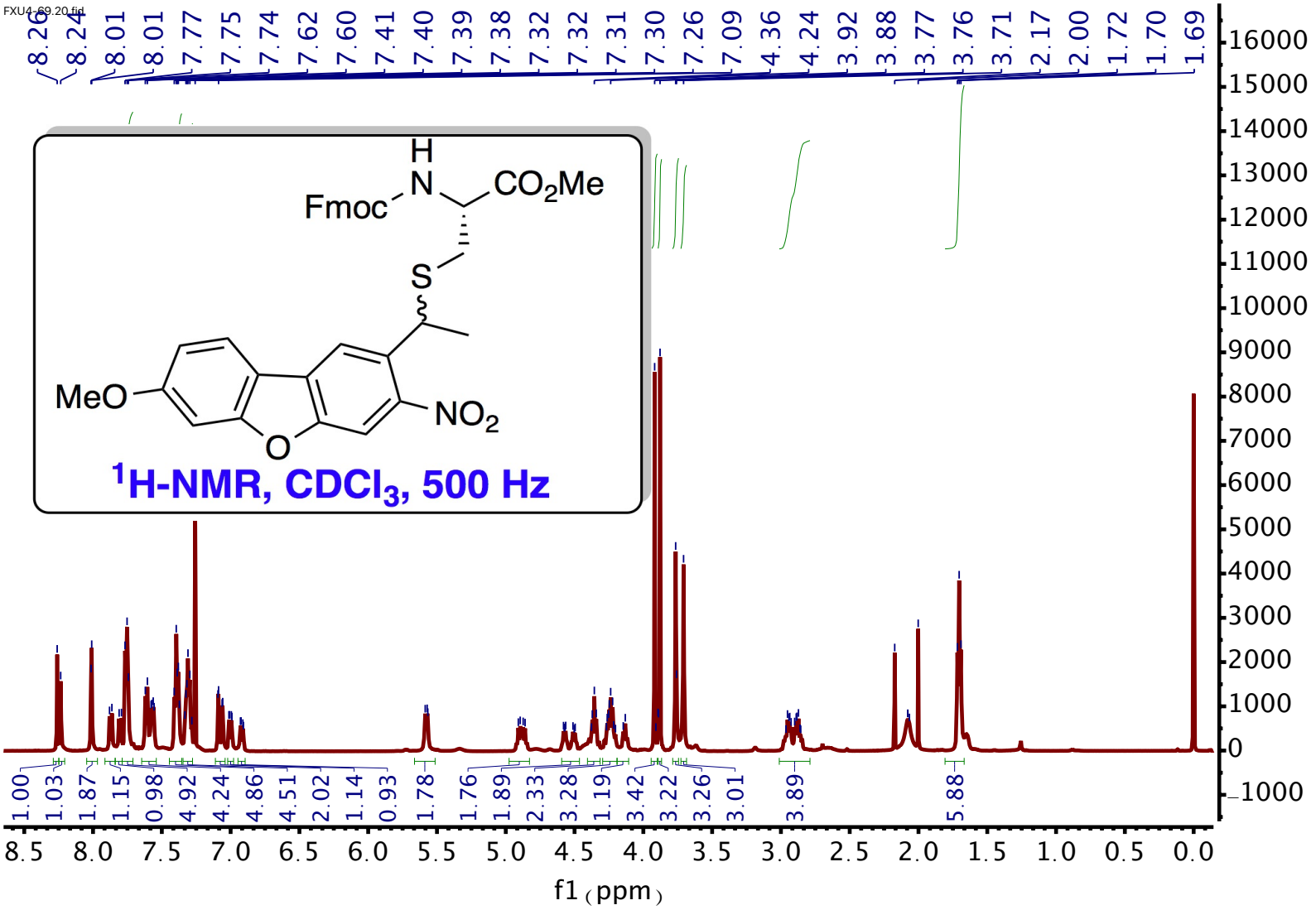

Compound **9**: ^{1}H NMR

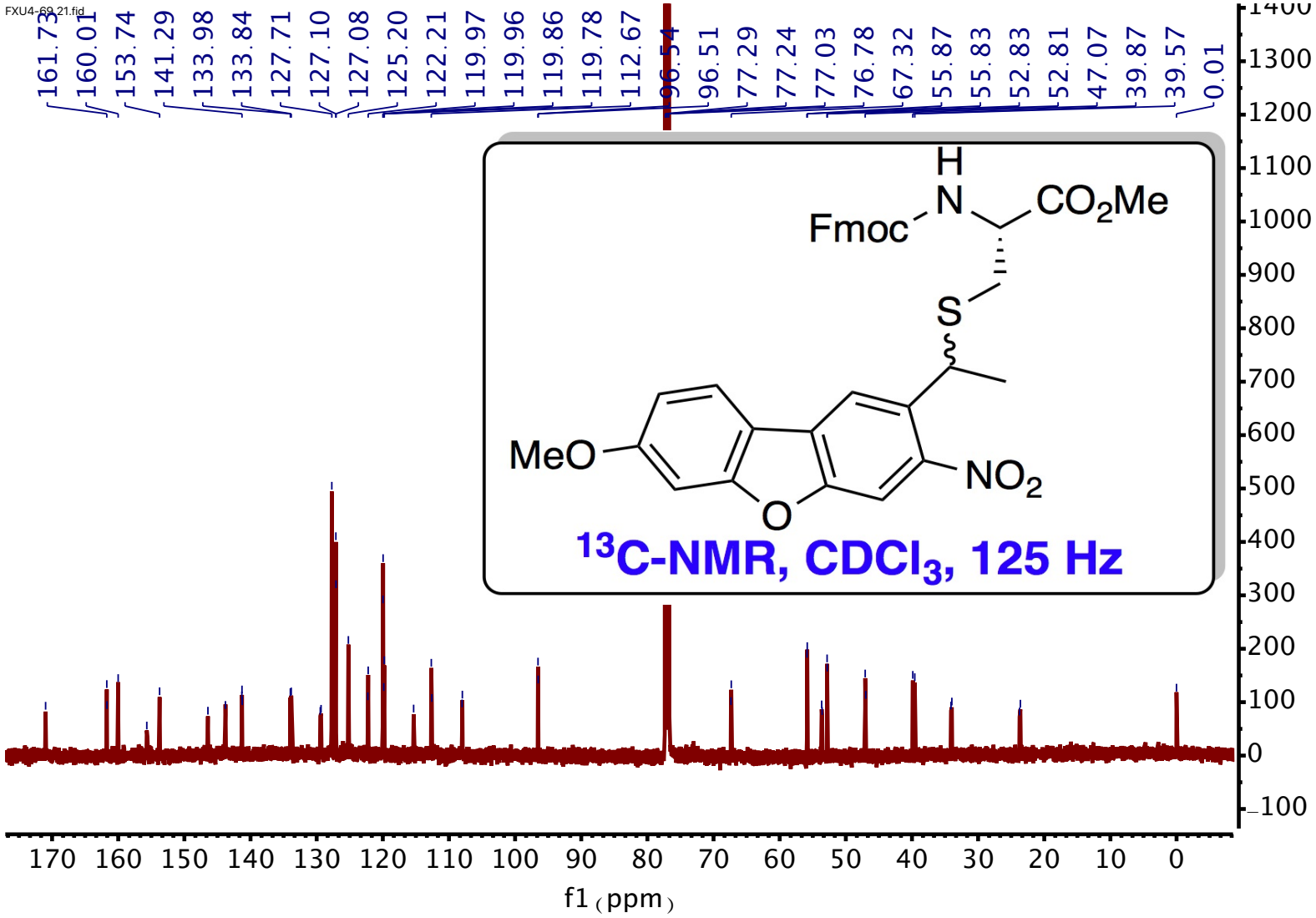

Compound **9**: ^{13}C NMR

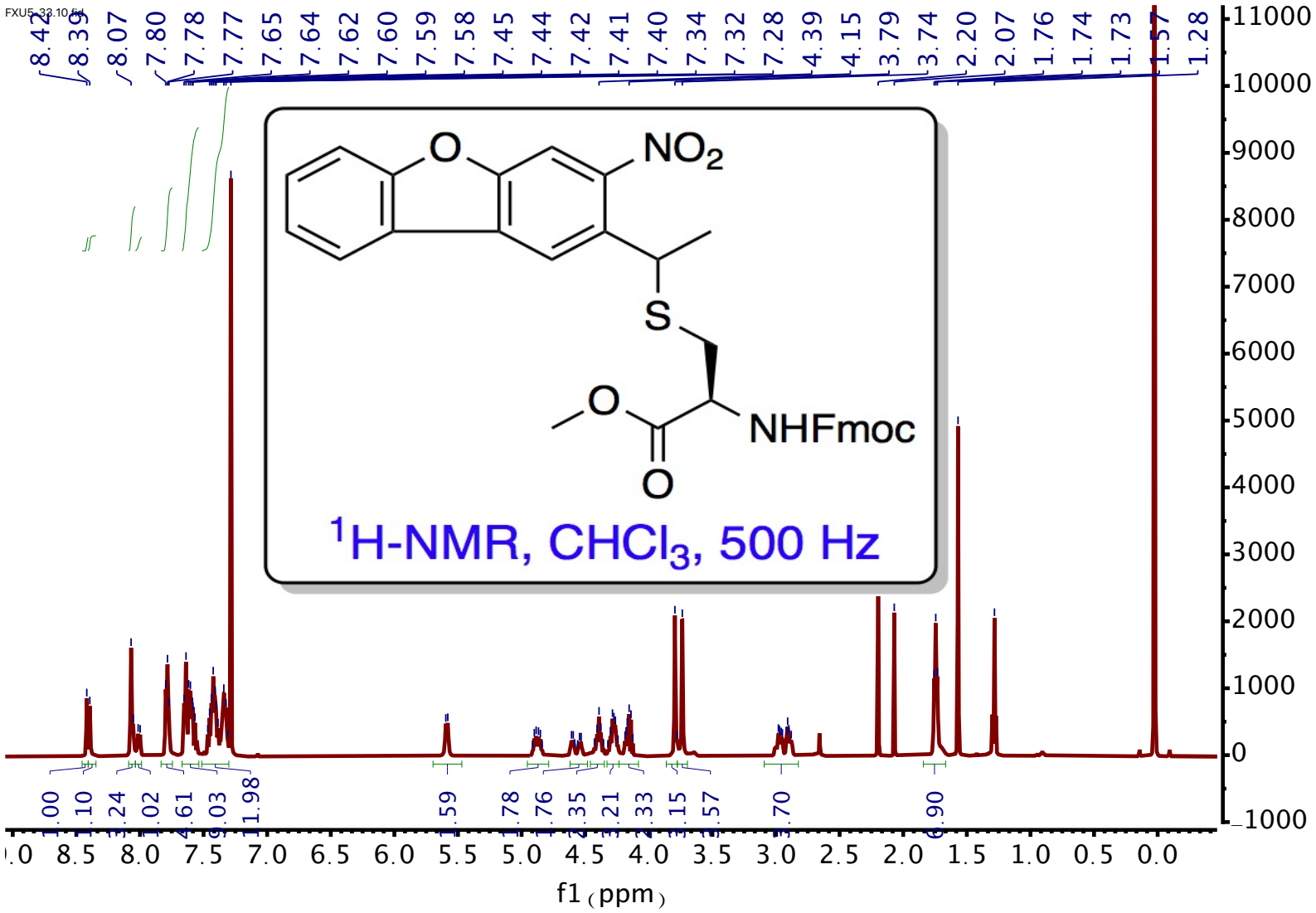

Compound **21b**: ^{1}H NMR

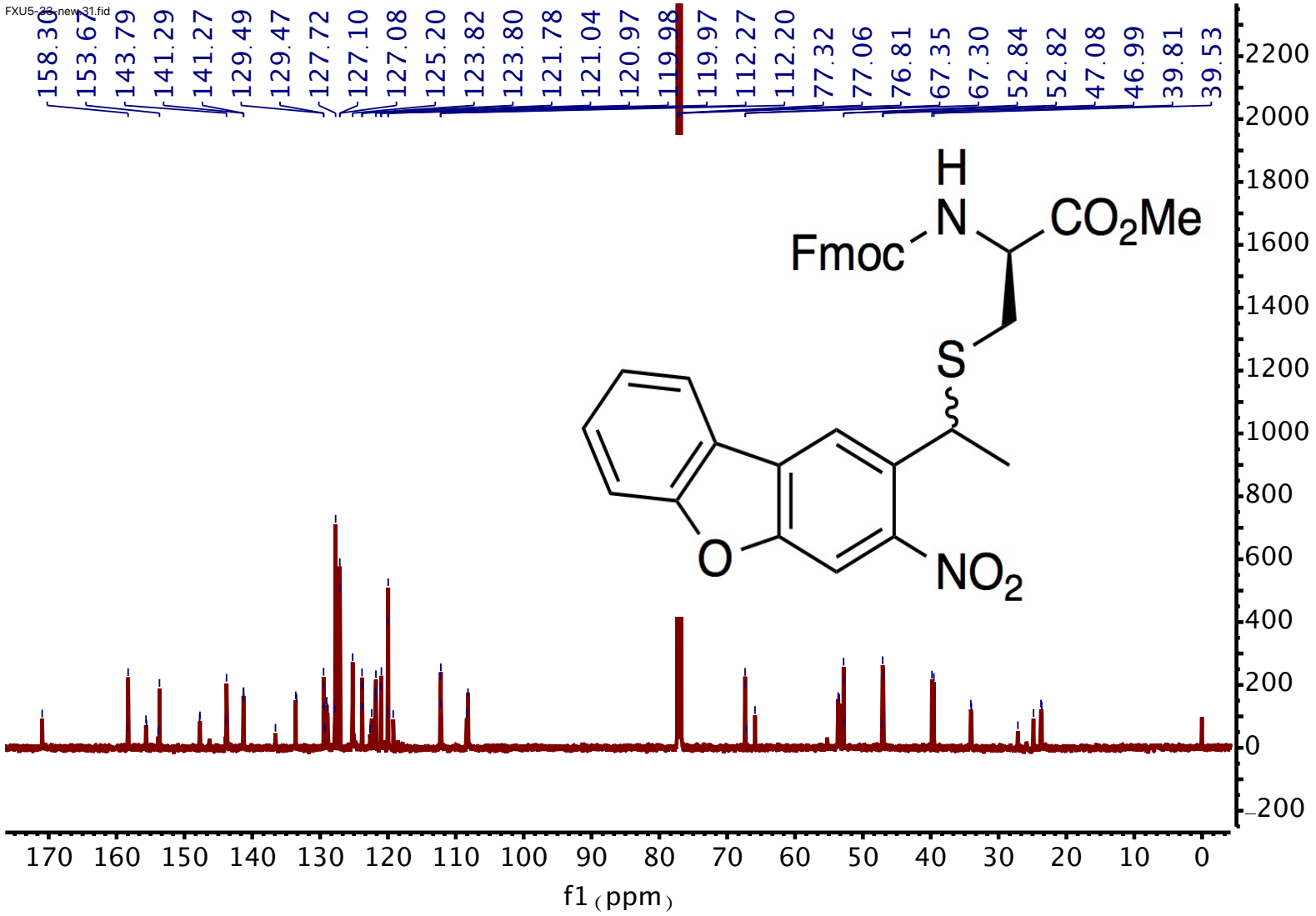

Compound **21b**: ^{13}C NMR

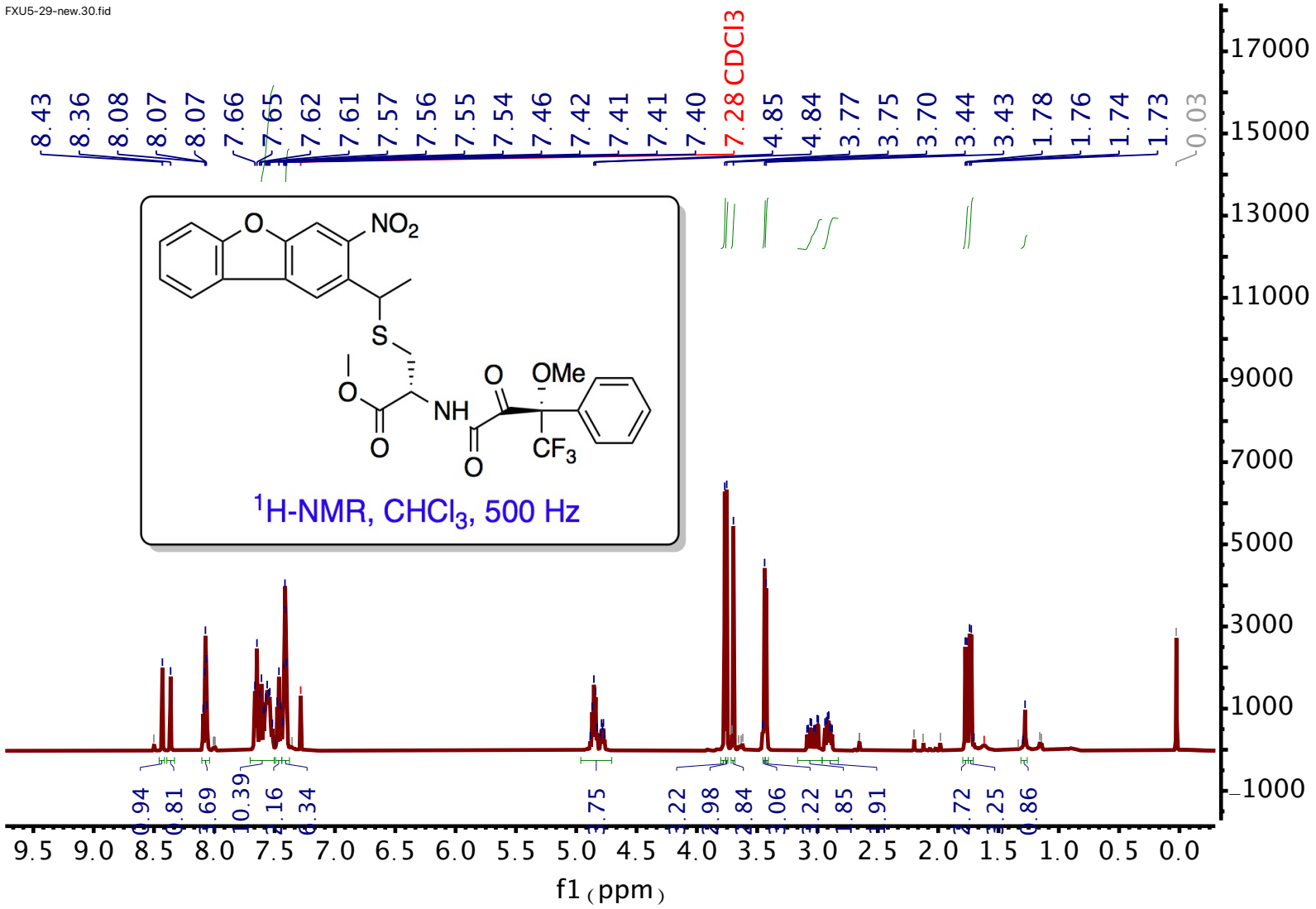

Compound **23a**: ^{1}H NMR

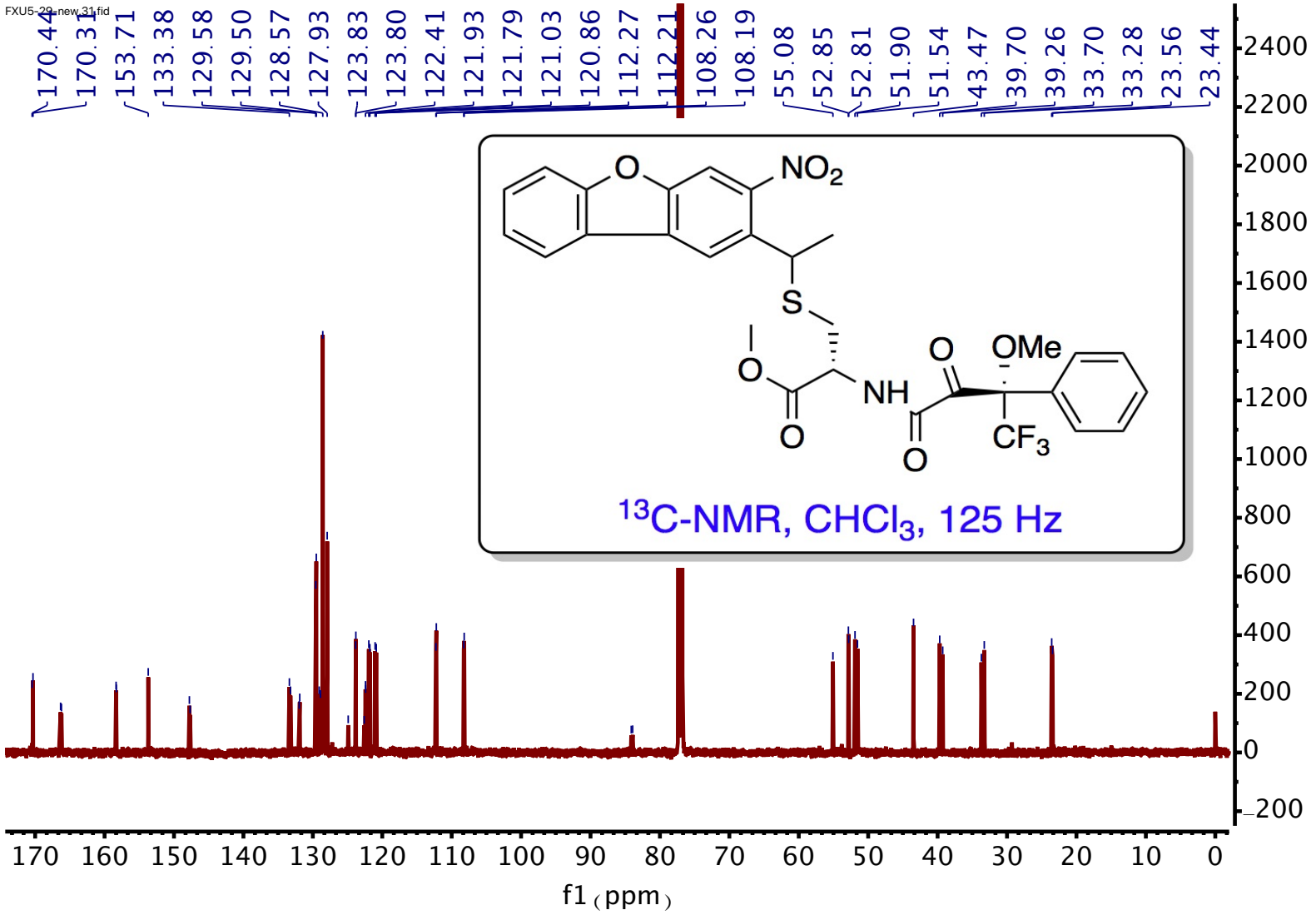

Compound **23a**: ^{13}C NMR

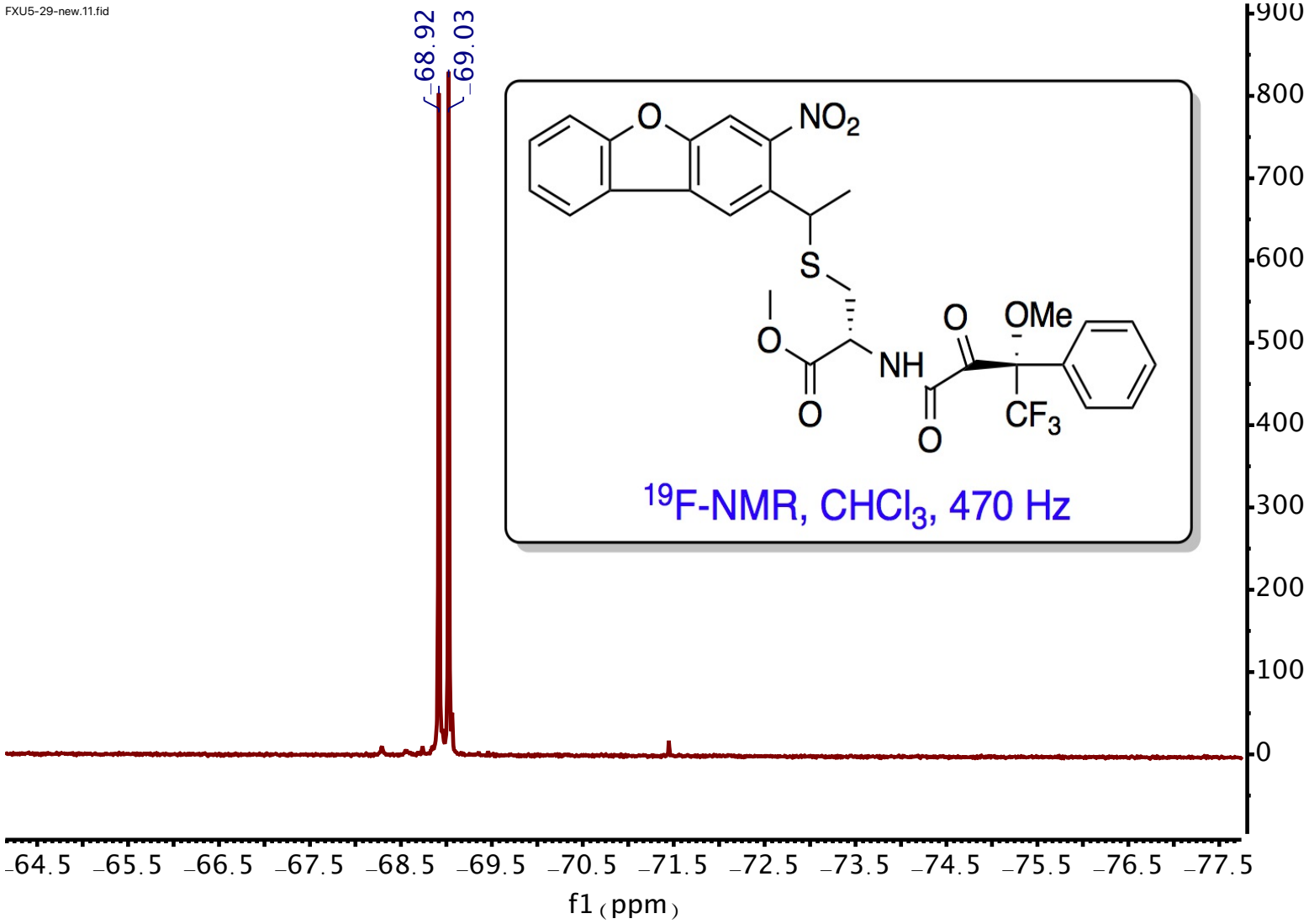

Compound **23a**: ^{19}F NMR

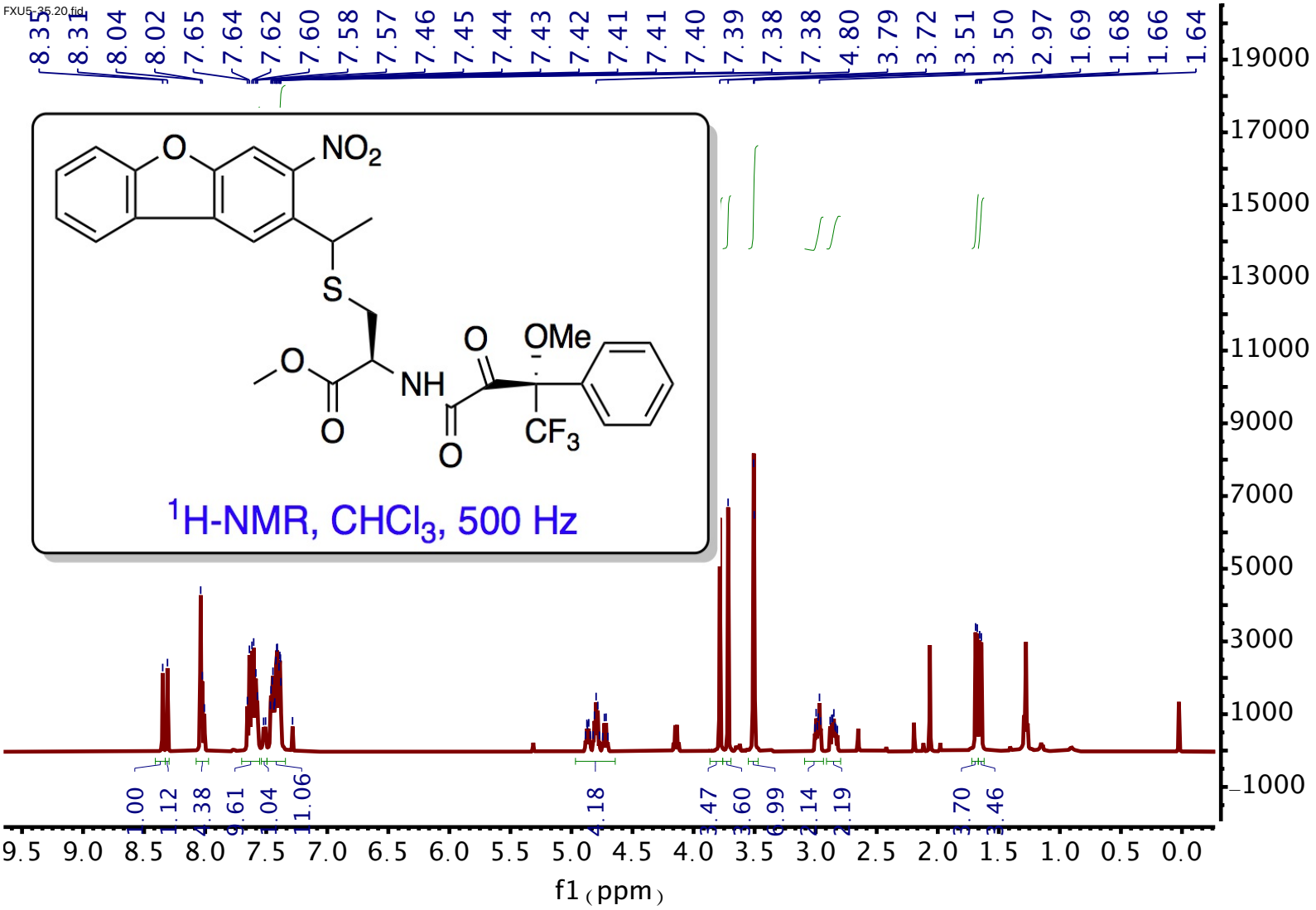

Compound **23b**: ^{1}H NMR

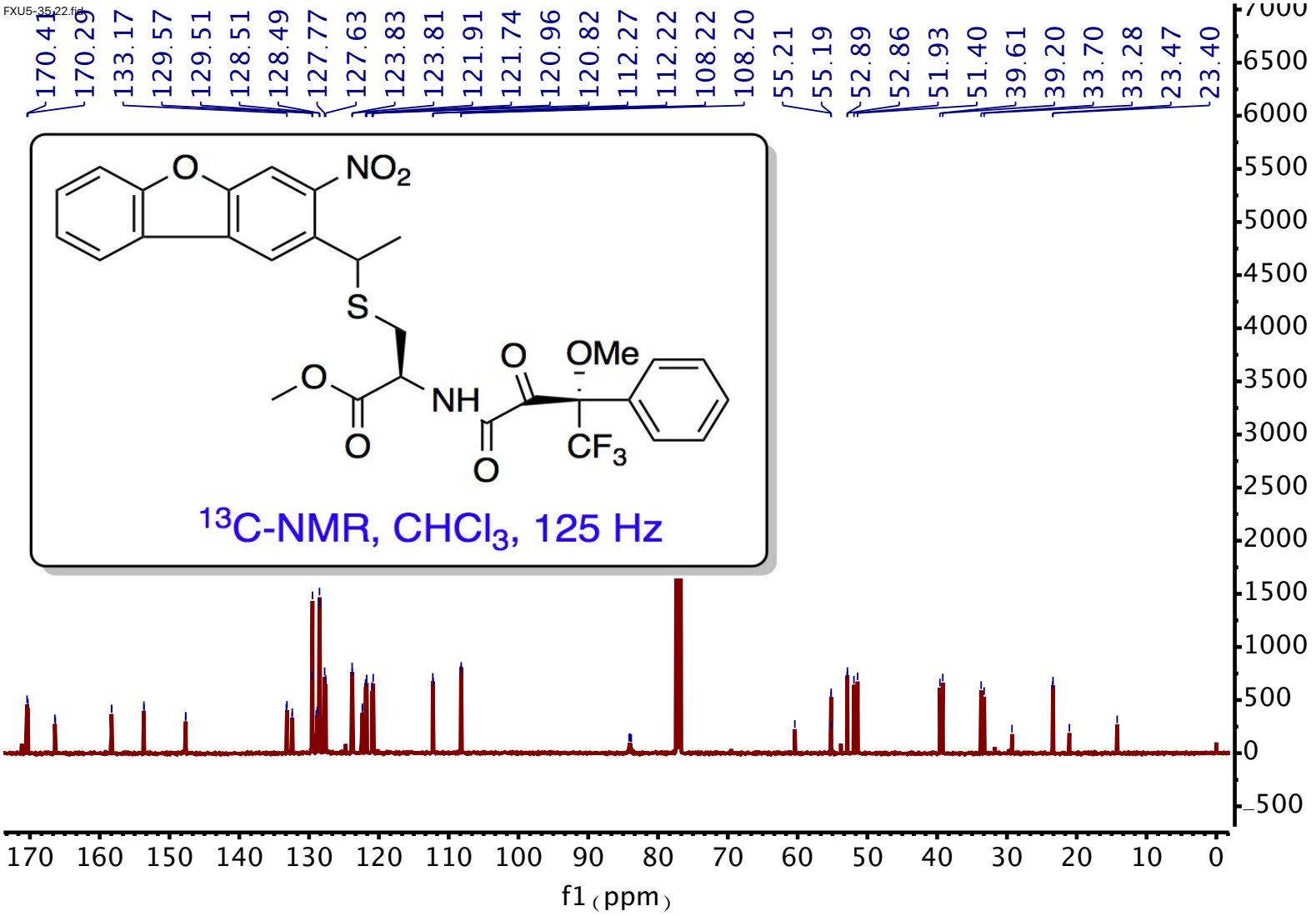

Compound **23b**: ^{13}C NMR

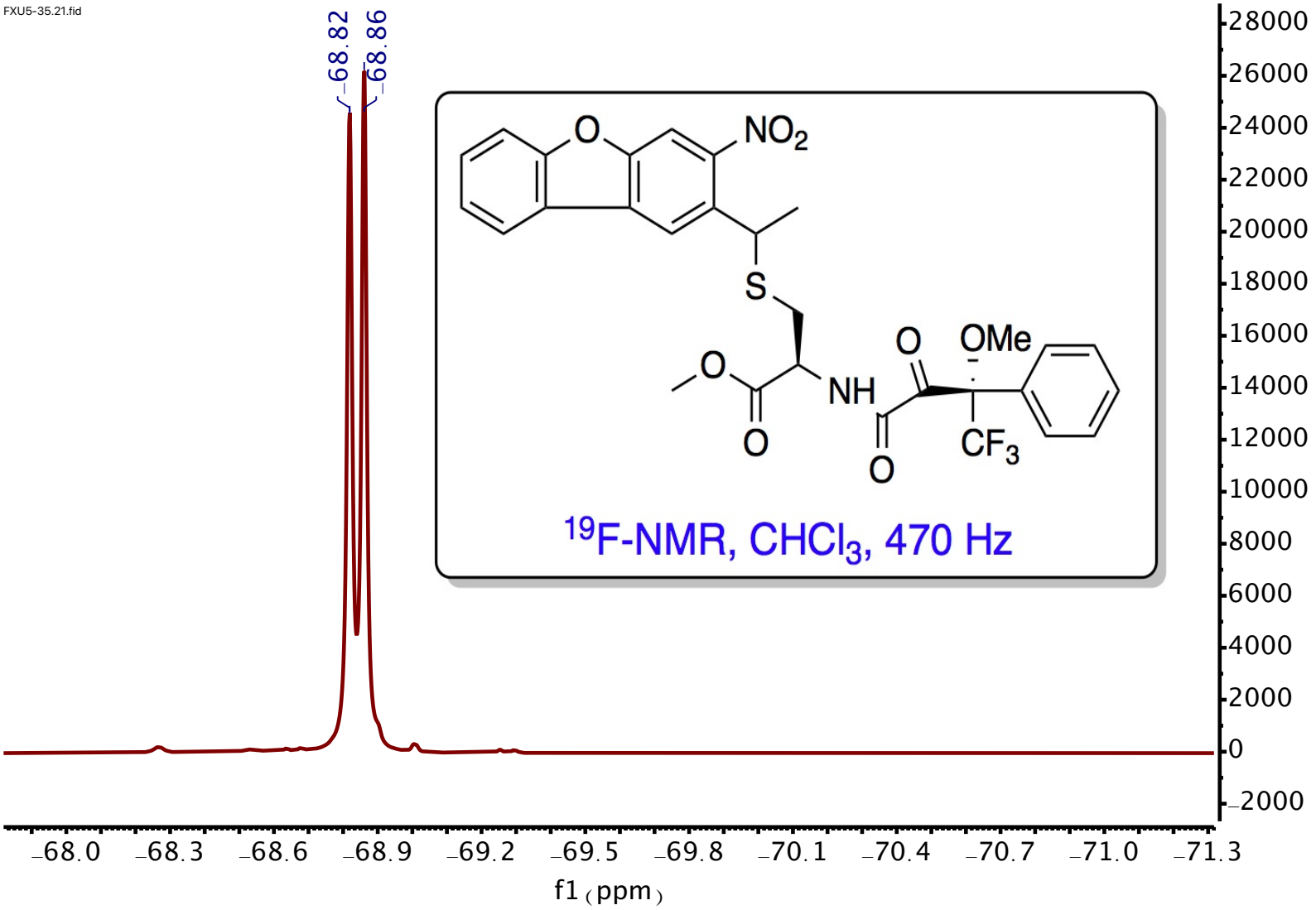

Compound **23b**: ^{19}F NMR

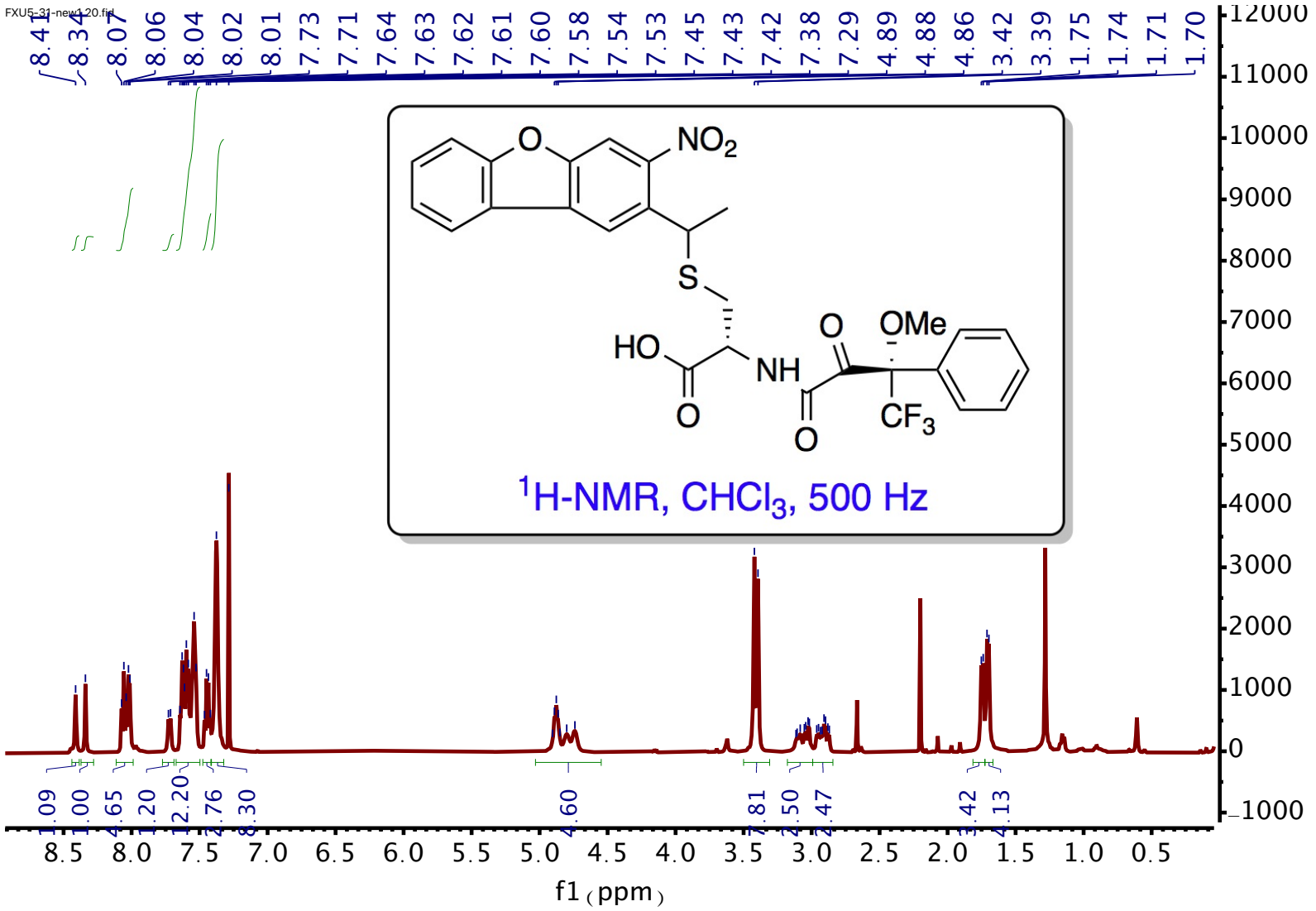

Compound **24a**: ^{1}H NMR

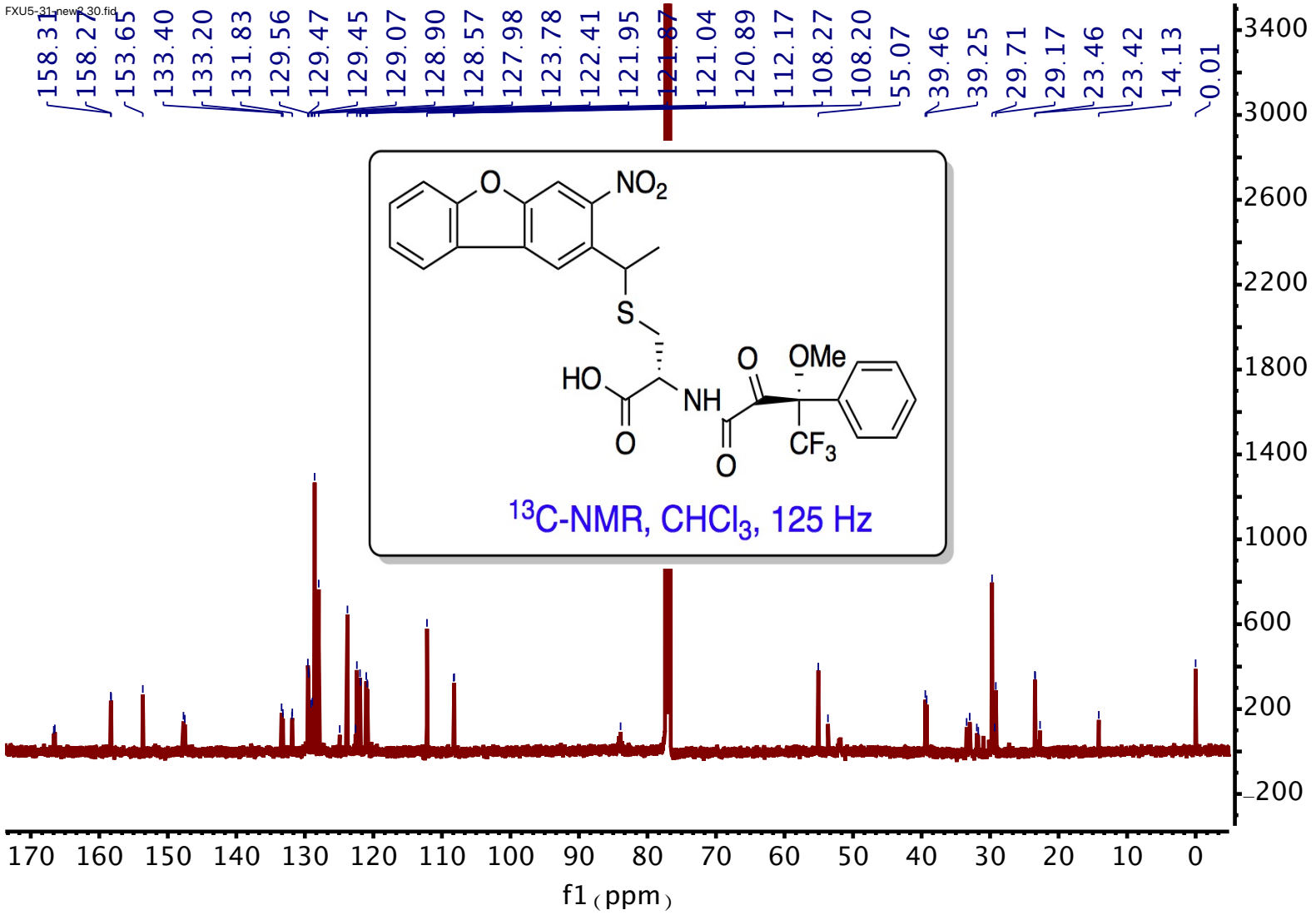

Compound **24a**: ^{13}C NMR

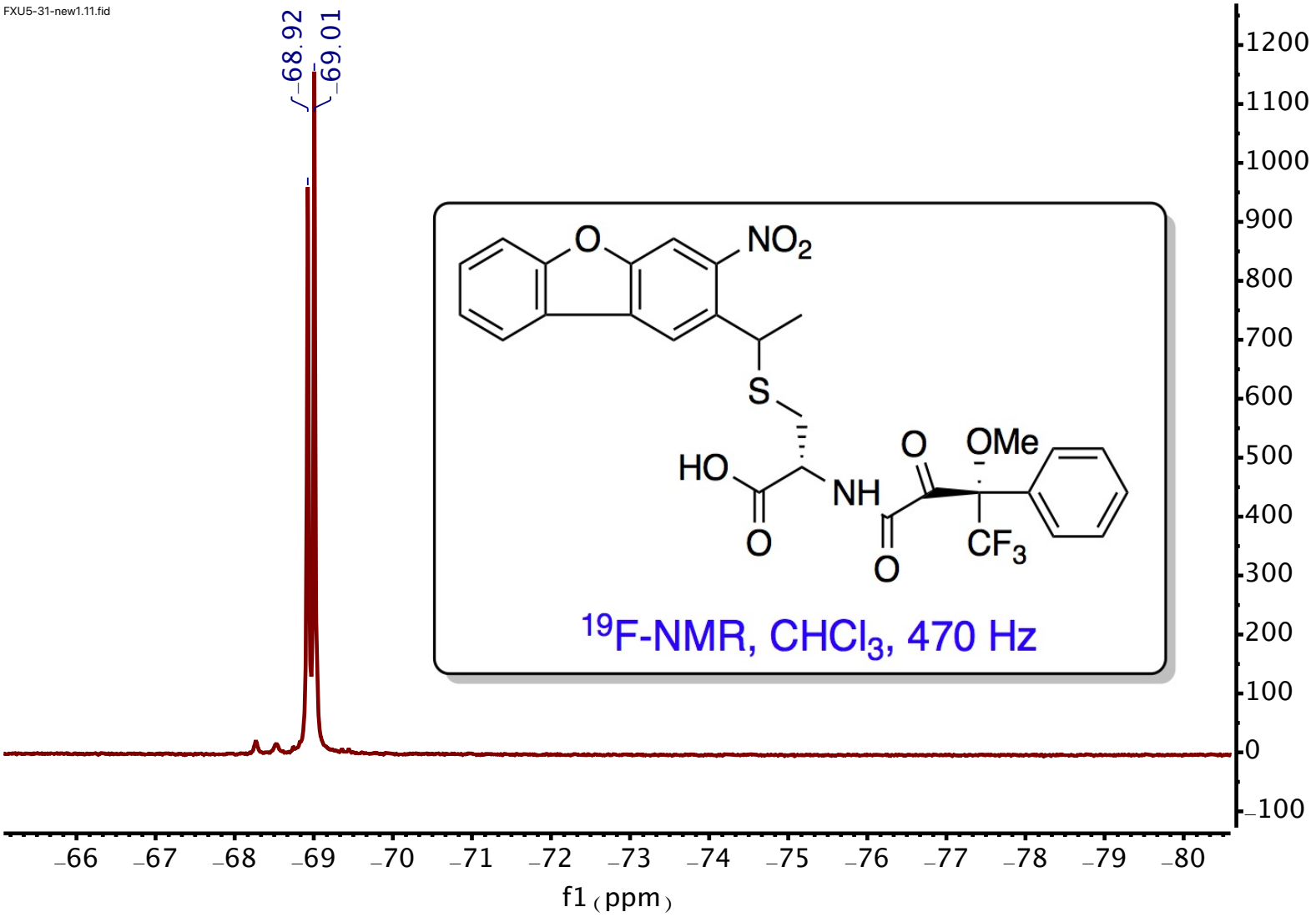

Compound **24a**: ^{19}F NMR

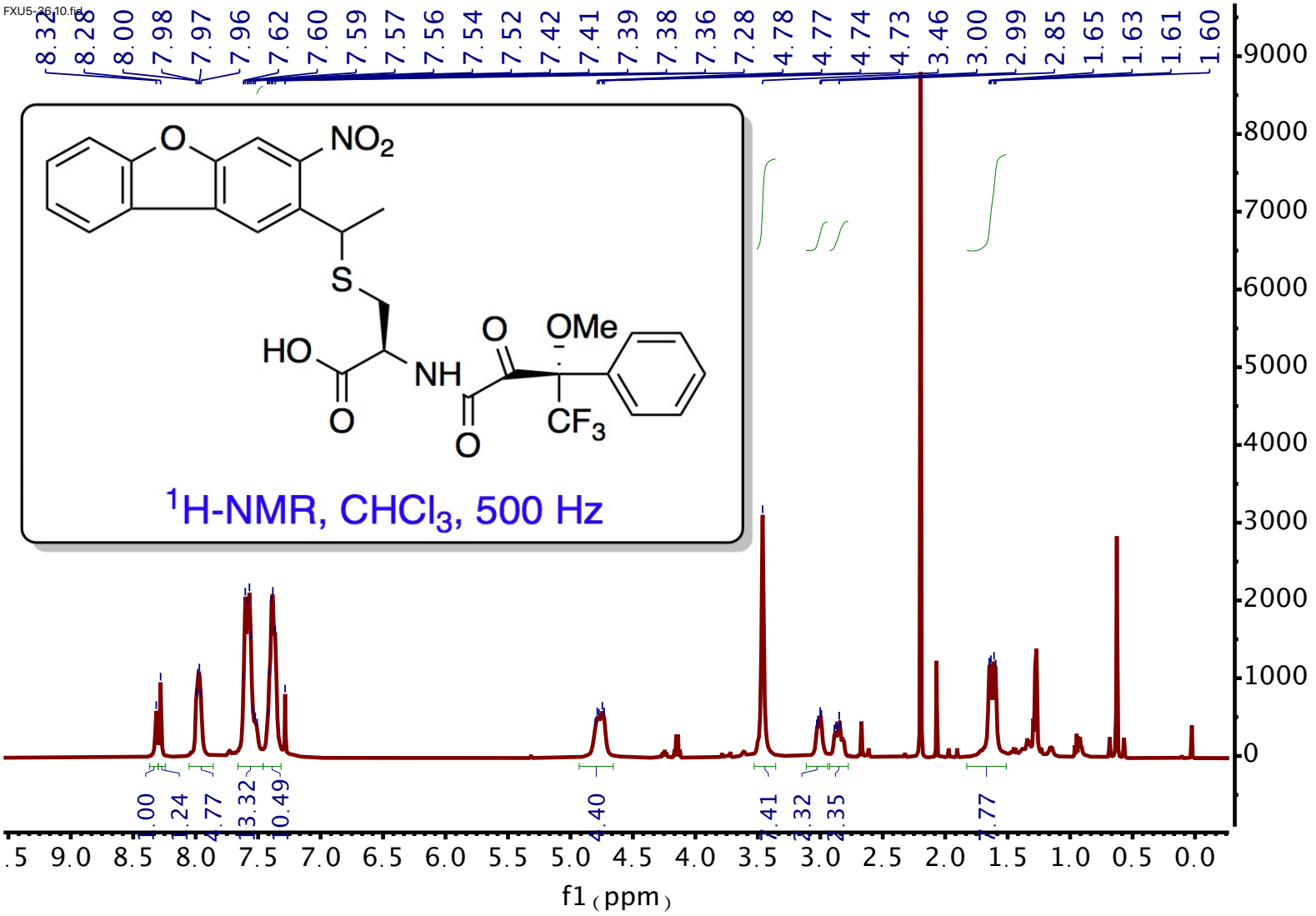

Compound **24b**: ^{1}H NMR

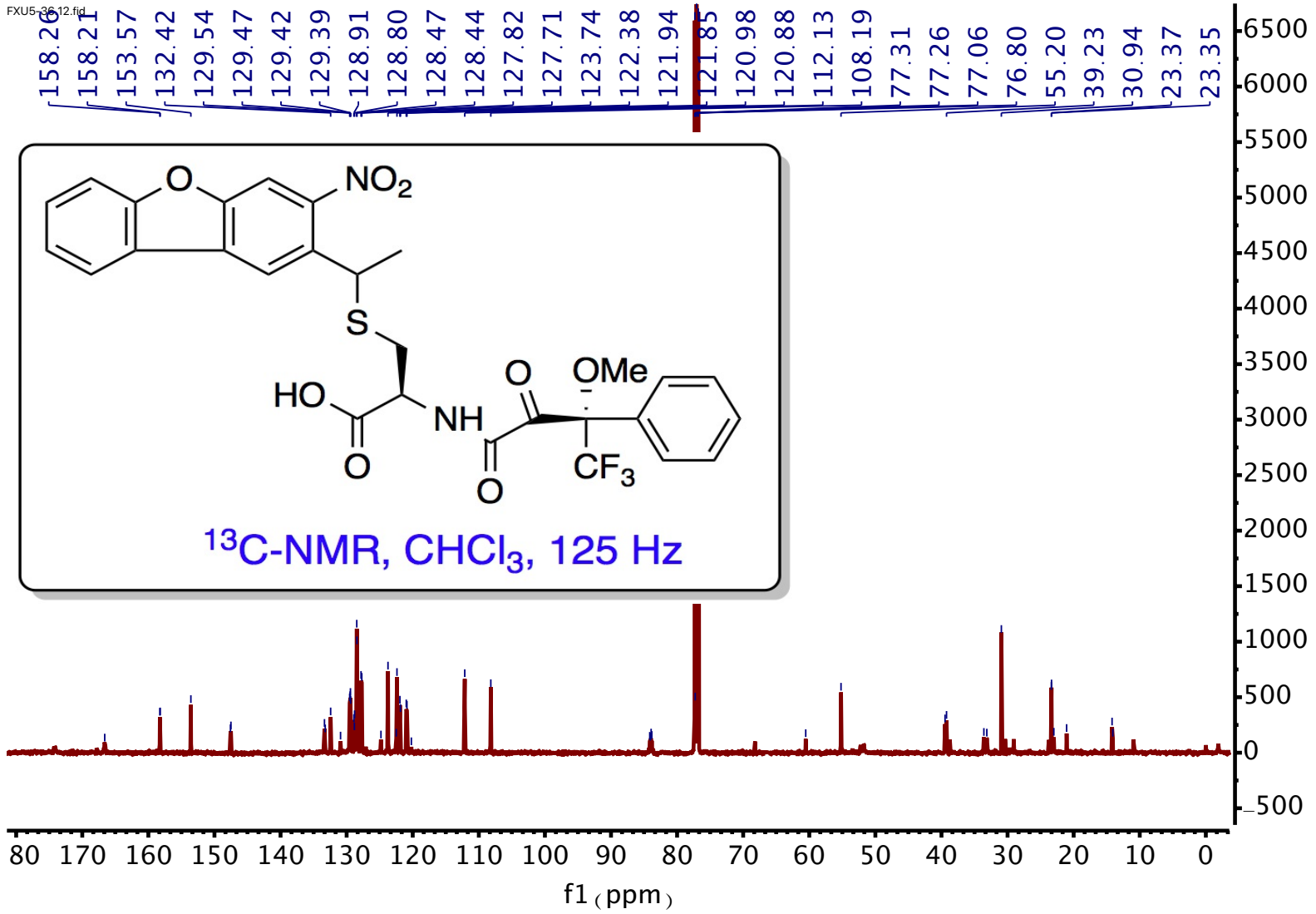

Compound **24b**: ^{13}C NMR

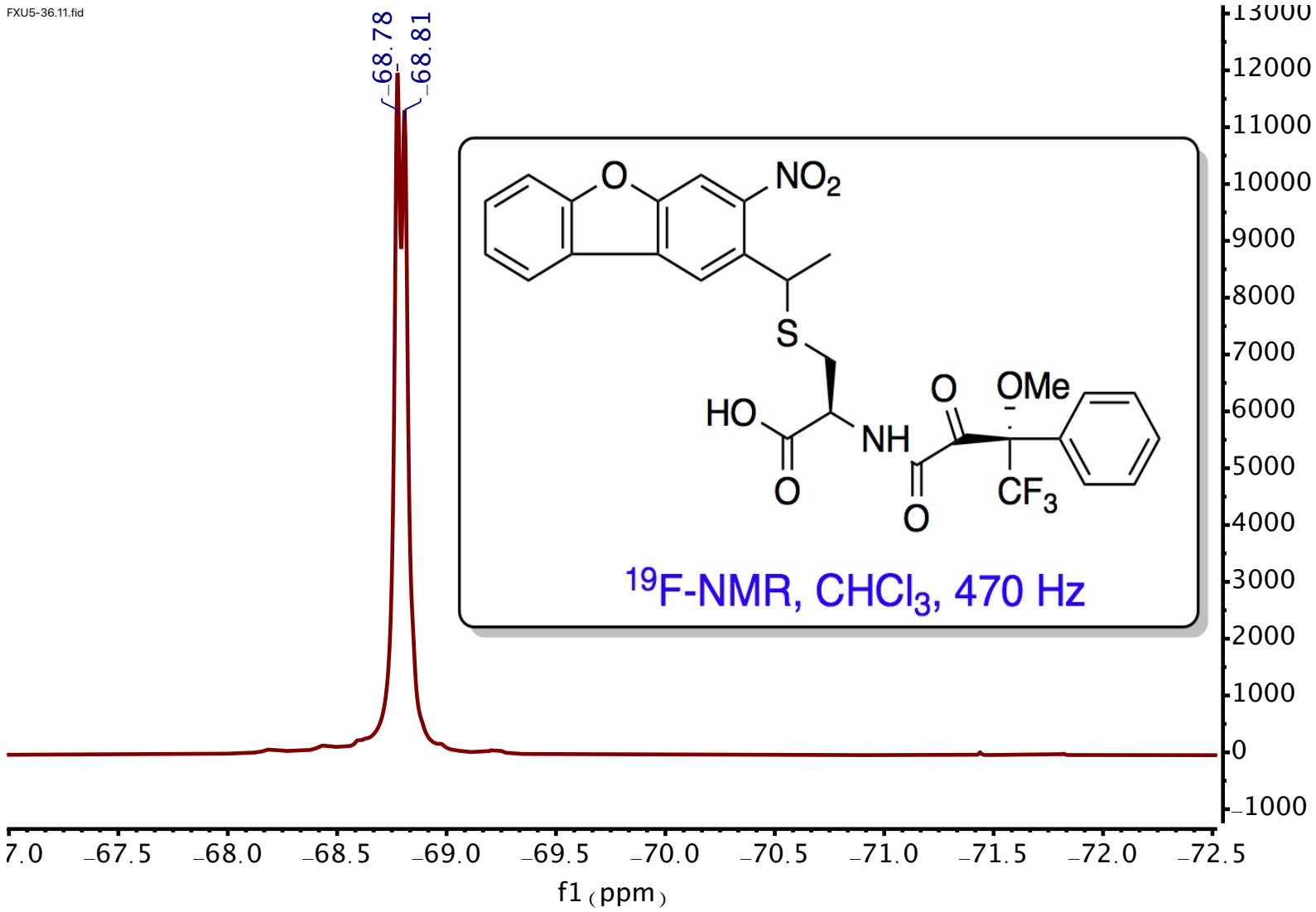

Compound **24b**: ^{19}F NMR